CHALMERS

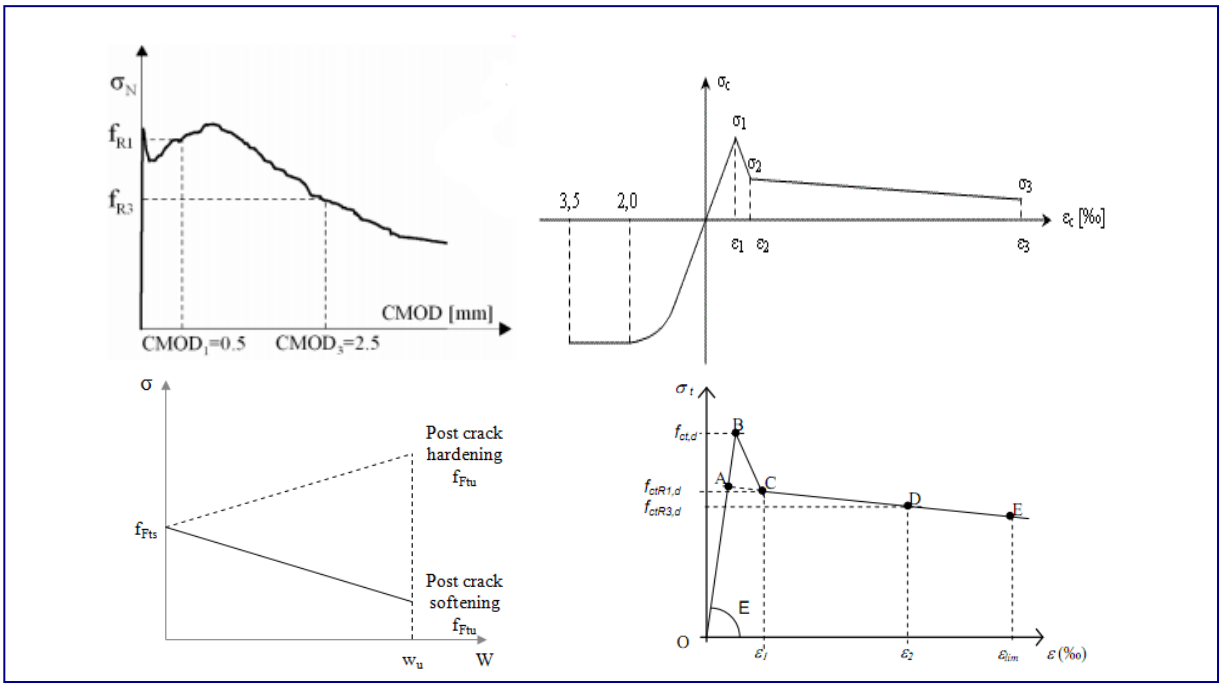

Design of Fibre Reinforced Concrete Beams and Slabs

Master of Science Thesis in the Master's Programme Structural Engineering and Building Performance Design

AMMAR ABID, KENNETH B. FRANZÉN

Department of Civil and Environmental Engineering
Division of Structural Engineering
Concrete Structures
CHALMERS UNIVERSITY OF TECHNOLOGY
Göteborg, Sweden 2011

Master's Thesis 2011:62

MASTER'S THESIS 2011:

Design of Fibre Reinforced Concrete Beams and Slabs

Master of Science Thesis in the Master's Programme Structural Engineering and Building Performance Design

AMMAR ABID, KENNETH B. FRANZÉN

Department of Civil and Environmental Engineering
Division of Structural Engineering
Concrete Structures
CHALMERS UNIVERSITY OF TECHNOLOGY
Göteborg, Sweden Göteborg, Sweden 2011

Design of Fibre Reinforced Concrete Beams and Slabs
AMMAR ABID, KENNETH B. FRANZÉN

Examensarbete / Institutionen för bygg- och miljöteknik,
Chalmers tekniska högskola 2011:62

Department of Civil and Environmental Engineering
Division of Structural Engineering
Concrete Structures
Chalmers University of Technology
SE-412 96 Göteborg
Sweden
Telephone: + 46 (0)31-772 1000

Cover:
Above: (Left) Figure 3.4: Results from a bending test with a softening material behaviour, (Right) Figure 3.15: Stress-strain diagram for fibre reinforced concrete, from RILEM TC-162 TDF
Below: (Left) Figure 3.5: Post crack constitutive law, from FIB model code 2010, (Right) Figure 3.25: Multi-linear stress-strain diagram, from Spanish EHE-08

Name of the printers / Department of Civil and Environmental Engineering Göteborg, Sweden Göteborg, Sweden 2011

Design of Fibre Reinforced Concrete Beams and Slabs

Master of Science Thesis in the Master's Programme Structural Engineering and Building Performance Design

AMMAR ABID, KENNETH B. FRANZÉN
Department of Civil and Environmental Engineering
Division of Structural Engineering
Concrete Structures
Chalmers University of Technology

ABSTRACT

Concrete is a material that needs strengthening in tension in order to meet the structural requirements. New techniques of strengthening concrete, besides the usual ordinary reinforcement bars, are developing, creating a need for new design methods. Fibre reinforcement is a method that has been in use over the last 30 years, yet it is unfamiliar to some and there is no common guideline for design using this method.

This project evaluates three of the existing guidelines, namely the FIB model code, RILEM TC-162-TDF (2003) and the Spanish EHE-08, regarding design of fibre reinforced concrete, aiming at detecting possible difficulties, limitations and possibilities.

Design calculations, regarding moment- and shear resistance in ultimate limit state and crack width calculations in serviceability limit state, were carried out in Mathcad for simply supported beams, with different combinations of ordinary reinforcement and fibre dosages. The design results were then compared with existing experimental results to assess the accuracy of the design codes. The simply supported slabs were also designed in Mathcad, where two reference slabs with ordinary reinforcement were compared to concrete slabs only reinforced with fibres.

Regarding accuracy, the variation between the design codes and guidelines was small. However when compared to the experimental results, underestimations were revealed in all the guidelines. The FIB model code and the Spanish EHE-08 proved to be the most accurate.

Out of the three guidelines, evaluated in this project, the FIB model code was most applicable due the fact that it was complete and clear in most regards.

The design of the simply supported slabs revealed that, it is possible to replace ordinary reinforcement with steel fibres but requires large fibre fractions, as those used in this project were not enough.

Key words: concrete, steel fibres, fibre reinforced concrete, moment resistance, shear resistance, crack width calculations, fibre fractions

Contents

Preface

This project is a part of a European project 'Tailor Crete' which aims at achieving more complex geometries in structures. This is done by developing new techniques such as different reinforcing methods.

The Report evaluates three of the existing national codes and guideline, namely the FIB model code, RILEM TC-162-TDF (2003) and the Spanish EHE-08, regarding design of fibre reinforced concrete, aiming at detecting possible difficulties, limitations and possibilities.

This master's thesis was carried out, between January 2011 and June 2011, at the Department of Civil and Environmental Engineering, Chalmers University of Technology, Göteborg, Sweden.

We would like to thank our examiner Ph.D. Karin Lundgren and supervisor Ph.D. Rasmus Rempling, at Chalmers, for their support and guidance throughout the entire project period. We would also like to thank Ph.D. student David Fall for all his support.

Göteborg June 2011

Ammar Abid and Kenneth B. Franzén

Notations

Roman upper case letters

A	Gross concrete section area
$A_{c,ef}$	Effective area of concrete
A_{ct}	Area of the tensile part of the concrete cross section
A_f	Area of the fibre cross section
A_p	Area of bonded active reinforcement
A_s	Area of steel reinforcement
A_{sw}	Area of shear reinforcement
E_c	Concrete modulus of elasticity
E_{cm}	Mean modulus of elasticity for concrete
E_s	Modulus of elasticity for steel
$F_{fc,t}$	Resulting residual tensile stress of the fibres
F_j	Load corresponding to crack mouth opening displacement
L	Span of the specimen
L	Length of the steel fibre
M_{cr}	Cracking moment
M_{Rd}	Yield moment
M_{uRd}	Ultimate moment
N_b	Number of fibres per unit area
N_{sd}	Longitudinal force in the section due to loading or pre-stressing
P	Prestressing force
V_{cd}	Shear resistance for members without shear reinforcement
V_{cu}	Shear resistance for members without shear reinforcement
V_d	Maximum shear resistance
V_f	Volume of the fibres in the concrete mix
V_{fd}	Contribution of fibres to shear resistance
V_{fu}	Contribution of fibres to shear resistance
V_{Rd}	Shear resistance
$V_{Rd,c}$	Concrete contribution to shear resistance
$V_{Rd,f}$	Fibre contribution to shear resistance
$V_{Rd,s}$	Shear reinforcement contribution to shear resistance
$V_{Rd,Fmin}$	Minimum value of shear resistance
V_{su}	Contribution of transverse reinforcement to the shear strength

V_{wd}	Contribution of stirrups or inclined bars to shear resistance
W_1	Section modulus
W_b	Section modulus

Roman lower case letters

a	Height of notch
b	Width of beam
b_f	Width of the flanges
b_w	Width of the web
c	Concrete cover
d	Effective depth
d_p	Depth of active reinforcement from the most compressed fibre in the section
d_s	Depth passive reinforcement
e	Eccentricity of the prestressing relative to the center of gravity of the gross section
f_{ck}	Cube strength
$f_{ck,cyl}$	Cylinder strength
f_{cm}	Mean concrete strength
f_{ctm}	Mean tensile concrete strength
f_{fcm}	Mean concrete compressive strength
$f_{ct,d}$	Design tensile strength, see Figure 3.25
$f_{ct,fl,d}$	Design value of the flexural tensile strength
$f_{ctR1,d}$	Design residual tensile strength, see Figure 3.25
$f_{ctR3,d}$	Design residual tensile strength, see Figure 3.25
f_{cv}	Compressive strength
$f_{fct,fl}$	Flexural tensile strength
$f_{fctm,fl}$	Mean residual tensile strength
f_{Fts}	Serviceability residual tensile strength, see Figure 3.7
f_{Ftu}	Ultimate residual tensile strength, see Figure 3.7
f_{pd}	Design value of the tensile strength of bonded active reinforcement
$f_{R,1,d}$	Design residual flexural strength
$f_{R,3,d}$	Design residual flexural strength

$f_{R,i}$	Residual flexural tensile strength corresponding to crack mouth opening displacement
$f_{R,j}$	Residual flexural tensile strength corresponding to crack mouth opening displacement
f_{su}	Ultimate steel reinforcement stress
f_{sy}	Yield steel reinforcement stress
f_{ywd}	Yield strength of the shear reinforcement
h	Height of beam
h_f	Height of the flanges
h_{sp}	Distance between the notch tip and the top of the specimen
k_1	Factor taking bond properties of ordinary reinforcement into account
k_2	Coefficient taking strain distribution into account
k	Factor taking size effect into account
k	Coefficient taking into account non-uniform self-equilibrating stresses leading to reduction of cracking force
k_c	Coefficient taking into account, the stress distribution in the cross section just before cracking and the change of inner lever arm
k_{cr}	Curvature at cracking
k_f	Factor taking contribution of flanges in T-section into account
k_h	Size factor
k_u	Ultimate curvature
k_v	Factor taking size effect into account
k_y	Curvature at yielding
l	Span of the specimen
l_{cs}	Critical length of the element
l_f	Fibre length
l_s	Free span length
$l_{s,max}$	The length over with slip between concrete and steel occurs
l_t	Span length
s	Spacing between shear reinforcement
s_m	Mean distance between cracks
s_{rm}	Mean crack spacing
w_d	Design crack width
w_u	Maximum allowed crack width
x	Height of compressive stress block

x_T	Fibres centre of gravity from the neutral axis
x_{tot}	Fibres centre of gravity seen from the top of the tensile zone given as a percentage of the distance
x_u	Height of compressive stress block in ultimate limit state
x_y	Distance from top of the beam to the neutral axis
y	Distance between the neutral axis and the tensile side of the cross section
z	Internal lever arm
z_f	Lever arm for the tensile zone

Greek lower case letters

α	Angle of shear reinforcement
α	Modular ratio
α_e	Modular ratio
β_1	Coefficient taking bond properties of the steel reinforcement bars into account
β_2	Coefficient taking duration of loading into account
β	Distance from the top of the beam to the center of the concrete compressive zone
β	Empirical coefficient to assess the mean strain over $l_{s,max}$
γ_c	Partial safety factor for concrete
δ_{peak}	Displacement at the maximum load
δ_{SLS}	Displacement at service load computed by performing a linear elastic analysis with the assumptions of uncracked condition and initial elastic Young's modulus
δ_u	Ultimate displacement
ε_{c2}	Strain in the concrete when the ordinary reinforcement reaches yielding
ε_{cm}	Average concrete strain over $l_{s,max}$
ε_{cs}	Concrete strain due to shrinkage
ε_{cu}	Ultimate strain in the concrete
$\varepsilon_{fc,max}$	Concrete compressive strain
$\varepsilon_{fc,t}$	Tensile strain
ε_r	Strain at cracking
ε_{sm}	Average steel strain over $l_{s,max}$
ε_{sy}	Yield strain of the ordinary reinforcement

ξ	Factor taking size effect into account
η	Factor that defines the effective strength
η_b	Fibre efficiency factor
$\eta_{b,beam}$	Fibre efficiency factor for beam elements
$\eta_{b,exp}$	Fibre efficiency factor obtained from the wedge splitting tests
η_r	Factor which takes long term effects into account
λ	Factor that reduces the height of the compression zone
ρ_1	Steel reinforcement ratio
$\rho_{s,ef}$	Effective steel reinforcement ratio
ρ_s	Steel reinforcement ratio
σ_1	Principal tensile stress
$\sigma_{b,beam}$	Bridging stress applicable for the beam elements
$\sigma_{b,exp}$	Experimental bridging stress from the wedge splitting tests
σ_{cp}	Average stress acting on the concrete cross section for an axial force
σ_{cd}	Contribution from axial compressive force or pre-stressing
σ_s	Steel stress in a crack
σ_{sr}	Maximum steel stress in a crack in the crack formation stage
τ_{bm}	Mean bond strength between reinforcing bars and concrete
τ_{fd}	Design value of increase in shear strength due to steel fibres
$\emptyset$	Diameter of the steel fibre
$\emptyset_b$	Ordinary reinforcement bar size
ϕ_s	Steel reinforcement diameter

Abbreviations

CEB	Euro-International concrete committee
CMOD	Crack mouth opening displacement
EHE	Spanish code on structural concrete
FIB	International federation for structural concrete
FIP	International federation for pre-stressing
FRC	Fibre reinforced concrete
LOP	Limit of proportionality
RILEM	International union of laboratory and experts in construction materials, systems and structures
UTT	Uni-axial tension tests
WST	Wedge splitting tests

1 Introduction

Concrete has proved to be a versatile material in the construction of structures due to the possibility of moulding it into virtually any shape and geometry. Utilizing this formable nature of the material, concrete architecture has made rapid progress in the recent years.

Concrete is a material with varying material behaviour with high strength in compression but poor in tension. This has led to a need for reinforcement in the tensile parts of the structures. Traditionally this has been done using ordinary reinforcing bars. However, the need for designing structures with more complex geometries has led to the development of relatively new reinforcement materials such as steel fibres, which have further raised the potential of designing such geometries. Steel fibres can partly or entirely replace conventional reinforcement owing to the fact that steel fibres also increase the load carrying capacity of structures and improve crack control.

Development of new reinforcing methods has left a need for the development of new design methods. Today, there are a number of different national guidelines and design codes for designing steel fibre reinforced concrete, but no general European design code exists.

1.1 Aim

The report aims at surveying the applicability and accuracy, in the ultimate limit state regarding moment and shear capacities and in the serviceability limit state regarding crack width calculations, from three of the existing design codes and guidelines namely FIB model code, RILEM TC-162-TDF (2003) and the Spanish EHE-08, in order to detect possible difficulties, limitations and possibilities.

1.2 Method

A literature study was done on fibre reinforced concrete to gain knowledge about the materials and their behaviour, strength and properties. In this report, results from experimental tests found in literature, on beams with varying fibre contents, performed by Gustafsson and Karlsson in 2006, were used as reference values and their material data and properties were used as input data for the design calculations. These design calculations were then compared with the results from the experimental tests to check the accuracy of the methods. Literature on full scale slab experimental tests was found but due to the difficulties in retrieving their material properties and data, the same material properties from the beam experiments were used for slab design.

1.3 Limitations

Only simply supported beams and flat slabs with rectangular cross sections were considered in the design. The report only treats short steel fibres, randomly spread in the concrete combined with ordinary reinforcement. The report has focused on steel fibre reinforced concrete elements with self-compacting concrete having a post crack softening behaviour for the reason that experimental results used for comparison had this behaviour. No long term effects were considered.

2 Literature study on fibre reinforced concrete

2.1 General

Fibre reinforced concrete (FRC) is a concrete mix containing water, cement, aggregate and discontinuous fibres of various shapes and sizes.

According to Bentur & Mindess (2006), fibres have been used as reinforcement for quite some time now. Asbestos was the first material widely used in the beginning of the 20th century. Man-made fibres produced from steel, glass, synthetics, asbestos and natural fibres such as cellulose, sisal and jute, are examples of materials that are used in FRC today.

Unreinforced concrete is as known, a brittle material with high compressive strength but low tensile strength. Therefore, concrete requires reinforcement. The most known method has been, using ordinary continuous reinforcing bars in order to increase the load carrying capacity in the tensile and shear zones. Fibres that are short materials randomly spread in the concrete mix, are however discontinuous. Fibres do not increase the (tensile) strength remarkably, but due to their random distribution in the mix, they are very effective when it comes to controlling cracks. As a result the ductility of fibre reinforced members is increased. Fibres can also be used in thin and complex members where ordinary reinforcement cannot fit.

2.2 Fibre types and classification

According to Naaman (2003), fibres used in cementitious composites can be classified with regard to:-

1. Origin of fibres
   According to origin, the fibres can be classified as:
   Natural organic (cellulose, sisal, bamboo, jute etc.), natural inorganic (asbestos, wollastonite, rock wool etc.) and man-made (steel, glass, synthetic etc.)

2. Physical/Chemical properties
   Fibres are classified based on their physical/chemical properties such as density, surface roughness, flammability, reactivity or non-reactivity with cementitious matrix etc.

3. Mechanical properties
   Fibres are also characterized on the basis of their mechanical properties e.g. specific gravity, tensile strength, elastic modulus, ductility, elongation to failure, stiffness, surface adhesion etc.

4. Shape and size
   Classification of fibres is also based on geometric properties, such as cross sectional shape, length, diameter, surface deformation etc. Fibres can be of any cross sectional shape such as circular, rectangular, diamond, square, triangular, flat, polygonal, or any substantially polygonal shape. Figure 2.1 and Figure 2.2 show the different cross sectional geometries of fibres.

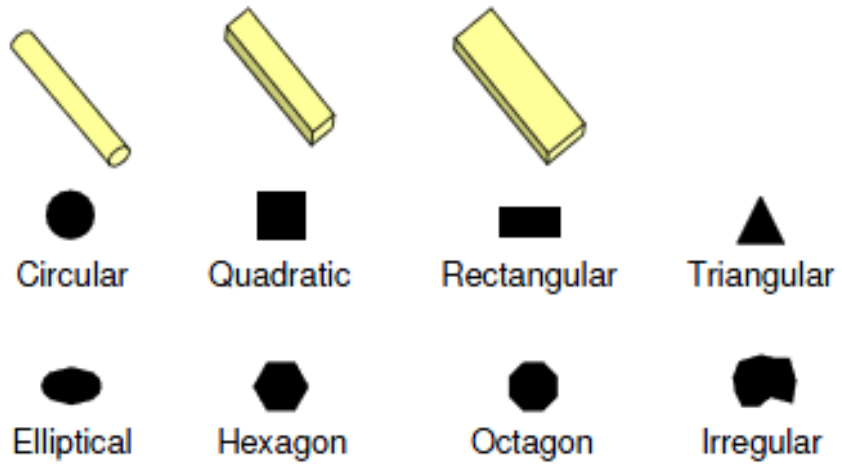

Figure 2.1 Cross sectional geometries of fibres, Löfgren (2005)

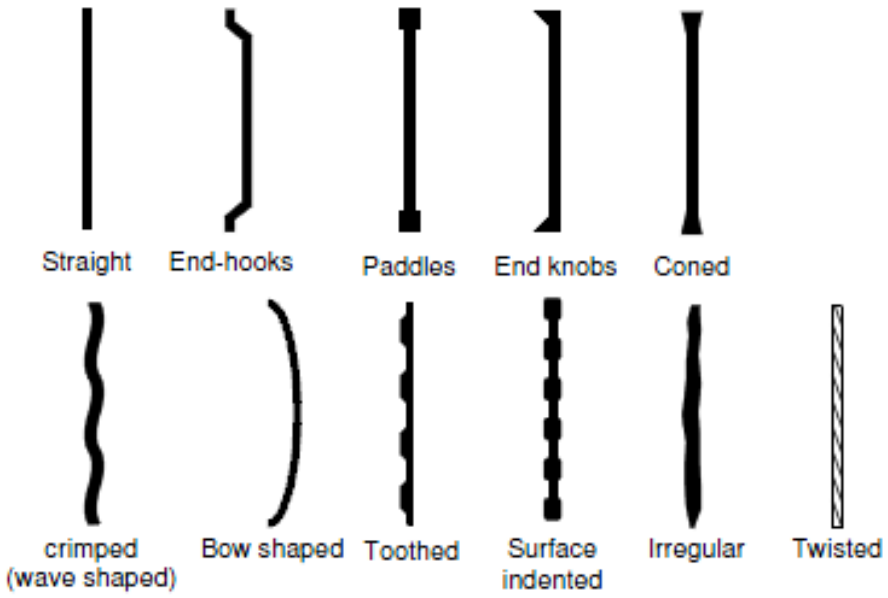

Fig 2.2 Typical geometries of fibres, Löfgren (2005)

The basic fibre categories are steel, glass, synthetic and natural fibre materials. In Table 2.1, typical physical properties of a few fibres are listed.

Table 2.1 Physical properties of typical fibre, from Löfgren (2005)

Type of Fibre	Diameter [µm]	Specific gravity [g/cm^3]	Tensile strength [MPa]	Elastic modulus [GPa]	Ultimate elongation [%]
Metallic					
Steel	5-1 000	7.85	200-2 600	195-210	0.5-5
Glass					
E glass	8-15	2.54	2 000-4 000	72	3.0-4.8
AR glass	8-20	2.70	1 500-3 700	80	2.5-3.6
Synthetic					
Acrylic (PAN)	5-17	1.18	200-1 000	14.6-19.6	7.5-50.0
Aramid (e.g. Kevlar)	10-12	1.4-1.5	2 000-3 500	62-130	2.0-4.6
Carbon (low modulus)	7-18	1.6-1.7	800-1 100	38-43	2.1-2-5
Carbon (high modulus)	7-18	1.7-1.9	1 500-4 000	200-800	1.3-1.8
Nylon (polyamide)	20-25	1.16	965	5.17	20.0
Polyester (e.g. PET)	10-8	1.34-1.39	280-1 200	10-18	10-50
Polyethylene (PE)	25-1 000	0.96	80-600	5.0	12-100
Polyethylene (HPPE)	-	0.97	4 100-3 000	80-150	2.9-4.1
Polypropylene (PP)	10-200	0.90-0.91	310-760	3.5-4.9	6-15.0
Polyvinyl acetate (PVA)	3-8	1.2-2.5	800-3 600	20-80	4-12
Natural - organic					
Cellulose (wood)	15-125	1.50	300-2 000	10-50	20
Coconut	100-400	1.12-1.15	120-200	19-25	10-25
Bamboo	50-400	1.50	350-50	33-40	-
Jute	100-200	1.02-1.04	250-350	25-32	1.5-1.9
Natural - inorganic					
Asbestos	0.02-25	2.55	200-1 800	164	2-3
Wollastonite	25-40	2.87-3.09	2 700-4 100	303-530	-

2.2.1 Steel fibres

Steel fibres are the most commonly used man-made metallic fibres generally made of carbon or stainless steel. The different mechanical properties for steel fibres are given in Table 2.1, according to which the tensile strength is in the range of 200-2600 MPa and ultimate elongation varies between 0.5 and 5%. It can be said, according to Jansson (2008), that pull-out tests, where the fibres have been of much higher strength than the concrete, yielding in the fibres has not been the issue but spalling of the concrete. With a minimum strength of 200 MPa, it can be concluded that the yielding strength is sufficient enough to prevent fibre rupture.

According to Bentur and Mindess (2006), fibres are added and treated as any other component in a concrete mix, but due to difficulties in handling, only about 2 volume percent can be applied.

Today, straight fibres are very rarely used due to their weak bonding with the cement matrix. It is however, quite common to use brass-coated straight fibres with high strength concrete mix since the bond obtained is relatively strong, see Lutfi (2004) and Marcovic (2006).

2.3 Steel fibre reinforced concrete

Steel fibre reinforced concrete is a composite material made up of a cement mix and steel fibres. The steel fibres, which are randomly distributed in the cementitious mix, can have various volume fractions, geometries, orientations and material properties, see Löfgren (2005).

It has been shown that fibres with low volume fractions (<1%), in fibre reinforced concrete, have an insignificant effect on both the compressive and tensile strength, Löfgren (2005). They however, contribute to the toughness and post cracking behaviour of the concrete. This behaviour can be measured as a flexural tensile strength and determined through different experimental test methods, where three point and four point bending tests are the most commonly used methods, see Löfgren (2005). Other noteworthy methods are wedge splitting tests (WST) and uni-axial tension tests (UTT).

Experiments, performed by Özcan et al. (2009), on steel fibre reinforced concrete beams with varying fibre dosages, revealed that fibres have a negative impact on the compressive strength and modulus of elasticity, as both decreased with increasing fibre dosages. The experiments however showed that the fibres have a positive effect on the toughness of the specimen, as the toughness increased with increasing fibre dosages, for more details see Özcan et al. (2009).

Today fibre reinforced concrete is mainly used on industrial ground floors, where the slabs on the ground are exposed to heavy repetitive loads from e.g. trucks and lifts, in order to increase the durability of the ground slabs and increase the strength against cracking. Another area where fibres are used is in tunnel linings, where the fibres contribute to increased strength against shrinkage and reduction of permeability as tunnels are often subjected to water or soil loads.

2.3.1 Post crack behaviour

The behaviour of fibre reinforced concrete, varies with composition and can have a softening or hardening behaviour, see Figure 2.3. Post crack hardening allows multiple cracks before failure while in post crack softening there is a reduction of strength after the first crack allowing no further cracks.

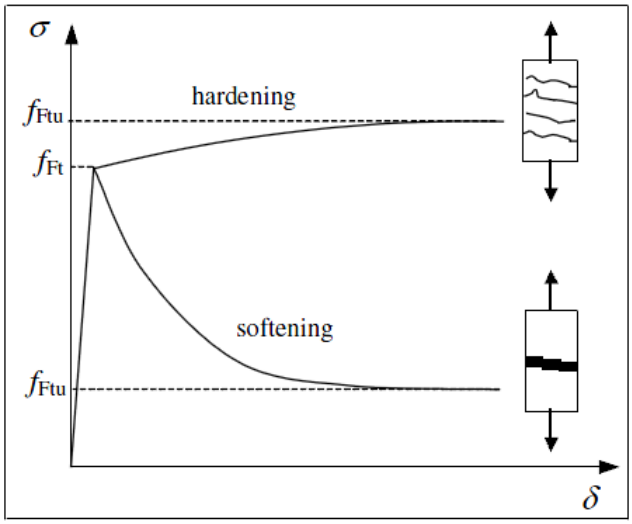

Figure 2.3 Post cracking behaviour of FRC in tension, from Jansson (2008)

3 Design of beam elements

Design of beam elements with three of the existing national guidelines and design codes was carried out to investigate differences and applicability. The design results were compared with experimental results to check their accuracy.

3.1 Experiments

The four point beam bending tests reviewed here have been carried out by Gustafsson and Karlsson (2006), see also Jansson (2008). The study contained 5 series with 3 beams tested in each series, see Table 3.1. The first series contained only conventional reinforcement, while the other series (2-5) contained different amounts of fibres as shown in Table 3.1 and Table 3.2. All tested beams had three reinforcing bars with a diameter of either 6mm or 8mm. The concrete composition used in the bending tests had a post crack softening behaviour.

Table 3.1 Details of test specimen reinforced with 8mm reinforcement bars

Series	Fibre Content %/[kg/m^3]	Reinforcement number and diameter [mm]	Number of beams	Number of WST cubes	Number of Compression cubes
1	-	3ø8	3	9	6
2	0.5/39.3	3ø8	3	9	6

Table 3.2 Details of test specimen reinforced with 6mm reinforcement bars

Series	Fibre Content %/[kg/m^3]	Reinforcement number and diameter [mm]	Number of beams	Number of WST cubes	Number of Compression cubes
3	0.5/39.3	3ø6	3	9	6
4	0.25/19.6	3ø6	3	9	6
5	0.75/58.9	3ø6	3	9	6

A self-compacting concrete, with w/b-ratio 0.55, was used in the experiments. For more information see Gustafsson and Karlsson (2006).

3.1.1 Compressive strength

In each series a total of 6 compression cubes have been tested in order to determine the compressive strength. The strength achieved for the concrete with only conventional reinforcing bars was 47 MPa while it varied between 36 MPa and 40

MPa for the fibre reinforced concrete, see Table 3.3. For equivalent cylindrical compression strength used in design, the cube strength is multiplied by a factor 0.8 derived from FIB model code 2010, Table 7.2-1 with both the strengths given and where, the cylinder strengths, f_{ck} are 80% of the cube strengths, $f_{ck,cube}$.

Table 3.3 Average values of cube compression strength and equivalent cylinder compression strength from the tests on beams with 8mm reinforcement bars.

Series	Reinforcement bars [mm]	Fibre content [%]	Compression cube strength [MPa]	Equivalent cylinder strength [MPa]
1	3ø8	0	47.0	37.6
2	3ø8	0.5	38.2	30.6

Table 3.4 Average values of cube compression strength and equivalent cylinder compression strength from the tests on beams with 6mm reinforcement bars.

Series	Reinforcement bars [mm]	Fibre content [%]	Compression cube strength [MPa]	Equivalent cylinder strength [MPa]
4	3ø6	0.25	39.2	31.4
3	3ø6	0.5	37.7	30.2
5	3ø6	0.75	36.8	29.4

From the test results in Table 3.3 and Table 3.4, it is noted that fibres had a negative impact on the compression strength, as it was reduced with higher fibre content. It should however be mentioned, that the concrete composition had little variation.

3.1.2 Tensile behaviour

Nine wedge splitting tests (WST), on small cubes with a volume of 0.1x0.1x0.1 m^3, were conducted for each series to determine the toughness of the steel fibres. For more details, also see Gustafsson and Karlsson (2006).

According to Löfgren (2005), it is necessary to consider fibre orientation and the number of fibres crossing a crack section. This is normally done by defining a fibre efficiency factor, η_b, see equation (3.1).

$$\eta_b = \frac{A_f}{V_f} N_b \tag{3.1}$$

where

A_f is the area of the fibre cross section

V_f is the fibre volume fraction

N_b is the number of fibres per unit area

The fibre efficiency factor obtained from the wedge splitting tests used in this report varied, according to Gustafsson and Karlsson (2006), between 0.49 and 0.56. The fibre efficiency factor for the beams was also calculated theoretically, according to Dupont and Vandewalle (2005), and the value obtained by Gustafsson and Karlsson was equal to 0.54. According to Löfgren (2005), experiments have shown that it is reasonable to assume a linear relationship between number of fibres and fibre bridging stresses as seen in equation (3.2).

$$\sigma_{b,beam} = \sigma_{b,exp} \frac{\eta_{b,beam}}{\eta_{b,exp}} \quad (3.2)$$

where

$\sigma_{b,beam}$ is the bridging stress applicable for the beam elements

$\sigma_{b,exp}$ is the experimental bridging stress from the wedge splitting tests

$\eta_{b,beam}$ is the fibre efficiency factor for beam elements

$\eta_{b,exp}$ is the fibre efficiency factor obtained from the wedge splitting tests

This method was used to transform the fibre bridging stresses obtained in the WSTs to beam stresses.

3.1.3 Conventional reinforcement

The reinforcement used in the beams consisted of 6mm and 8mm diameter bars. The measured yield stress and ultimate stress capacities are shown in Table 3.5.

Table 3.5 Yield and ultimate stress capacities from tests on reinforcing bars done by Gustafsson and Karlsson (2006)

Reinforcement Bars	Yield Stress Capacity, f_{sy} [MPa]	Ultimate Stress Capacity, f_{su} [MPa]
6 mm	660	784
8 mm	590	746

3.1.4 Results

Four point bending tests were performed on series of simply supported beams with loading conditions and dimensions as shown in Figure 3.1. The tests were performed using load control.

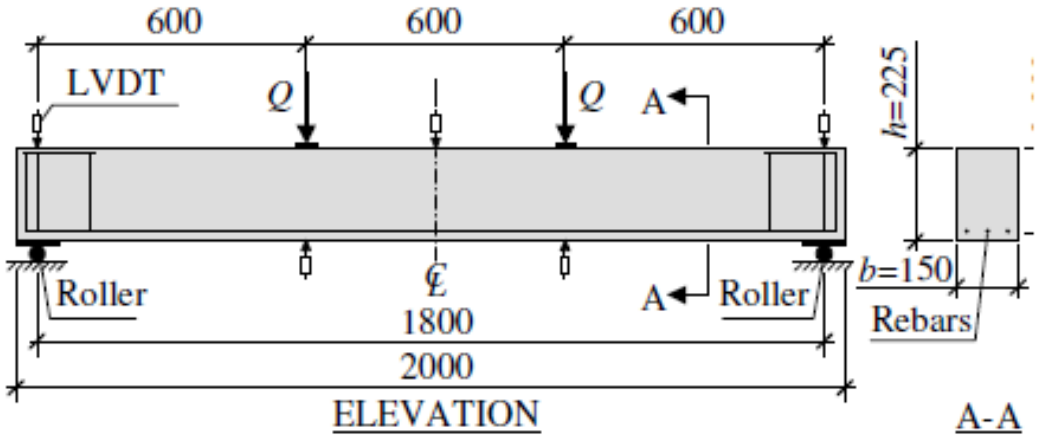

Figure 3.1 Dimensions and loading conditions for the beam tests, from Jansson (2008)

From the test results, values of loads, deflections at mid-span, support settlements and crack widths were obtained. More details in Gustafsson and Karlsson (2006). The results from the three beams in each series were presented as average moment-curvature curves and are shown in the Figure 3.2 and Figure 3.3.

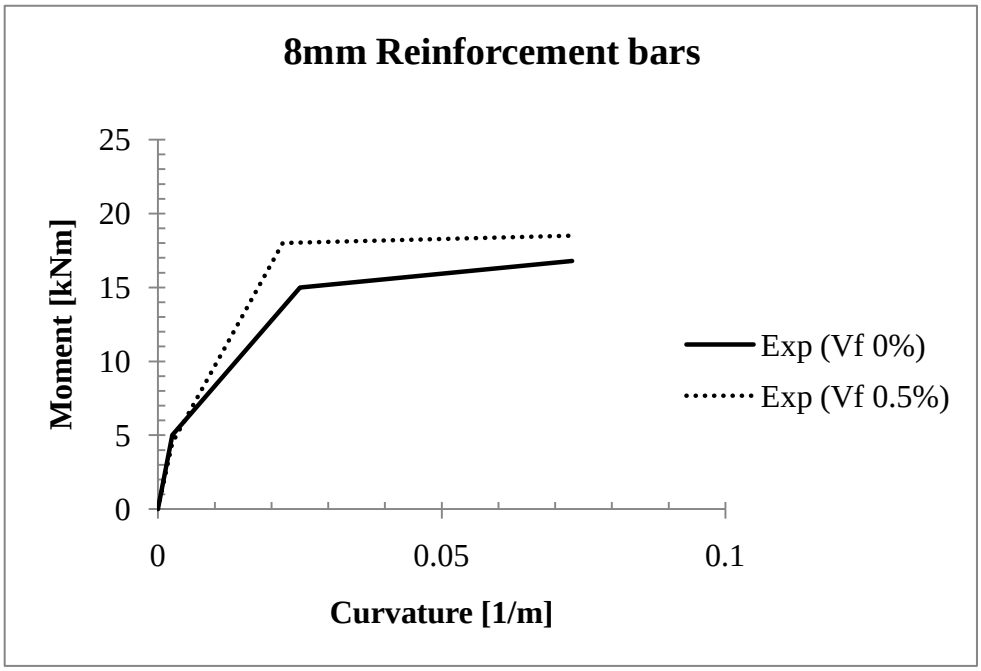

Figure 3.2 Moment versus curvature diagrams from the beam tests with reinforcement bar ø8 mm

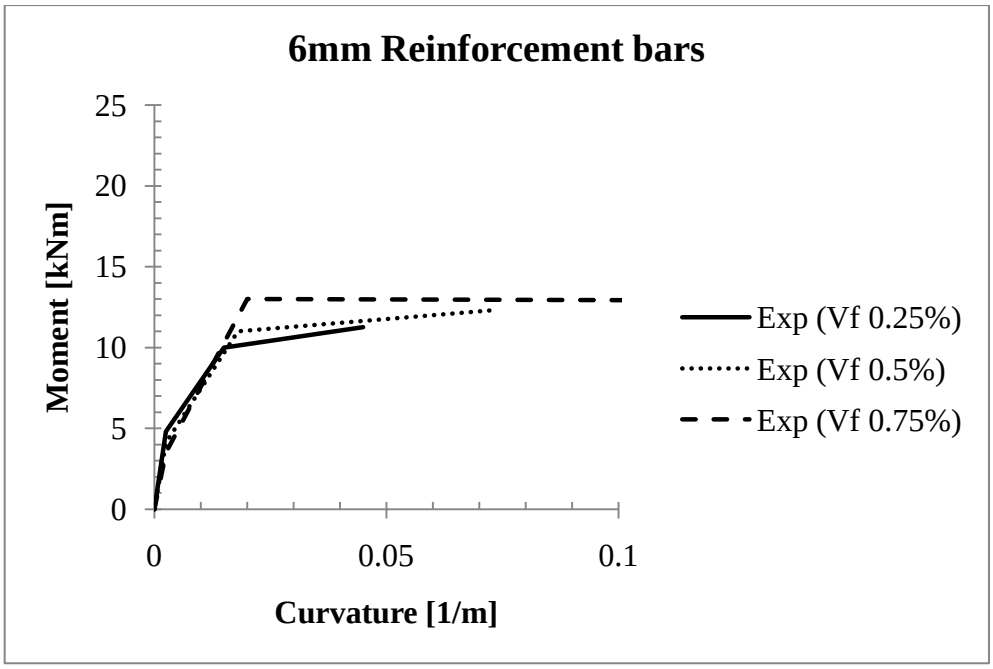

Figure 3.3 Moment versus curvature diagrams from the beam tests with reinforcement bar ø6 mm

Table 3.6 Ultimate moment capacities from experiments, for beam series with 8 mm reinforcement bars

Series	V_f (%)	Reinforcement	Moment Capacity (kNm)	Increase of capacity due to addition of fibres (%)
1	0	3ø8	16.8	-
2	0.5	3ø8	18.9	12.5

Table 3.7 Ultimate moment capacities from experiments, for beam series with 6 mm reinforcement bars

Series	V_f (%)	Reinforcement	Moment Capacity (kNm)	Increase of capacity due to varying fibre volume (%)
4	0.25	3ø6	11.3	-
3	0.50	3ø6	12.3	8.8
5	0.75	3ø6	12.8	13.3

3.2 Design according to FIB model code

FIB (fédération Internationale du béton) is an international federation for structural concrete which was formed when the Euro-International concrete committee (CEB) and the International federation for pre-stressing (FIP) were joined together, see FIB bulletin 1, volume 1.

According to FIB model code, bulletin 56, volume 2, the following assumptions, when determining the ultimate limit moment resistance of reinforced or prestressed concrete sections are made;

- Plane sections remain plane
- The strain in bonded reinforcement or bonded prestressing tendons, whether in tension or in compression, is the same as that in the surrounding concrete
- The tensile strength of the concrete is ignored
- The stresses in the concrete are derived from stress-strain relations for the design of cross-sections.
- The stresses in the reinforcing and prestressing steel are derived from design curves given in subclause 7.2.3.2 and 7.2.3.3 in the FIB model code.
- The initial strain in the prestressing tendons is taken into account when assessing the stresses in the tendons.

When designing fibre reinforced concrete sections, all points above are valid except point three, where the concrete tensile strength is ignored.

Equation (3.3) to equation (3.6), taken from FIB model code, were used to derive the concrete tensile stresses, f_{ctm}, and modulus of elasticity, E_{cm}, with all the stresses in MPa

$$f_{cm} = f_{ck} + 8 \tag{3.3}$$

$$f_{ctm} = 0.30 f_{ck}^{2/3} \tag{3.4}$$

With f_{ck} being the cylindrical compressive fibre reinforced concrete strength.

$$E_{cm} = \left(\frac{f_{cm}}{10}\right)^{0.3} \tag{3.5}$$

$$\varepsilon_{cu} = 3.5 \times 10^{-3} \tag{3.6}$$

It should however, be noted that equation (3.5) is incomplete, as the mean concrete modulus of elasticity,E_{cm}, cannot be smaller than the mean compressive strength. So equation (3.7), given by RILEM TC-162-TDF (2003), was used.

$$E_{cm} = 9500(f_{fcm})^{\frac{1}{3}} \tag{3.7}$$

3.2.1 Residual flexural tensile strength

According to FIB model code, the strength of fibres is measured as a residual flexural tensile strength, $f_{R,j}$. This can be done by performing crack mouth opening displacement (CMOD) tests. A CMOD test is a deformation controlled loading test, where the crack opening is measured as a horizontal deflection. The test setup requires a beam, notched to prevent horizontal cracking, and devices for recording the

applied load and the crack opening, which is referred to as CMOD. The FIB model code proposes that it is to be done in accordance with EN 14651 (2005). The CMOD, for the experimental data used in this report, was however from the wedge splitting tests which are basically the same tests but performed on small cubes, for more details see Gustafsson and Karlsson (2006), see also Jansson (2008).

$$f_{R,j} = 3\frac{F_j l}{2bh_{sp}^2} \quad \text{(MPa)} \tag{3.8}$$

where

$f_{R,j}$ is the residual flexural tensile strength corresponding to $CMOD_j$, with [j=1,2,3,4]

F_j is the load corresponding to $CMOD_j$

$CMOD_j$ is the crack mouth opening displacement

l is the span of the specimen

b is the width of the specimen

h_{sp} is the distance between the notch tip and the top of the specimen

The values f_{R1} and f_{R3} are obtained from the corresponding F_{R1}- $CMOD_1$ and F_{R3}- $CMOD_3$ values as shown in Figure 3.4.

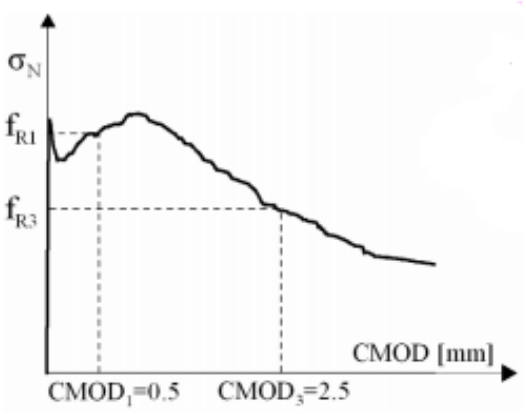

Figure 3.4 An example of typical results from a bending test with a softening material behaviour. From FIB model code, bulletin 55, vol. 1

The FIB model code simplifies the real response in tension, as shown in Figure (3.4), into two stress-crack opening constitutive laws, a linear post crack softening or hardening behaviour, see Figure (3.5), and a plastic rigid behaviour, see Figure (3.6).

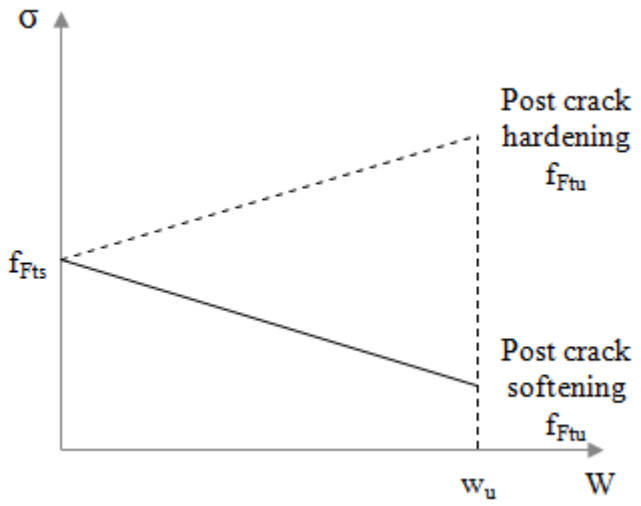

Figure 3.5 Simplified post-crack constitutive laws; linear post cracking stress-crack opening. From FIB model code, bulletin 55, vol. 1

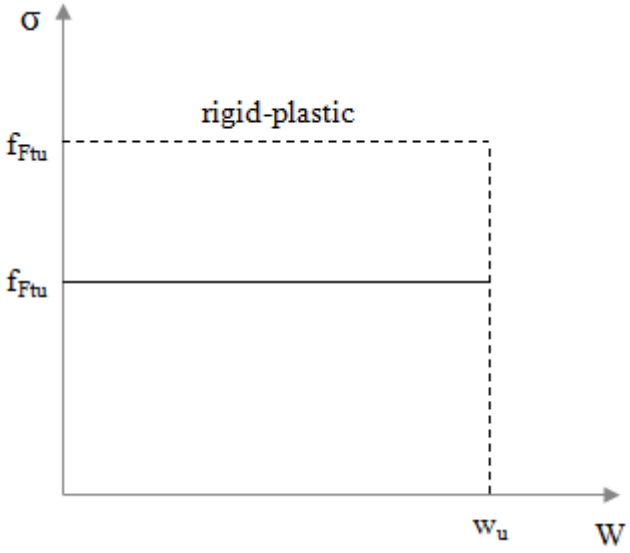

Figure 3.6 Simplified post-crack constitutive laws; plastic-rigid behaviour. From FIB model code, bulletin 55, vol. 1

Two reference values are introduced, f_{Fts} representing the serviceability residual strength and f_{Ftu} representing the ultimate residual strength. See equation (3.9) and equation (3.10). No partial safety factors were used, due to comparison with experiments.

$$f_{Fts} = 0.45 f_{R1} \quad (3.9)$$

where

f_{Fts} is the serviceability residual strength

f_{R1} is the residual flexural tensile strength corresponding to $CMOD_1$

$$f_{Ftu} = f_{Fts} - \frac{w_u}{CMOD_3}(f_{Fts} - 0.5 f_{R3} + 0.2 f_{R1}) \geq 0 \quad (3.10)$$

where

f_{Ftu} is the ultimate residual strength

w_u is the ultimate crack opening accepted in structural design, see equation (3.11)

f_{R3} is the residual flexural tensile strength corresponding to $CMOD_3$

$CMOD_1$ is the crack mouth opening displacement and is equal to 0.5mm

$CMOD_3$ is the crack mouth opening displacement and is equal to 2.5mm

Equation (3.10) gives the values of f_{Ftu} where, $w_u \neq CMOD_3$. Using a linear constitutive law between $CMOD_1$ corresponding to serviceability limit state and $CMOD_3$ corresponding to the crack opening of 2.5mm, any value up to w_u can be obtained, see Figure (3.7). The crack width, w_u, is the maximum crack opening accepted in structural design, where it's value depends on the required ductility, and therefore should not exceed 2.5mm, according to the FIB model code. w_u is calculated as equation (3.11).

$$w_u = \varepsilon_{Fu} l_{cs} \tag{3.11}$$

where

ε_{Fu} is assumed to be equal to 2% for variable strain distribution in cross section and 1% for only tensile strain distribution along the cross section

l_{cs} is the structural characteristic length, calculated in equation (3.12).

$$l_{cs} = min\{s_{rm}, y\} \tag{3.12}$$

where

s_{rm} is the mean crack spacing

y is the distance between the neutral axis and the tensile side of the cross section

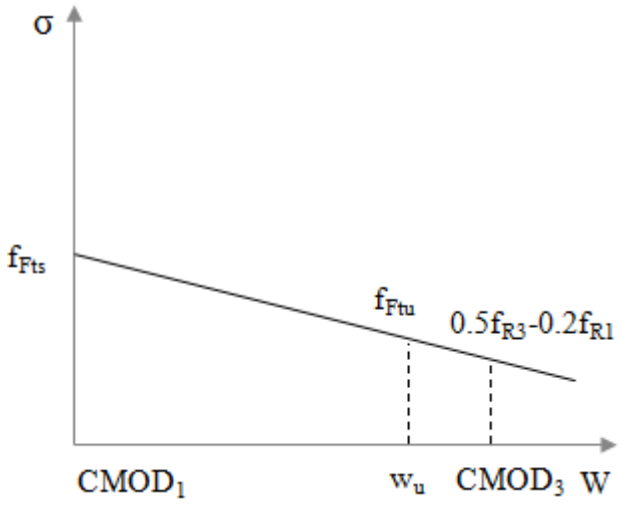

Figure 3.7 Simplified linear post-cracking constitutive law. From FIB model code, bulletin 55, vol.1

The requirements in equation (3.13) and equation (3.14) need to be fulfilled, according to FIB model code, if fibre reinforcement is to partially or entirely substitute the ordinary reinforcement in ultimate limit state.

$$f_{R1k}/f_{Lk} > 0.4 \quad (3.13)$$

$$f_{R3k}/f_{R1k} > 0.5 \quad (3.14)$$

where

f_{Lk} is the limit of proportionality

f_{R1k} is the flexural tensile strength corresponding to $CMOD_1$

f_{R3k} is the flexural tensile strength corresponding to $CMOD_3$

3.2.2 Moment resistance

The residual flexural tensile strength of the fibres is added as a stress block as seen in Figure 3.8. For bending moment and axial force in the ultimate limit state, a simplified stress/strain relationship is given by the FIB model code. The simplified stress distributions can be seen in Figure 3.8 where the linear post cracking stress distribution is to the left and the rigid plastic stress distribution is to the right, with η = 1 and λ = 0.8 for concrete with compressive strength below or equal to 50MPa. However, it should be noticed that the safety factor, γ_F, has been removed for the reason that, the moment resistance is compared with experimental results. The linear stress distribution to the left was used for design in this report, see Appendix D for application.

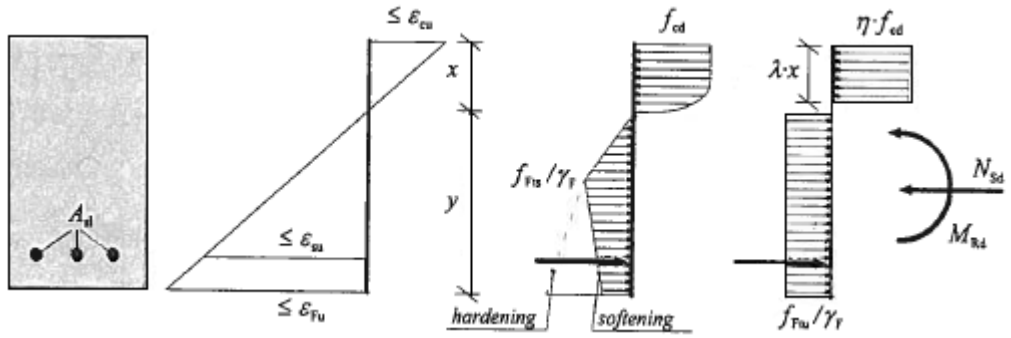

Figure 3.8 Simplified stress/strain relationship including the residual flexural tensile strength of fibres, from FIB model code, bulletin 56

Moments at cracking, yielding and ultimate stage were calculated for all beam series using the FIB model code. The flexural cracking moment for all the series was calculated as:

$$M_{cr} = W_1 f_{ctm} \quad (3.15)$$

where

M_{cr} is the cracking moment resistance

f_{ctm} is the mean tensile strength of the concrete mix

W_1 is the sectional modulus calculated as equation (3.16)

$$W_1 = \frac{bh^2}{6} \tag{3.16}$$

With b being the width of the cross section, and h the height of the cross section

The moments at yielding and ultimate stage were calculated using the simplified stress-strain relationship, in accordance with FIB model code, see Figure 3.8.

The yield moment was calculated using the linear post cracking constitutive law, see stress distribution to the left in Figure 3.8. The total contribution of fibres to the moment resistance was referred to as f_{Ft} and used in calculations, see Appendix D for details.

$$M_{Rd} = f_{sy}A_s(d - \beta x) + f_{Ft}(h - x)b[\beta x + x_{tot}y] \tag{3.17}$$

where

f_{sy} is the yield strength of the ordinary reinforcement

β is the distance from the top of the beam to the center of the concrete compressive zone

A_s is the area of the ordinary reinforcement bars

d is the effective depth

f_{Ft} is the total stress of the tensile stress block from the fibre contribution

h is the height of the beam

x is the distance from top of the beam to the neutral axis

x_{tot} is the centre of gravity for the tensile zone of fibre stress, given as a percentage of the total height

y is the height of the tensile stress block

The ultimate moment resistance was also calculated using the simplified linear post-cracking stress distribution in Figure 3.8.

$$M_{Rdu} = f_{sy}A_s(d - \beta x) + f_{Ft}(h - x)b[\beta x + x_{tot}y] \tag{3.18}$$

For the definition of the variables, see equation (3.17).

The corresponding curvatures were calculated according to equation (3.19) to equation (3.23).

$$k_{cr} = \frac{\varepsilon_r}{h/_2} \tag{3.19}$$

where,

k_{cr} is the curvature at cracking

ε_r is the elastic strain in the concrete calculated as equation (3.20)

$$\varepsilon_r = \frac{f_{ctm}}{E_{cm}} \tag{3.20}$$

$$k_y = \frac{\varepsilon_{c2}}{x} \tag{3.21}$$

where

k_y is the curvature at yielding

ε_{c2} is the strain in the concrete when the ordinary reinforcement reaches yielding and calculated as equation (3.22)

$$\varepsilon_{c2} = \frac{\varepsilon_{sy}}{\left(\frac{d-x}{x}\right)} \quad (3.22)$$

where

ε_{sy} is the yield strain of the ordinary reinforcement

$$k_u = \frac{\varepsilon_{cu}}{x} \quad (3.23)$$

with,

k_u is the ultimate curvature

ε_{cu} is the ultimate strain in the concrete equal to 3.5×10^{-3}

The moment-curvature relationships for the different beam series obtained when designed using the FIB model code are given in Figure 3.9 for beams with 8mm ordinary reinforcement bars and in Figure 3.10 for beams with 6mm ordinary reinforcement bars. In both Figure 3.9 and Figure 3.10, it can be seen that the moment resistance slightly increases with increased fibre volume; it is however, evident from these figures that, the moment resistance does not significantly increase with the addition of fibres.

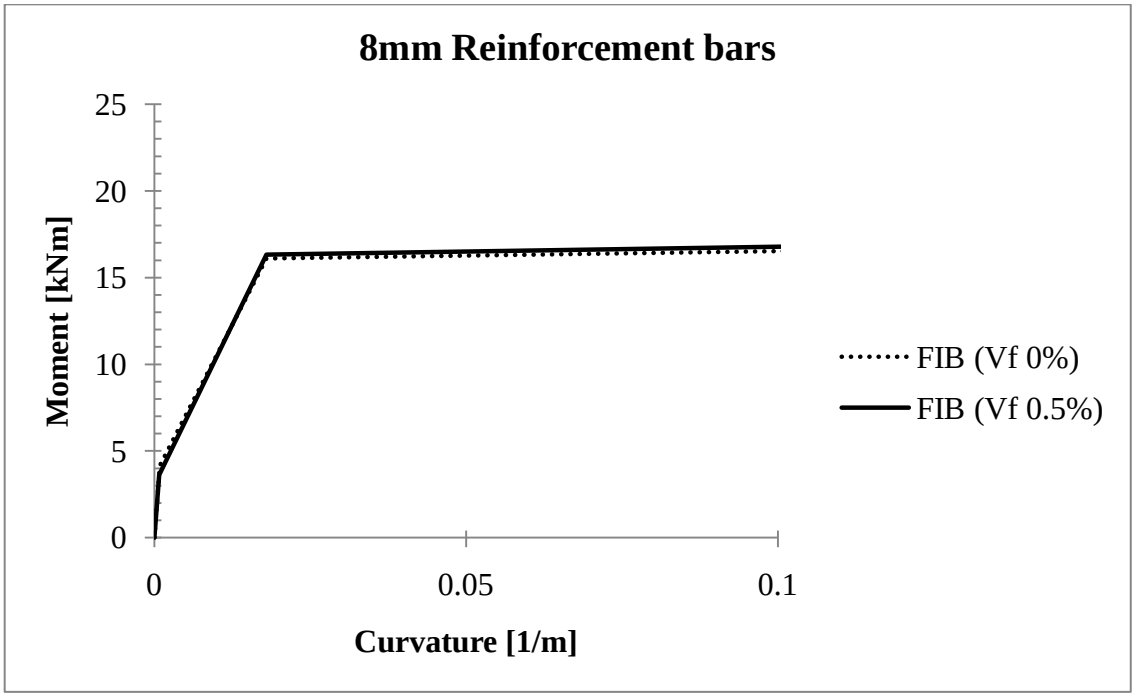

Figure 3.9 Moment versus curvature diagrams for beams with reinforcement bar ø8 mm, designed according to FIB model code

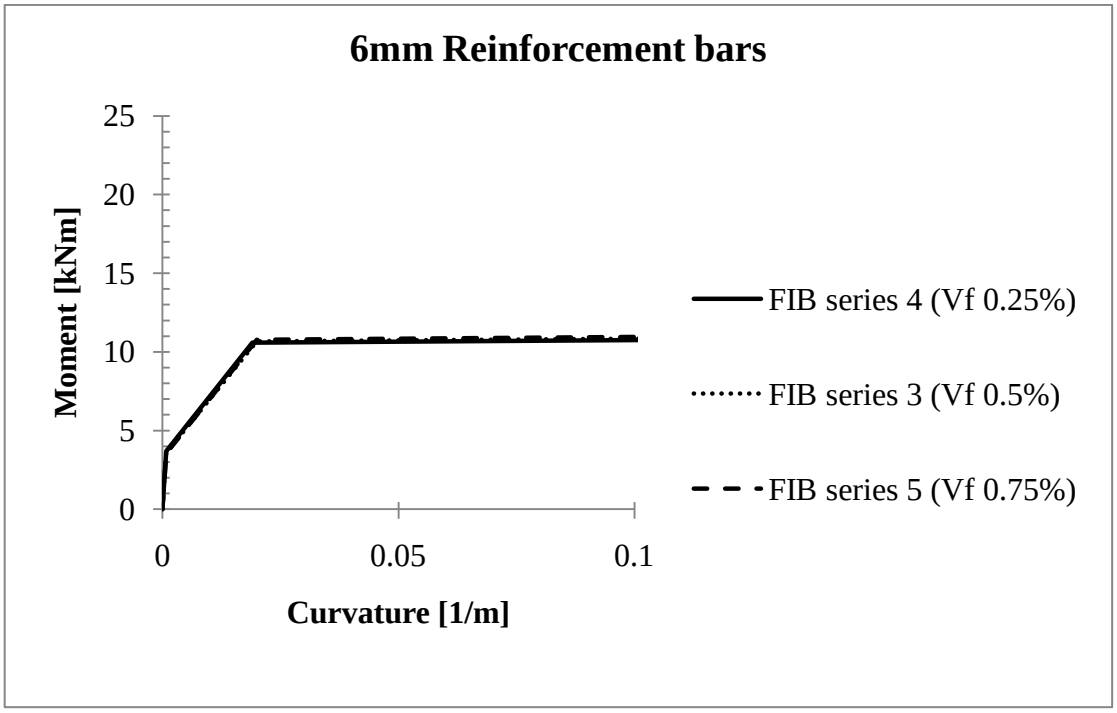

Figure 3.10 Moment versus curvature diagrams for beams with reinforcement bar ø6 mm, designed according to FIB model code

In Table 3.8, it can be seen that addition of 0.5% fibre volume in a beam reinforced with 8mm diameter ordinary reinforcement bars increases the moment capacity by 0.6%.

Table 3.8 Moment capacities for beam series with 8 mm reinforcement bars, designed according to FIB model code.

Series	V_f (%)	Reinforcement	Moment Capacity (kNm)	Increase of capacity due to addition of fibres (%)
1	0	3ø8	16.9	-
2	0.5	3ø8	17.0	0.6

Decreasing the diameter of ordinary reinforcement bars from 8mm to 6mm significantly reduces the moment resistance. This reduction can however be complemented by addition of sufficient amount of fibres. Table 3.9 shows how the moment capacity increases with variation of fibre volume from 0.25% to 0.75%. Here it is clear that much more fibre fractions are needed in order to compensate for this reduction.

For beams reinforced with 6mm diameter reinforcement bars, no reference beam without fibres was tested, but it can still be noted that increase in fibre volume increases the moment capacity.

Table 3.9 Moment capacities for beam series with 6 mm reinforcement bars, designed according to FIB model code.

Series	V_f (%)	Reinforcement	Moment Capacity (kNm)	Increase of capacity due to varying fibre volume (%)
4	0.25	3ø6	11.0	-
3	0.50	3ø6	11.1	0.9
5	0.75	3ø6	11.2	1.8

When designing fibre reinforced concrete beams without the presence of ordinary reinforcement, the FIB model code proposes that the same stress strain relationship in section 3.2.2 applies, excluding the contribution of the steel reinforcement. The equation for moment resistance for beams without ordinary reinforcement can be seen in equation (3.24).

$$M_{Rdu} = f_{Ftm}(h - x)b[\beta x + x_{tot}y] \quad (3.24)$$

For definitions of variables, see equation (3.17).

The results of the ultimate moment capacities from design of beams without ordinary reinforcement, designed using the FIB model code, are presented in Table 3.10. The results revealed that the moment capacity increased with increasing fibre volumes, the results however showed very low moment capacities for the chosen fibre fractions.

Table 3.10 Ultimate moment resistances for beams without ordinary reinforcement bars designed according to FIB model code

Series	Fibre Volume (%)	$M_{ultimate}$ (kNm)	Percentage increase (%)
4	0.25	0.29	-
3	0.5	0.43	48
5	0.75	0.60	107

When designing in ultimate limit state, ductility requirements need to be fulfilled. FIB takes this into account by implying that ductility requirements are fulfilled when the need for minimum ordinary reinforcement amount is satisfied. The minimum reinforcement is calculated as equation (3.25).

$$A_{s,min} = k_c k (f_{ctm} - f_{Ftsm}) \frac{A_{ct}}{\sigma_s} \quad (3.25)$$

where

f_{ctm} is the mean concrete tensile strength

f_{Ftsm} is the residual tensile strength of fibre reinforced concrete

A_{ct} is the tensile part of the concrete cross section

σ_s is the maximum tensile reinforcement at cracking stage

k_c is the coefficient taking into account the stress distribution in the cross section just before cracking and the change of inner lever arm

k is the coefficient taking into account non-uniform self-equilibrating stresses leading to reduction of cracking force

Table 3.11 illustrates that the ductility requirements were fulfilled as the steel reinforcement, A_s, was larger than the minimum required reinforcement, $A_{s,min}$.

Table 3.11 Results of the ductility requirements for beam series with 8 mm reinforcement bars, designed according to FIB model code

Series	Reinforcement	Fibre Volume (%)	A_s (mm^2)	$A_{s,min}$ (mm^2)	Ductility
2	3ø8	0.5	150.8	134.9	Fulfilled

For the beams with a smaller amount of reinforcement, the ductility requirements were not fulfilled for the used fibre content, see Table 3.12. Thus, less ordinary reinforcement can be compensated by adding more fibres. Table 3.12 illustrates that more than 0.75% fibre content is needed in order to fulfil the ductility requirements.

Table 3.12 Results of the ductility requirements for beam series with 6 mm reinforcement bars, designed according to FIB model code

Series	Reinforcement	Fibre Volume (%)	A_s (mm^2)	$A_{s,min}$ (mm^2)	Ductility
4	3ø6	0.25	84.8	131.0	Not Fulfilled
3	3ø6	0.5	84.8	123.7	Not Fulfilled
5	3ø6	0.75	84.8	117.4	Not Fulfilled

According to FIB model code, ductility requirements can be satisfied in fibre reinforced concrete structures without minimum ordinary reinforcement if one of the conditions in equations (3.26) and (3.27) are fulfilled.

$$\delta_u \geq 20\delta_{SLS} \quad (3.26)$$

$$\delta_{peak} \geq 5\delta_{SLS} \quad (3.27)$$

where

δ_u is the ultimate displacement

δ_{peak} is the displacement at the maximum load

δ_{SLS} is the displacement at service load computed by performing a linear elastic analysis with the assumptions of uncracked condition and initial elastic Young's modulus.

The values in equation (3.26) and equation (3.27) are obtained from experiments.

The ductility requirements were fulfilled for all the series, see Appendix D for details, but for beams without ordinary reinforcement, no experimental data on load-deformation conditions is available

The ductility requirements in equation (3.26) and equation (3.27) are valid for design of fibre reinforced concrete without ordinary reinforcement if ultimate load is higher than the cracking load.

3.2.3 Shear capacity

The shear capacity was also calculated for all the beam series, using the FIB model code. The total shear resistance is the sum of contributions from concrete as well as the shear reinforcement. However, in the present case, there was no shear reinforcement, thus the resistance was provided only by concrete.

$$V_{Rd} = V_{Rd,c} + V_{Rd,s} \quad (3.28)$$

where

$V_{Rd,s} = 0$ since there was no shear reinforcement

The shear resistance for the beam without fibres was calculated by using equation (3.29), in which,

$$V_{Rd,c} = k_v \frac{\sqrt{f_{ck,cyl}}}{\gamma_c} zb \quad (3.29)$$

where

γ_c is a partial safety factor for concrete, but was removed in this design due to the comparison with experiments

$z = 0.9d$ is the internal lever arm

$f_{ck,cyl}$ is the equivalent cylinder strength

k_v is the factor that takes into account the size factor

The shear resistance for the beam series with varying fibre contents reinforced with ordinary reinforcement bars and without shear reinforcement was calculated using the formula in equation (3.30), given by the FIB model code. The shear resistance was calculated by using the mean value of the tensile strength of concrete mix.

$$V_{Rd} = \left[\left(\frac{0.18}{\gamma_c}\right) k \left[100\rho_1 \left(1 + 7.5\frac{f_{Ftu}}{f_{ctm}}\right) f_{ck,cyl}\right]^{\frac{1}{3}} + 0.15\sigma_{cp}\right] bd \quad (3.30)$$

where

f_{Ftu} is the fibres ultimate residual tensile strength

$f_{ck,cyl}$ is the equivalent cylinder compressive strength for the corresponding series

f_{ctm} is the mean concrete tensile strength

σ_{cp} is the average stress acting on the concrete due to loading or prestressing

b is the width of the cross-section

d is the effective depth of the cross-section

γ_c is the partial safety factor for concrete without fibres which was not used in design due to comparison with experimental results

ρ_1 is the reinforcement ratio for ordinary reinforcement

k is a factor that takes size effect into account

The code also defines a minimum value for the shear resistance, which is given by equation (3.31):

$$V_{Rd,Fmin} = \left(v_{min} + 0.15\sigma_{cp}\right) bd \quad (3.31)$$

where

$$v_{min} = 0.035 k^{\frac{3}{2}} f_{ck,cyl}^{\frac{1}{2}} \quad (3.32)$$

For definitions of variables, see equation (3.30)

The shear resistance (V_d) is the maximum of the values V_{Rd} , $V_{Rd,Fmin}$ as given in equation (3.33):

$$V_d = \max\left(V_{Rd}, V_{Rd,Fmin}\right) \quad (3.33)$$

The results for the shear resistance of different beam series are given in the Table 3.13 and Table 3.14. From the results, it can be inferred that fibre volume does have an influence on the shear capacity of beams as it increases with increasing fibre volume.

Table 3.13 Shear resistance results for beam series with 8mm reinforcement bars, designed according to FIB model code.

Series	V_f (%)	Reinforcement	Shear resistance (kN)	Increase of capacity due to addition of fibres (%)
1	0	3ø8	24.8	-
2	0.5	3ø8	30.4	22.6

Table 3.14 Shear resistance results for beam series with 6mm reinforcement bars, designed according to FIB model code.

Series	V_f (%)	Reinforcement	Shear resistance (kN)	Increase of capacity due to varying fibre volume (%)
4	0.25	3ø6	24.4	-
3	0.50	3ø6	25.0	2.5
5	0.75	3ø6	25.9	6.1

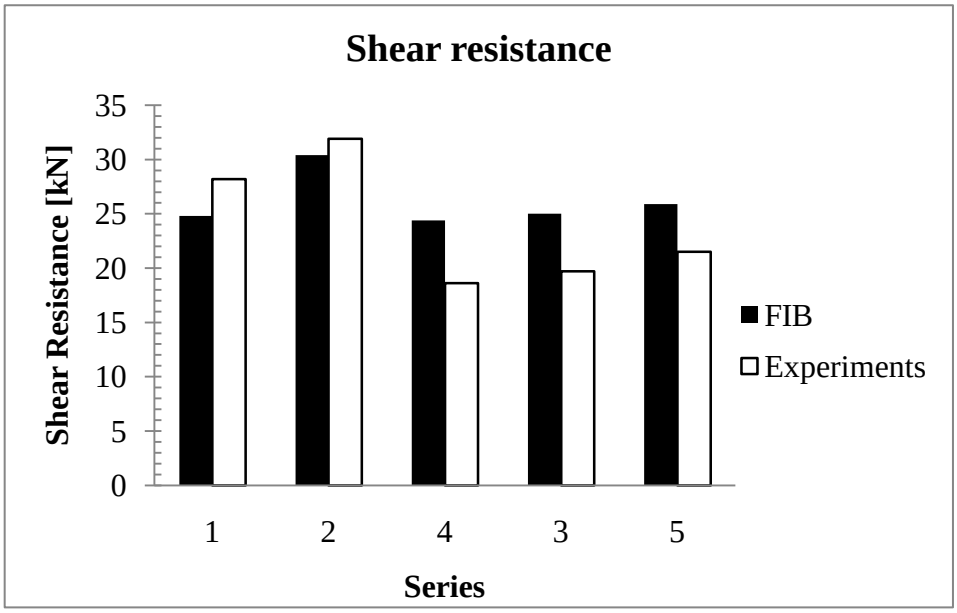

Figure 3.11 Shear resistance compared to experimental results for all beam series

It is not possible to evaluate shear resistance accuracy for the reason that the beams tested failed in bending and not in shear. Figure 3.11 shows that, the shear capacity for beam series 1 and 2, with 8mm ordinary reinforcement bars, is lower than the experimental shear load, and since shear was not the failure mode, the capacity is underestimated.

Regarding design of shear resistance in beams without ordinary- and shear reinforcement, the FIB model code suggests that the principal tensile stress, σ_1, shall not exceed the design value of the tensile strength given in equation (3.34). This is however, only valid for fibre reinforced concrete with tensile hardening behaviour. The beams designed in this report have a tensile softening behaviour and there is therefore no method for the designing of shear resistance in FRC with softening behaviour.

$$\sigma_1 = \frac{f_{Ftuk}}{\gamma_F} \quad (3.34)$$

where

f_{Ftuk} is the characteristic value of the ultimate residual tensile strength

γ_F is the partial safety factor for fibres

3.2.4 Crack width

Cracking occurs in concrete structures. This is however, not a problem in the serviceability limit state for the structural system itself other than the fact that it gives an unattractive appearance. Still, there is a need for controlling the crack widths in order to meet the requirements in the serviceability limit state. This can be done with the presence of:

- conventional reinforcement bars
- normal compressive forces e.g. compressive axial loading and/or pre-stressing

FIB model code suggests that for all stages of cracking, in members with ordinary reinforcement, the crack width,w_d, is calculated according to equation (3.35).

$$w_d = 2l_{s,max}(\varepsilon_{sm} - \varepsilon_{cm} - \varepsilon_{cs}) \quad (3.35)$$

where

ε_{sm} is the average steel strain over $l_{s,max}$

ε_{cm} is the average concrete strain over $l_{s,max}$

ε_{cs} is the concrete strain due to shrinkage

$l_{s,max}$ is the length over which slip between concrete and steel occurs, see equation (3.36)

$$l_{s,max} = \frac{1}{4}\frac{\emptyset_s}{\rho_s}\frac{f_{ctm}}{\tau_{bm}} \quad (3.36)$$

Adding equation (3.35) with equation (3.36), equation (3.37) is obtained.

$$w_d = \frac{1}{2}\frac{\emptyset_s}{\rho_{s,ef}}\frac{f_{ctm}}{\tau_{bm}}(\sigma_s - \beta\sigma_{sr} + \eta_r\varepsilon_r E_s)\frac{1}{E_s} \quad (3.37)$$

where

f_{ctm} is the mean concrete tensile strength

E_s is the modulus of elasticity of steel

σ_s is the actual steel stress

η_r is a factor which takes long term effects into account. For short term effects, this factor is equal to 0.

τ_{bm} is the mean bond strength between reinforcement bars and concrete

β is the empirical coefficient for assessing mean strain over $l_{s,max}$. $l_{s,max}$, is the length over which slip between concrete and steel occurs

ε_r is the strain at the onset of cracking

σ_{sr} is the maximum steel stress in the crack at crack formation stage, see equation (3.38)

$$\sigma_{sr} = \frac{f_{ctm}}{\rho_{s,ef}}(1 + \alpha_e \rho_s) \quad (3.38)$$

where

ρ_s is the steel reinforcement ratio

α_e is the modular ratio

$\rho_{s,ef}$ is the effective steel reinforcement ratio, see equation (3.39)

$$\rho_{s,ef} = \frac{A_s}{A_{c,ef}} \quad (3.39)$$

where

A_s is the steel reinforcement area

$A_{c,ef}$ is the effective area of concrete

The steel stress was calculated by carrying out state II analysis of the beam in cracked state. The crack width design formula in equation (3.40) has however, a small error which pertains to dividing the whole formula with the steel modulus of elasticity. Equation (3.35), for crack width calculations, contains strains while equation (3.40) contains stresses. This is missing in the crack width equation given by the FIB model code, bulletin 56, vol.2.

$$w_d = \frac{1}{2}\frac{\emptyset_s}{\rho_{s,ef}}\frac{f_{ctm}}{\tau_{bm}}(\sigma_s - \beta\sigma_{sr} + \eta_r \varepsilon_r E_s) \quad (3.40)$$

For definition of variables, see equation (3.37)

When considering design crack width, the effect of steel fibres in fibre reinforced concrete is similar to that of ordinary reinforced concrete. The steel fibre tensile strength,f_{Fts}, which is not equal to zero, is taken as constant all over the cracked section. The design crack widths for fibre reinforced concrete beams with ordinary reinforcement were calculated, according to FIB model code, using equation (3.41) and here it is clear that the stresses are divided with the steel modulus of elasticity, E_s.

$$w_d = \frac{1}{2}\frac{\emptyset_s}{\rho_{s,ef}}\frac{(f_{ctm} - f_{Fts})}{\tau_{bm}}(\sigma_s - \beta\sigma_{sr})\frac{1}{E_s} \quad (3.41)$$

where

f_{Fts}, is the serviceability residual strength for the corresponding series.

All other variables are defined in equation (3.35).

Stabilized cracking is reached when the moment is between cracking and yield moment. To make a fair comparison between the crack widths, a moment of 15kNm is used for series 1 and 2 and a moment of 10 kNm is used for series 3, 4 and 5. The results for crack widths calculated using this assumption, for different beam series are given in Table 3.15 and Table 3.16.

Table 3.15 Crack width results for beam series with 8mm reinforcement bars, designed according to FIB model code, calculated at a moment resistance of 15kNm.

Series	V_f (%)	Reinforcement	Crack width (mm)	Change due to addition of fibres (%)
1	0	3ø8	0.244	-
2	0.5	3ø8	0.264	8.2

Table 3.16 Crack width results for beam series with 6mm reinforcement bars, designed according to FIB model code, calculated at a moment resistance of 15kNm.

Series	V_f (%)	Reinforcement	Crack width (mm)	Change due to change of fibre volume (%)
4	0.25	3ø6	0.327	-
3	0.5	3ø6	0.322	-1.5
5	0.75	3ø6	0.314	-3.9

From the results in Table 3.15, it can be seen that an addition of 0.5% fibres did not result into a reduction, but to an increase of the crack width. The reason for this unexpected outcome, is due to the fact that the concrete tensile strength, f_{ctm}, was derived from the concrete compressive strength which was 47 MPa for series 1 and 37.6 MPa for series 2. It is therefore difficult to make a fair comparison. It can however be noted, in Table 3.16, that under comparable circumstances, fibres do have a positive impact on crack control as an increase of fibre volume decreases the crack width.

The FIB model code does not give any suggestions for the calculation of crack width for fibre reinforced concrete beams without ordinary reinforcement.

3.2.5 Comparison with experimental results

The moment resistance results were compared with the experimental results, for all the beam series, in order to identify the accuracy of the FIB model code.

Figure 3.12 and Figure 3.13 illustrate the comparison of the design results with experimental results and in all cases with fibres, it was noted that there was an underestimation of the moment resistance when designing according to FIB model code.

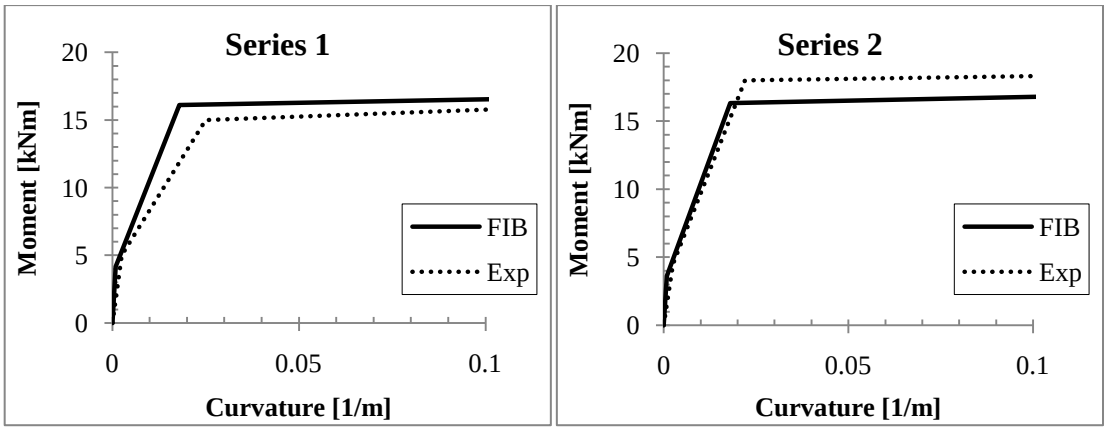

(a) *(b)*

Figure 3.12 Comparison of moment-curvature diagrams, according to FIB model code and the experimental results for (a) beams with V_f = 0 % and rebar ø8 mm, (b) beams with V_f = 0.5 % and rebar ø8 mm

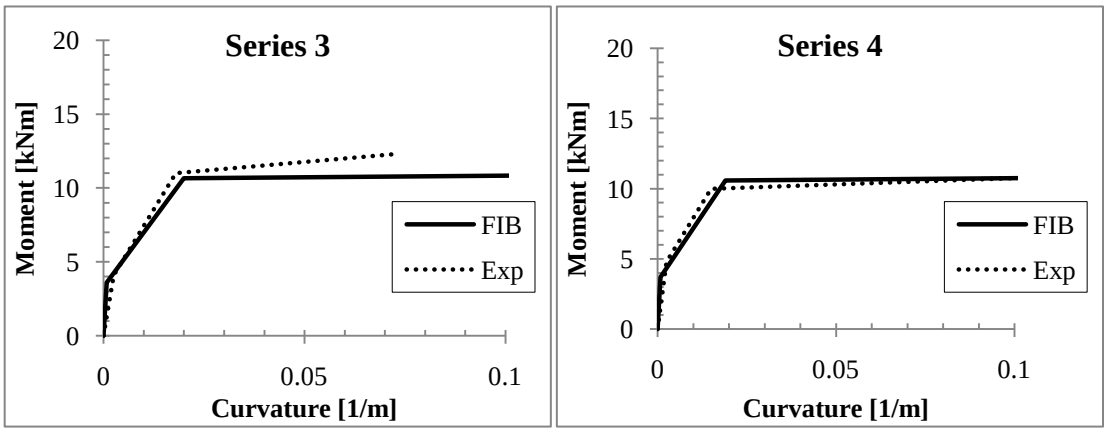

(a) *(b)*

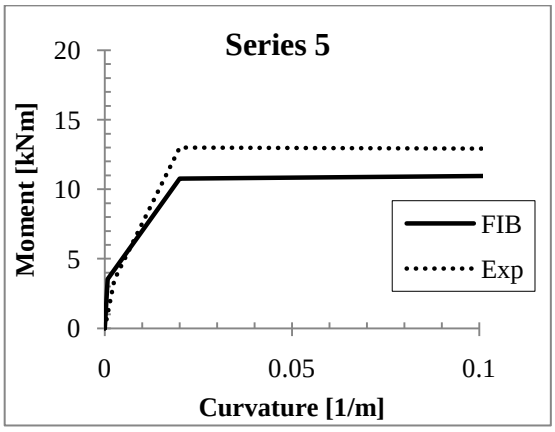

(c)

Figure 3.13 Comparison of moment-curvature diagrams, according to FIB model code and the experimental results for (a) beam with V_f = 0.5 % and rebar ø6 mm, (b) beam with V_f = 0.25 % and rebar ø6 mm, (c) beam with V_f = 0.75 % and rebar ø6 mm

The percentage over/under-estimation of the moment capacities for beams with 8 mm diameter ordinary reinforcement bars can be seen in Tables 3.17 and for beams with 6 mm diameter bars in Table 3.18. The maximum underestimation goes up to 12.5%.

Table 3.17 Comparison of moment capacity for beams with 8mm reinforcement bars

$M_{ultimate}$		
Series	1	2
V_f (%) and reinforcement	0 3Ø8mm	0.5 3Ø8mm
FIB	16.9	17.0
Experimental	16.8	18.9
Difference (%)	0.6	-9.0

Table 3.18 Comparison of moment capacity for beams with 6mm reinforcement bars

$M_{ultimate}$			
Series	4	3	5
V_f (%) and reinforcement	0.25 3Ø6mm	0.5 3Ø6mm	0.75 3Ø6mm
FIB	11.0	11.1	11.2
Experimental	11.3	12.3	12.8
Difference (%)	-2.6	-9.7	-12.5

3.2.6 Conclusions

The moment resistance obtained, when designing using the FIB model code, confirmed the experimental results that the moment resistance increases with increased amount of fibres. There were however, slight underestimations of the ultimate bending moment capacities for all beams with fibres, designed according to FIB model code. This underestimation might be due to the variation in material properties for the different samples as, three experimental results from the same concrete mix varied significantly, where the mean value was used for comparison. See Appendix C.

The shear resistance calculations using the FIB model code revealed that the shear resistance increases with addition and increasing amount of fibres. It is however, difficult to determine the accuracy of the code since the comparison with the experimental shear loads revealed a slight underestimation for the beam series with 8 mm ordinary reinforcement bars, as the beam experiments failed in flexure and not shear. The beam series with 6 mm reinforcement bars proved to be more accurate due to the fact that the shear resistance was higher than the experimental shear load.

Crack width calculations were carried out to see the effect of fibres and the results showed that addition of fibres decreases the crack width. The results also revealed that if there is a need for reduction of ordinary reinforcement, addition of a considerable amount of fibres could compensate this reduction.

3.3 Design of beams using RILEM

Rilem is an international committee of experts which aims at advancing the scientific knowledge in structures, systems and construction materials. Among their aims, Rilem is to assess scientific research data and publish their recommendations as guidelines.

In this section, all the beams series, designed according to RILEM TC-162-TDF (2003), are evaluated. The section also includes comparison with experimental results in section 3.1.4.

3.3.1 Flexural tensile strength

The flexural tensile strength is derived from the compressive strength obtained from the test results mentioned in section 3.1.1. RILEM TC-162-TDF (2003) recommends the following formulas for mean and characteristic flexural tensile strength of steel fibre reinforced concrete:

With compression strength known:

$$f_{fctm} = 0.3(f_{fck})^{\frac{2}{3}} \quad (3.42)$$

where

f_{fctm} is the mean tensile strength of the concrete
f_{fck} is the concrete cylindrical compressive strength

$$f_{fctk} = 0.7 f_{fctm} \quad (3.43)$$

with f_{fctk} being the characteristic value of the tensile strength

With flexural tensile strength known:

$$f_{fct} = 0.6 f_{fct,fl} \quad (3.44)$$

with $f_{fct,fl}$ being the flexural tensile strength

$$f_{fctk,fl} = 0.7 f_{fctm,fl} \quad (3.45)$$

with $f_{fctm,fl}$ being the mean flexural tensile strength.

Since the experimental data, considered in this report, was obtained from tests on compression cubes, the compressive strength is known and therefore, equation (3.42) and equation (3.43) are used.

3.3.2 Residual flexural tensile strength

RILEM TC-162-TDF (2003) also refers to crack mouth opening displacement (CMOD) for determining the residual tensile strength in equation (3.46), where the residual tensile strengths, f_{R1} and f_{R4} are determined following $CMOD_1$ and $CMOD_4$ respectively, for $CMOD$ values see Figure 3.14.

$$f_{R,i} = 3\frac{F_{R,i}L}{2bh_{sp}^2} \qquad (3.46)$$

where

$f_{R,i}$ is the residual flexural tensile strength corresponding to $CMOD_i$, with [i=1,2,3,4]

$F_{R,i}$ is the load corresponding to $CMOD_i$

$CMOD_i$ is the crack mouth opening displacement

l is the span of the specimen

b is the width of the specimen

h_{sp} is the distance between the notch tip and the top of the specimen

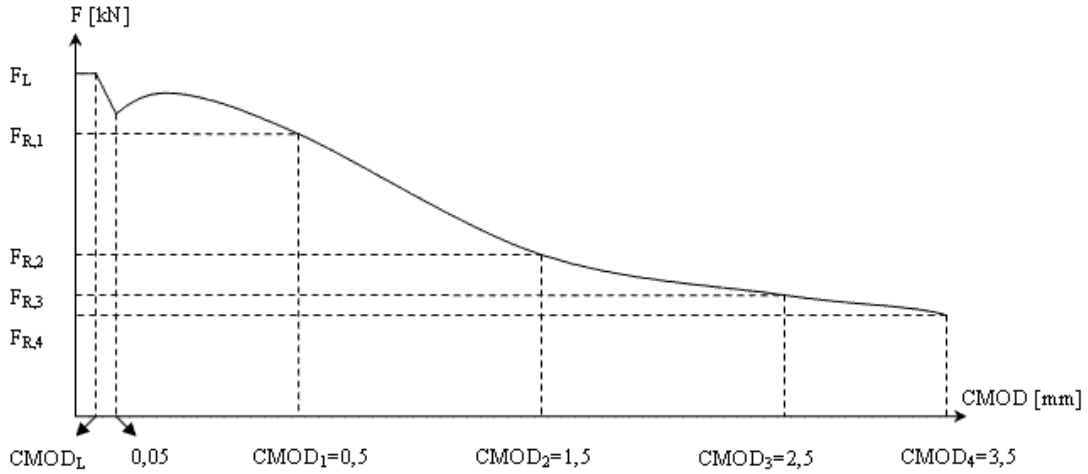

Figure 3.14 Load–CMOD diagram used to obtain the residual flexural tensile strength, from RILEM TC-162-TDF (2003)

In order to design in ultimate limit state, regarding bending and axial force, RILEM TC-162-TDF (2003) makes the following assumptions:

- Plane sections remain plane

- The stresses in the steel fibre reinforced concrete in tension as well as in concrete are derived from the stress strain diagram shown in Figure 3.15
- The stresses in the reinforcement bars are derived from an idealized bi-linear stress strain diagram
- For cross sections subjected to pure axial compression, the compressive strain in the steel fibre reinforced concrete is limited to $-2x10^{-3}$. For cross sections not fully in compression, the limiting compressive strain is taken as $-3.5x10^{-3}$. In intermediate situations, the strain diagram is defined by assuming that the strain is $-2x10^{-3}$ at a level of $\frac{3}{7}$ of the height of the compressed zone, measured from the most compressed face.
- For steel fibre reinforced concrete which is additionally reinforced with bars, the strain is limited to $25x10^{-3}$ at the position of the reinforcement, see Figure 3.17
- To ensure enough anchorage capacity for the steel fibres, the maximum deformation in the ultimate limit state is restricted to 3.5mm. If crack width larger than 3.5mm are used, the residual flexural tensile strength corresponding to that crack width and measured during the bending test has to be used to calculate σ_3

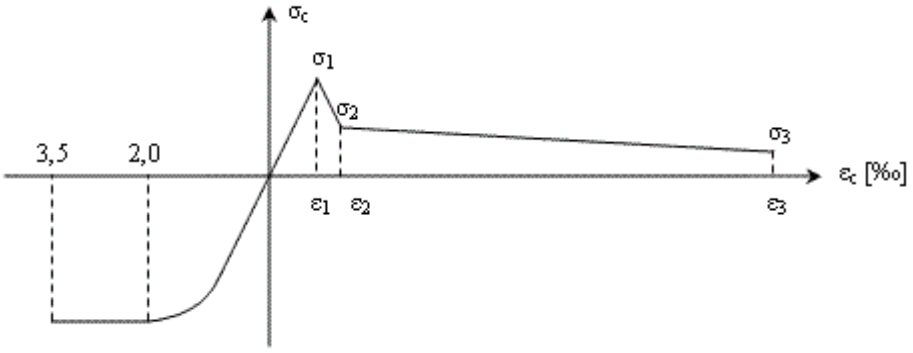

Figure 3.15 Stress strain diagram for fibre contribution, from RILEM TC-162-TDF (2003)

The values in Figure 3.15 are, according to RILEM TC-162-TDF (2003), calculated by the following formulas:

$$\sigma_1 = 0.7 f_{fctm,fl}(1.6 - d) \quad (3.47)$$

where

d is the effective depth in meters
$f_{fctm,fl}$ is the mean concrete flexural tensile strength

$$\sigma_2 = 0.45 f_{R1} k_h \quad (3.48)$$

where

k_h is the size factor
f_{R1} is the residual flexural tensile strength at $CMOD_1$

$$\sigma_3 = 0.37 f_{R4} k_h \quad (3.49)$$

where,

f_{R4} is the residual flexural tensile strength at $CMOD_4$

$$E_c = 9500(f_{fcm})^{\frac{1}{3}} \quad (3.50)$$

where

E_c is the concrete modulus of elasticity
f_{fcm} is the mean concrete compressive strength

$$\varepsilon_1 = \frac{\sigma_1}{E_c} \quad (3.51)$$

$$\varepsilon_2 = \varepsilon_1 + 0.1‰ \quad (3.52)$$

$$\varepsilon_3 = 25‰$$

$$k_h = 1.0 - 0.6\,\frac{h[cm]-12.5}{47.5} \quad [12.5 \leq h \leq 60\ [cm]]\text{ , Figure 3.16} \quad (3.53)$$

with h being the height of the beam in cm

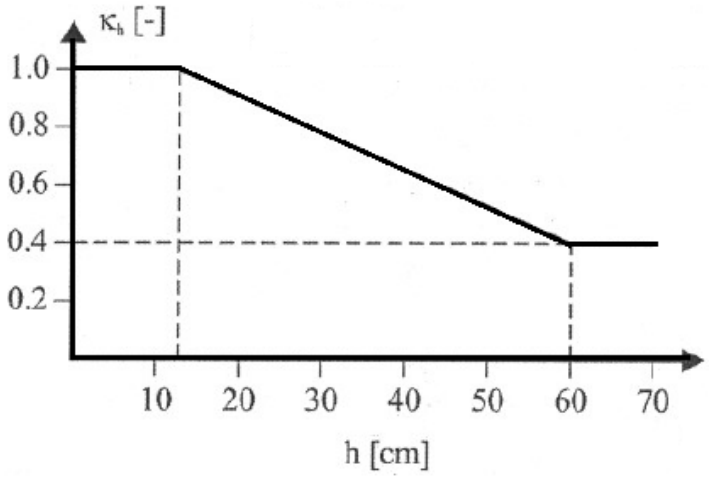

Figure 3.16 Range of the size factor,k_h, from RILEM TC-162-TDF (2003)

The size factor, k_h, in equation (3.53) and Figure 3.16 is used in RILEM TC-162-TDF (2003) to compensate the overestimation in the load carrying capacity which was detected when the design results were compared to experimental tests. According to RILEM TC-162-TDF (2003), the origin of the need for this size factor requires further studies. The design guideline points out that it might be due to variation of the material properties in different samples. It could also be built in the method used or both.

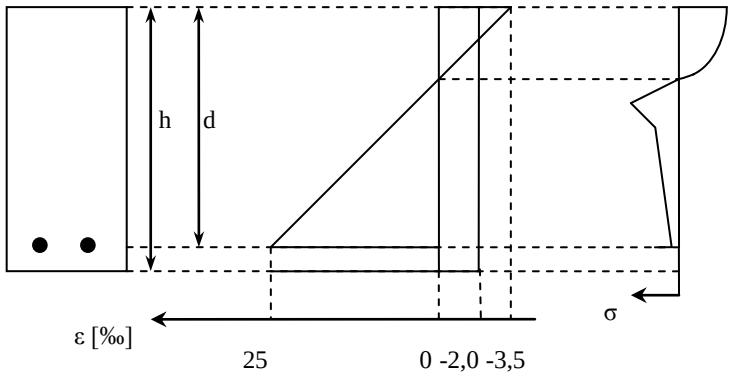

Figure 3.17 Stress strain distribution, from RILEM TC-162-TDF (2003)

3.3.3 Moment resistance

Moments at cracking, yielding and ultimate stage were as well calculated for all beam series using RILEM TC-162-TDF (2003), see Appendix E for application. Here, the flexural cracking moment, M_f, for all the series was calculated as:

$$M_{cr} = W_1 \sigma_1 \tag{3.54}$$

where

W_1 is the sectional modulus, see equation (3.55)

$$W_1 = \frac{bh^2}{6} \tag{3.55}$$

σ_1 is the cracking stress

For the beam without fibres, the moment at yielding and at ultimate stage was calculated by carrying out sectional analysis following equation (3.56) and equation (3.57) respectively.

For yield moment,

$$M_{Rd} = A_S f_{sy}(d - \beta x) \tag{3.56}$$

where

f_{sy} is the yield strength of the ordinary reinforcement

βx is the distance from the top of the beam to the center of the concrete compressive zone

A_s is the area of the ordinary reinforcement bars

d is the effective depth

x is the distance from top of the beam to the neutral axis

For ultimate moment,

$$M_{uRd} = A_S f_{sy}(d - \beta x) \tag{3.57}$$

For definition of variables see equation (3.56)

For the beam series with fibres, the moments at yielding and at ultimate stage were calculated using the stress-strain distribution shown in Figure 3.17 and stress strain relationship given in Figure 3.15. The fibre tensile stress block resultant and neutral axis were calculated using area balance in accordance with details given in the stress strain diagram in Figure 3.18, see Appendix D for application.

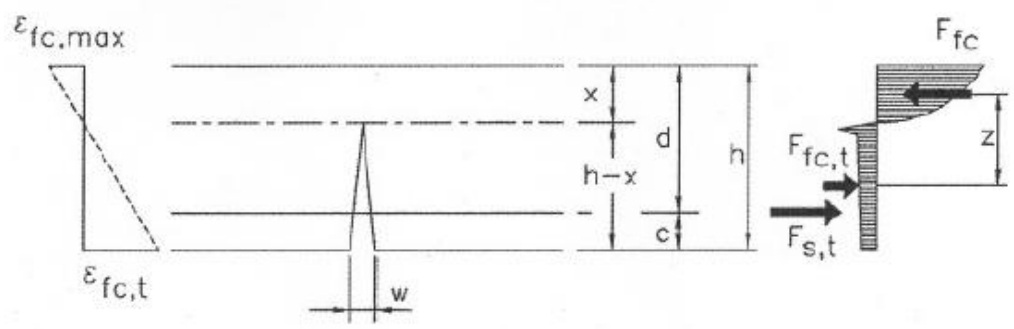

Figure 3.18 Stress strain relationship of steel fibre reinforced concrete with ordinary reinforcing bars, from RILEM TC-162-TDF (2003)

The yield and ultimate moments were derived from the stress strain relationship in Figure 3.17 and are given in equation (3.58) and equation (3.59):

Yield moment,

$$M_{Rd} = A_S f_{sy}\left(d - \frac{x}{2}\right) + F_{fc,t}(h - x)bz \qquad (3.58)$$

where

$F_{fc,t}$ is the resulting residual tensile force of the fibres

$z = [\beta x + x_T(h - x)]$, is the internal lever arm. See Figure 3.18.

x_T is the centre of gravity for the tensile zone of fibre stress, given as a percentage of the total height

f_{sy} is the yield strength of the ordinary reinforcement

βx is the distance from the top of the beam to the center of the concrete compressive zone

A_s is the area of the ordinary reinforcement bars

d is the effective depth

h is the height of the beam

x is the distance from top of the beam to the neutral axis

Ultimate moment,

$$M_{uRd} = A_S f_{sy}\left(d - \frac{x}{2}\right) + F_{fc,t}(h - x)bz \qquad (3.59)$$

For definition of variables see equation (3.58)

The moment-curvature relationships for the different beam series obtained, when designed using RILEM TC-162-TDF (2003), are given in Figure 3.19 and Figure 3.20. From these figures it is difficult to see whether the moment capacity increases with increasing fibre volumes.

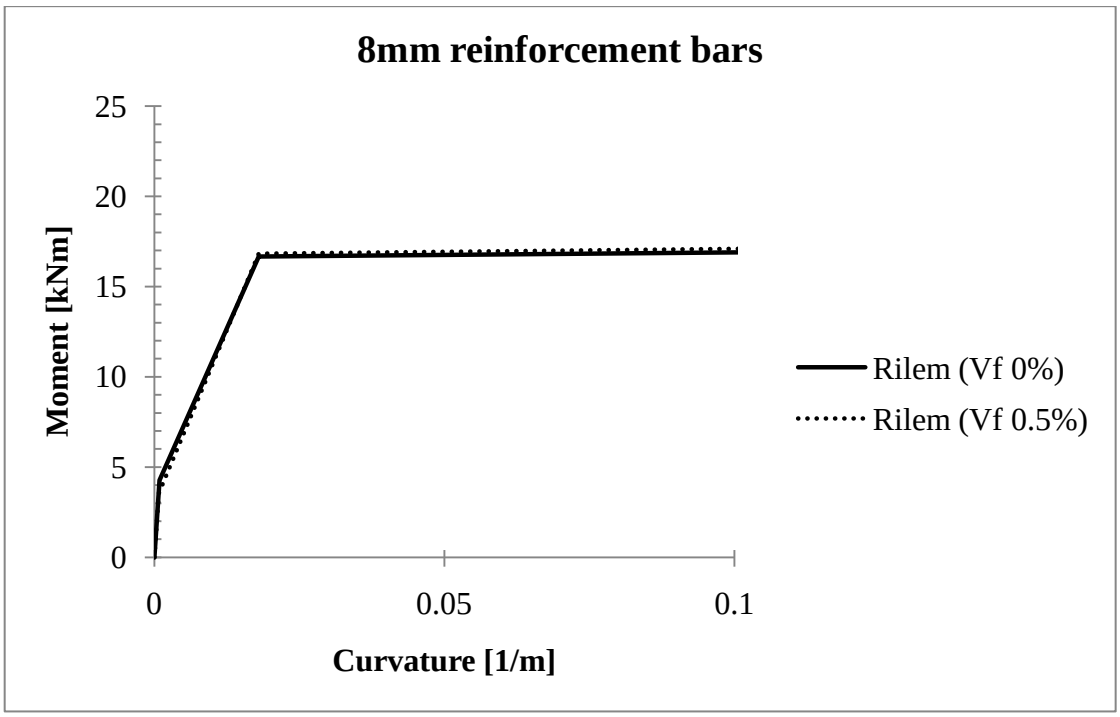

Figure 3.19 Moment curvature results, according to RILEM TC-162-TDF (2003), for beams with 8 mm diameter reinforcement bars

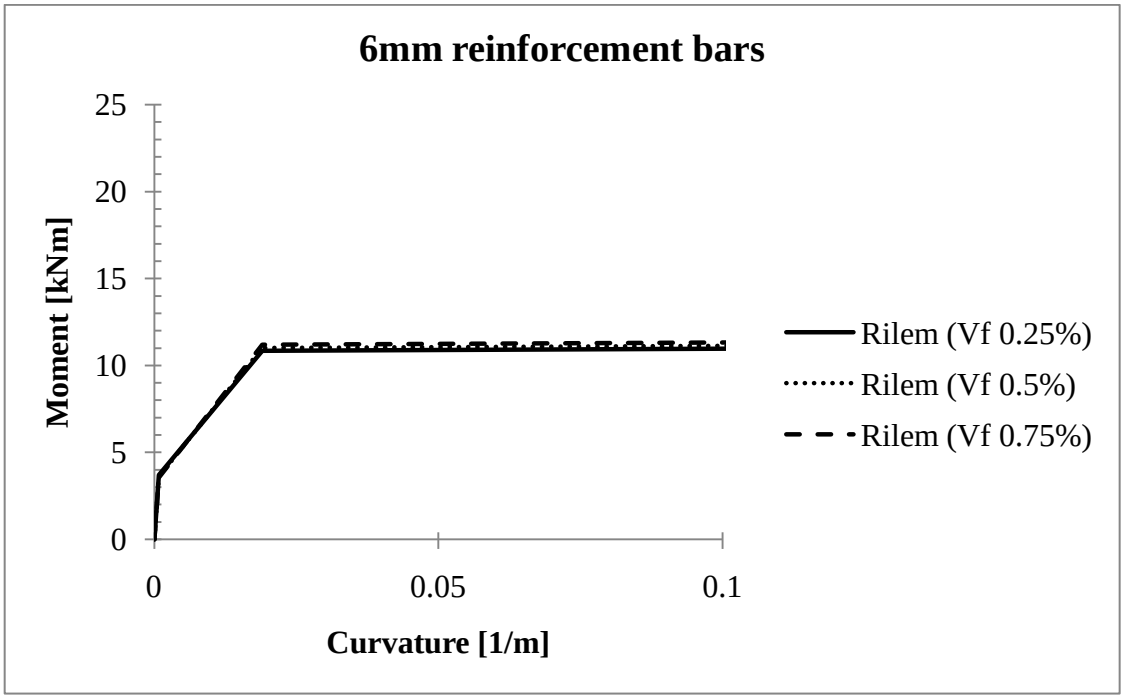

Figure 3.20 Moment curvature results, according to RILEM TC-162-TDF (2003), for beams with 6 mm diameter reinforcement bars

The results in Table 3.19 and Table 3.20 show the ultimate moment capacities, in numbers. The tables also show the increase of moment capacity in percentage due to variation of fibre volume. Table 3.19 indicates that addition of 0.5% fibres does not have any effect on the ultimate moment resistance. It can however be seen, in Table 3.20, that there is a slight increase in the ultimate moment resistance.

Table 3.19 Ultimate moment capacities for beam series with 8 mm reinforcement bars, designed according to RILEM TC-162-TDF (2003).

Series	V_f (%)	Reinforcement	Moment Capacity (kNm)	Increase of capacity due to addition of fibres (%)
1	0	3ø8	17.2	-
2	0.5	3ø8	17.2	0.0

Table 3.20 Ultimate moment capacities for beam series with 6 mm reinforcement bars, designed according to RILEM TC-162-TDF (2003).

Series	V_f (%)	Reinforcement	Moment Capacity (kNm)	Increase of capacity due to varying fibre volume (%)
4	0.25	3ø6	11.2	-
3	0.50	3ø6	11.3	0.8
5	0.75	3ø6	11.5	2.6

RILEM TC-162-TDF (2003) does not give any recommendations regarding ductility requirements when designing steel fibre reinforced concrete.

For design of beams without ordinary reinforcement, RILEM TC-162-TDF (2003) suggests the same method as used in section 3.3.3 for beams with ordinary reinforcement, excluding the steel bars as shown in Figure 3.21.

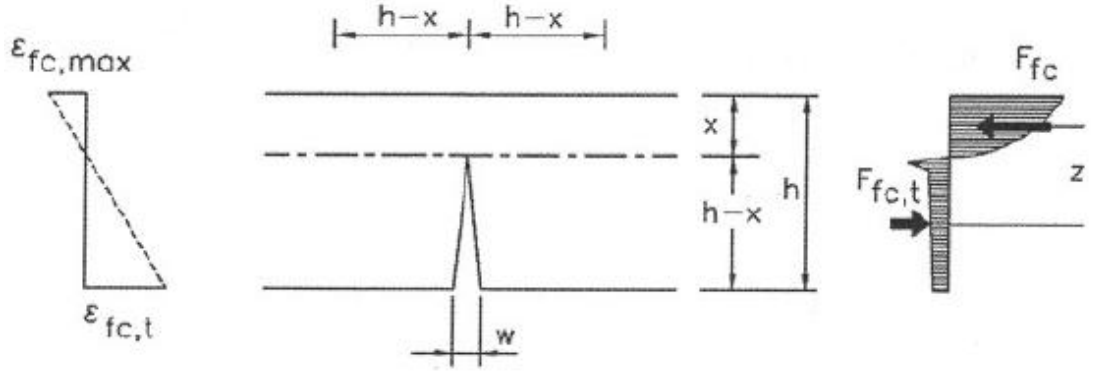

Figure 3.21 Stress strain distribution for beams without ordinary reinforcement, from RILEM TC-162-TDF (2003).

The ultimate moment capacities for beams designed with RILEM TC-162-TDF (2003) are presented in Table 3.21. The results show very low ultimate moment capacities, but it is clear from Table 3.21 that the ultimate moment capacities increase with increased fibre volume.

Table 3.21 Ultimate moment capacities, designed using RILEM TC-162-TDF (200 3), for beams without ordinary reinforcement bars

Series	Fibre Volume (%)	$M_{ultimate}$ (kNm)	Percentage increase (%)
4	0.25	0.365	-
3	0.5	0.609	67
5	0.75	0.849	133

3.3.4 Shear Capacity

The shear capacity was also calculated for all the beam series with the recommendations laid down by RILEM TC-162-TDF (2003), where it is clearly stated that the given method is only valid for beams and plates reinforced with traditional reinforcement bars. In the presence of axial compression forces, this method is also applicable for pre-stressed members and columns.

The proposed design method for shear resistance given by RILEM TC-162-TDF (2003) can be seen in equation (3.60),

$$V_{Rd,3} = V_{cd} + V_{fd} + V_{wd} \quad (3.60)$$

where

V_{cd} is the shear resistance for members without shear reinforcement given in equation (3.61)

V_{wd} is the contribution of stirrups or inclined bars to shear resistance, see equation (3.69)

V_{fd} is the contribution of fibres to shear resistance, see equation (3.65)

$$V_{cd} = \left[0.12k\left[100\rho_1 f_{fck}\right]^{\frac{1}{3}} + 0.15\sigma_{cp}\right]bd \quad (3.61)$$

where

k is the factor taking size effect into account and is given in equation (3.62)

$$k = 1 + \sqrt{\frac{200}{d}} \quad \text{(d in mm)} \quad \text{and } k \leq 2 \quad (3.62)$$

ρ_1 is the steel reinforcement ratio given in equation (3.63)

$$\rho_1 = \frac{A_s}{bd} \leq 2\% \quad (3.63)$$

σ_{cp}, takes into account compression forces in the section due to loading or pre-stressing

$$\sigma_{cp} = \frac{N_{sd}}{A_c} \quad (3.64)$$

where

N_{sd} is the longitudinal force in the section due to loading or pre-stressing

$\sigma_{cp} = 0$ due to the fact that there is no longitudinal force in the section.

$$V_{fd} = 0.7k_f k_1 \tau_{fd} bd \quad (3.65)$$

$k_1 = k$ where k is expressed in equation (3.62)

τ_{fd} is the design value of increase in shear strength due to steel fibres given in equation (3.66)

$$\tau_{fd} = 0.12 f_{Rk,4} \quad (3.66)$$

k_f is the factor taking contribution of flanges in T-section into account given in equation (3.67)

$$k_f = 1 + n\left(\frac{h_f}{b_w}\right)\left(\frac{h_f}{d}\right) \text{ and } k_f \leq 1.5 \quad (3.67)$$

where

h_f is the height of the flanges, b_f is the width of the flanges and b_w is the width of the web

$$n = \frac{b_f - b_w}{h_f} \leq 3 \qquad \text{and} \qquad n \leq \frac{3b_w}{h_f} \tag{3.68}$$

$$V_{wd} = \frac{A_{sw}}{s} 0.9 d f_{ywd} (1 + cot\alpha) sin\alpha \tag{3.69}$$

With,

s is the spacing between shear reinforcement

α is the angle of shear reinforcement

f_{ywd} is the yield strength of the shear reinforcement

A_{sw} is the area of shear reinforcement

Since there are no stirrups or inclined reinforcement bars, the shear resistance, V_{wd}, due to shear reinforcement is equal to zero. The formula in equation (3.60) is thus reduced to equation (3.70).

$$V_{Rd,3} = V_{cd} + V_{fd} \tag{3.70}$$

The results from calculations of the shear resistance are shown in Table 3.22 for beams reinforced with 8 mm ordinary reinforcement bars and Table 3.23 for beams with 6 mm reinforcement bars. It can be concluded from Tables 3.22 and 3.23 that the shear resistance increases with increasing fibre volume.

Table 3.22 Shear resistance results for beam series with 8 mm reinforcement bars, designed according to RILEM TC-162-TDF (2003)

Series	V_f (%)	Reinforcement	Shear resistance (kN)	Increase of capacity due to addition of fibres (%)
1	0	3ø8	19.2	-
2	0.5	3ø8	20.1	4.7

Table 3.23 Shear resistance results for beam series with 6 mm reinforcement bars, designed according to RILEM TC-162-TDF (2003).

Series	V_f (%)	Reinforcement	Shear resistance (kN)	Increase of capacity due to varying fibre volume (%)
4	0.25	3ø6	16.2	-
3	0.50	3ø6	16.9	4.3
5	0.75	3ø6	17.7	9.3

The shear capacities are also illustrated in the bar diagram in Figure 3.22. Here, the shear resistance is compared with the shear load from the experimental results. It can be concluded from the bar diagram, that the shear resistance is lower than the shear load in all analyses which is acceptable, since the failure mode in the experiments was flexure and not shear.

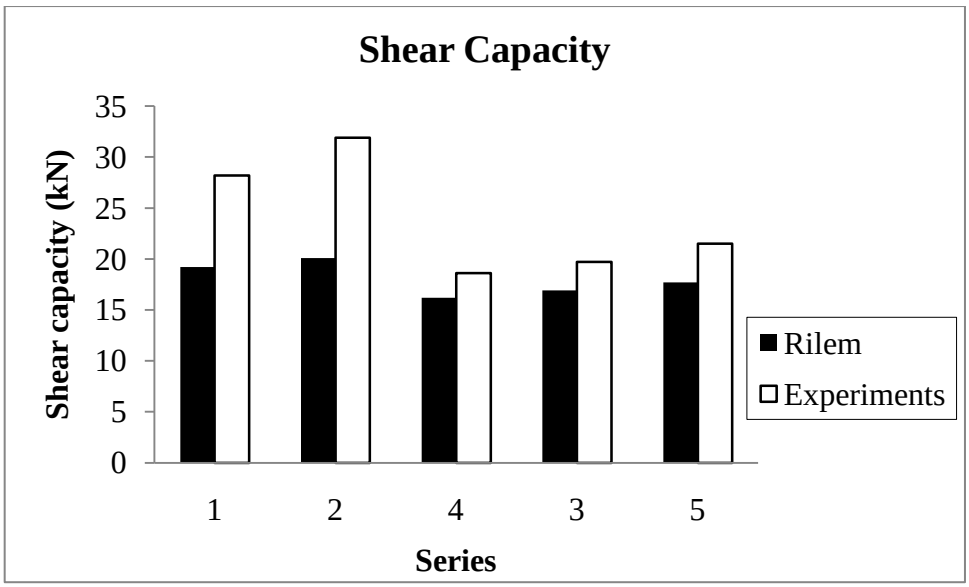

Figure 3.22 Shear resistance compared to experimental results for all beam series.

It is clearly stated in RILEM TC-162-TDF (2003), that there is no approved calculation method for shear resistance in steel fibre reinforced concrete elements, in the absence of ordinary reinforcement or compressive zone.

3.3.5 Crack width

The crack width calculations were carried out at a moment of 15kNm for series 1 and 2 and a moment of 10 kNm for series 3, 4 and 5 in order to make a fair comparison between the crack widths.

For the calculation of crack width,w_k, RILEM TC-162-TDF (2003) proposes the formula given in equation (3.71):

$$w_k = \beta s_{rm} \varepsilon_{sm} \tag{3.71}$$

with,

β being the coefficient taking loading conditions into account. The value is 1.7 for load induced cracking and 1.3 in restrained cracking.

ε_{sm}, is the mean steel strain in the reinforcement, see equation (3.72).

$$\varepsilon_{sm} = \frac{\sigma_s}{E_s}\left[1 - \beta_1 \beta_2 \left(\frac{\sigma_{sr}}{\sigma_s}\right)^2\right] \tag{3.72}$$

where,

σ_s is the actual stress in tensile reinforcement in a cracked section

σ_{sr} is the stress in the tensile reinforcement at the crack formation stage

β_1 is the coefficient taking bond properties of the steel reinforcement bars into account. $\beta_1 = 1.0$ for high bond bars and $\beta_1 = 0.5$ for plain bars.

β_2 is the coefficient taking duration of loading into account. $\beta_2 = 1.0$ for single short term loading and 0.5 for sustained loading.

s_{rm} is the average final crack spacing

$$s_{rm} = \left(50 + 0.25 k_1 k_2 \frac{\emptyset_b}{\rho_r}\right)\left(\frac{50}{L/\emptyset}\right) \tag{3.73}$$

where

$\emptyset_b$ is the ordinary reinforcement bar size

k_1 is a factor taking bond properties of ordinary reinforcement into account. $k_1 = 0.8$ for high bond bars and $k_1 = 1.6$ for plain bars.

k_2 is a coefficient taking strain distribution into account. $\mathrm{k}_2 = 0.5$ for bending and $\mathrm{k}_2 = 1.0$ for pure tension.

$$\rho_r = \frac{A_s}{A_{c,eff}} \tag{3.74}$$

where,

L is the length of the steel fibre

$\emptyset$ is the diameter of the steel fibre

$\frac{50}{L/\emptyset} \leq 1$ is the fibre contribution to the average final crack spacing

$L/\emptyset$ is the slenderness ratio of steel fibres.

It can be noted that the final crack spacing in equation (3.73) only takes slenderness ratio of the fibres into account and not the fibre dosage, implying that the amount of fibres has no effect on the crack spacing which is incorrect in reality. As a result of this ignorance, the results in Table 3.25 give almost the same crack width in all the series. Still, fibres do have an effect on crack width, according to RILEM TC-162-TDF (2003), which can be observed in Table 3.24, where there is a reduction of approximately 30% with an addition of 0.5% fibre volume.

Table 3.24 Crack width results for beam series with 8 mm reinforcement bars, according to RILEM TC-162-TDF (2003), calculated at a moment resistance of 15kNm.

Series	V_f (%)	Reinforcement	Crack width (mm)	Reduction due to addition of fibres (%)
1	0	3ø8	0.384	-
2	0.5	3ø8	0.297	-29.3

Table 3.25 Crack width results for beam series with 6 mm reinforcement bars, designed according to RILEM TC-162-TDF (2003), calculated at a moment resistance of 10kNm.

Series	V_f (%)	Reinforcement	Crack width (mm)	Reduction due to change of fibre volume (%)
4	0.25	3ø6	0.367	-
3	0.5	3ø6	0.370	-0.8
5	0.75	3ø6	0.372	-1.3

Crack width calculations for beams without ordinary reinforcement can be calculated, according to RILEM TC-162-TDF (2003), using the formula in equation (3.75).

$$w = \varepsilon_{fc,t}(h - x) \tag{3.75}$$

With,

$$\varepsilon_{fc,t} = \varepsilon_{fc,max}\frac{h-x}{x} \tag{3.76}$$

where

$\varepsilon_{fc,max}$ is the concrete compressive strain, for strain distribution see Figure 3.21

$\varepsilon_{fc,t}$ is the tensile strain

The results in Table 3.26 show the crack width calculations in the ultimate state. The results are exceedingly higher than the allowable crack width. In order to meet this requirement, very large amounts of fibres are needed.

Table 3.26 Crack width results for beams without ordinary reinforcement bars, designed according to RILEM TC-162-TDF (2003)

Series	Fibre Volume (%)	Crack width (mm)	Crack width Reduction (%)
4	0.25	175.5	-
3	0.5	107.4	63
5	0.75	77.1	128

3.3.6 Comparison with experimental results

The overall results from design of fibre reinforced concrete beams using RILEM TC-162-TDF (2003), were in most cases underestimated when compared with the experimental results, which can be seen in Figure 3.23 and in Figure 3.24.

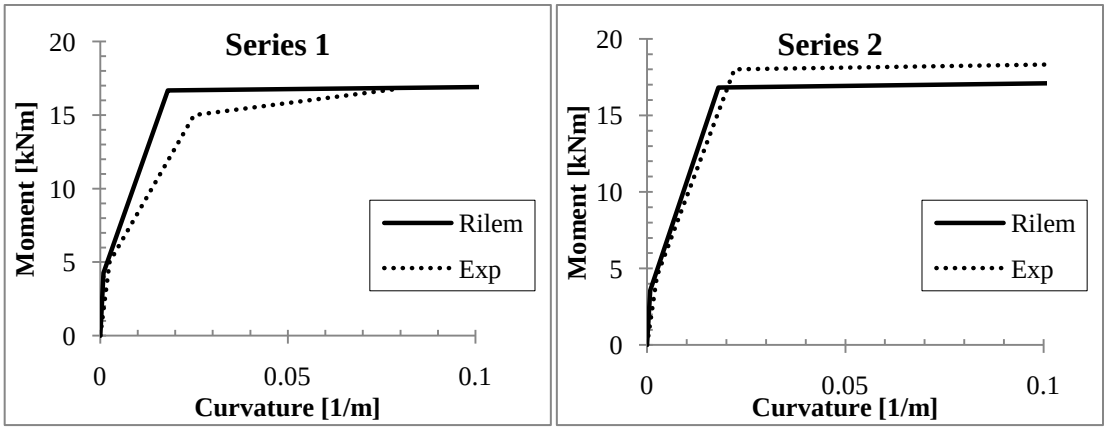

(a) *(b)*

Figure 3.23 Moment curvature results, for beam series with 8 mm rebars, from design according to RILEM TC-162-TDF (2003) and the experimental results for (a) beams with V_f = 0%, (b) beams with V_f = 0.5 %

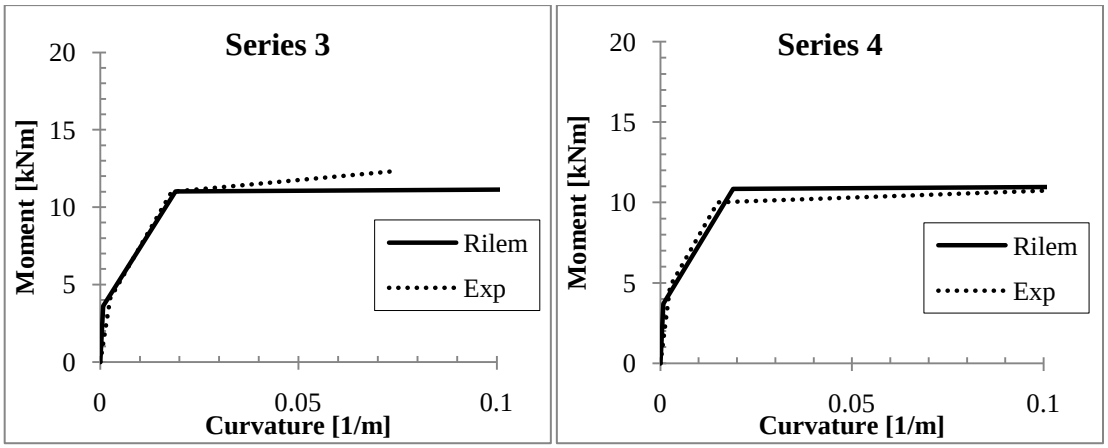

(a)

(b)

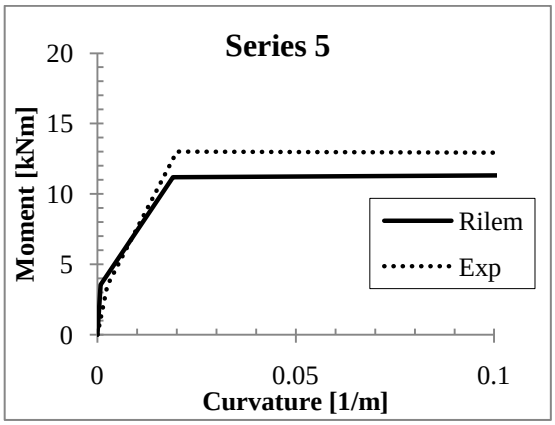

(c)

Figure 3.24 Moment curvature results, for beam series with 6 mm rebars, from design according to RILEM TC-162-TDF (2003) and the experimental results for (a) beams with V_f = 0.5 %, (b) beams with V_f = 0.25 %, (c) beams with V_f = 0.75 %

In Table 3.27 and Table 3.28, the ultimate moment capacities are compared with the experimental results and the under- or overestimations are checked and presented in percent. It is observed from these tables that there are no overestimations in the beams with fibres but underestimations, where the largest underestimation is 10.2% and found in series 5, see Table 3.28.

Table 3.27 Ultimate moment capacities from RILEM TC-162-TDF (2003) and experiments for beams with 8mm reinforcement bars

$M_{ultimate}$		
Series	1	2
V_f (%) and reinforcement	0 3Ø8mm	0.5 3Ø8mm
Rilem	17.2	17.2
Experimental	16.8	18.9
Difference (%)	2.4	-8.9

Table 3.28 Ultimate moment capacities from RILEM TC-162-TDF (2003) and experiments for beams with 6mm reinforcement bars

$M_{ultimate}$			
Series	4	3	5
V_f (%) and reinforcement	0.25 3Ø6mm	0.5 3Ø6mm	0.75 3Ø6mm
Rilem	11.2	11.3	11.5
Experimental	11.3	12.3	12.8
Difference (%)	-0.8	-8.1	-10.2

3.3.7 Conclusions

The moment resistance, when designing according to RILEM TC-162-TDF (2003), hardly increased with addition of fibres in the concrete mix. When compared with experimental results, an underestimation of the ultimate moment resistance was revealed in all the cases with fibres, where the largest underestimation, found in series 5, was 10.2%. For the beam series without fibres, the ultimate moment resistance was overestimated. This overestimation was considerably small.

The moment resistance obtained from the design of beams without ordinary reinforcement increased with more fibre fractions but also revealed that very large amounts of fibres are needed, if fibres are to replace ordinary reinforcement.

The design of shear resistance using RILEM TC-162-TDF (2003) also indicated that fibres have a positive effect on the shear resistance as it increases with the addition of fibres. However, when compared to the shear load, the shear resistance was much underestimated in all analyses. This is acceptable since the failure modes were flexure and not shear.
The design code proposed no method for designing shear resistance for beams without ordinary reinforcement.

Design of crack width, using RILEM TC-162-TDF (2003), revealed that fibres have a positive effect on crack width as an addition of fibres reduced the crack width, see Table 3.24. Increasing fibre amount did not give any reduction in crack width, see Table 3.25. The reason for this is due to the fact that the formula of the final crack spacing, suggested by RILEM TC-162-TDF (2003) in equation (3.73), does not account for the amount of fibres used in the concrete mix, but the slenderness ratio of the fibres. Since the same type of fibres is used in all the beam series, there is no significant difference in the design crack width.

3.4 Design according to Spanish Guidelines

In this section, the method and considerations for the design of beam elements, as laid down in the Spanish (EHE-08) recommendations, are discussed. The beams were designed considering the models mentioned in the code and the moment and shear capacities were determined. Furthermore, calculations were made to check the crack width in serviceability limit state. Comparison of the design results with the experimental data is also included in this section.

EHE-08 is the abbreviation for Instrucción de hormigón estructura 2008, which is the Spanish code on structural concrete. EHE-08 lays down the requirements that have to be fulfilled by the concrete structures/elements in order to satisfy the safety standards.

3.4.1 Residual flexural tensile strength

The Spanish guideline EHE-08 makes the same assumptions as FIB model code and RILEM TC-162-TDF (2003), regarding linear post cracking distribution for the residual tensile strength f_{R1d} and f_{R3d}. The design residual tensile strengths $f_{ctR1,d}$ and $f_{ctR3,d}$ and their corresponding strains are, according to EHE-08, determined using the multi-linear stress strain diagram shown in Figure 3.25, where the values are expressed in equations (3.77) to (3.81).

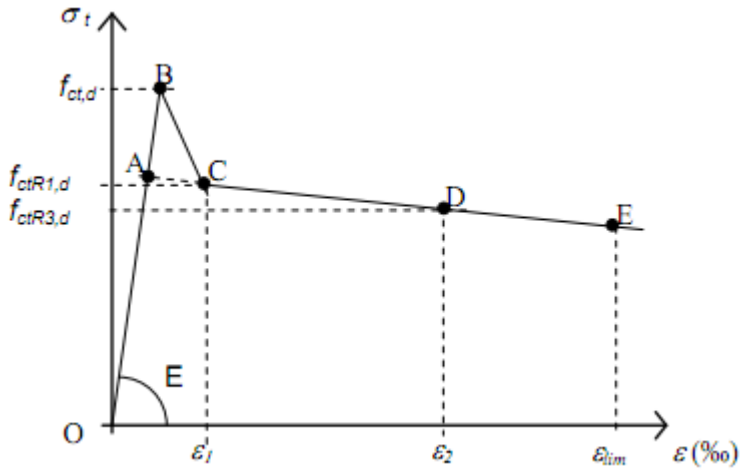

Figure 3.25 Multi-linear stress strain diagram, from EHE-08

$$f_{ct,d} = 0.6 f_{ct,fl,d} \tag{3.77}$$

where

$f_{ct,d}$ is the design tensile strength

$f_{ct,fl,d}$ is the design value of the flexural tensile strength

$$f_{ctR1,d} = 0.45 f_{R,1,d} \tag{3.78}$$

where

$f_{ctR1,d}$ is the design residual tensile strength

$f_{R,1,d}$ is the design residual flexural strength

$$f_{ctR3,d} = k_1\left(0.5 f_{R,3,d} - 0.2 f_{R,1,d}\right) \tag{3.79}$$

where

$f_{ctR3,d}$ is the design residual tensile strength

$f_{R,3,d}$ is the design residual flexural strength

$k_1 = 1$ for sections subjected to bending and 0 for sections subjected to tension

$$\varepsilon_1 = 0.1 + \frac{1000 f_{ct,d}}{E_{c0}} \tag{3.80}$$

$$\varepsilon_2 = \frac{2.5}{l_{cs}} \tag{3.81}$$

l_{cs} is the critical length of the element, see equation (3.82)

$$l_{cs} = min(s_m, h - x) \tag{3.82}$$

where

s_m is the mean distance between cracks

h-x is the distance from the neutral axis to the most highly tension end

$\varepsilon_{lim} = 20 \times 10^{-3}$ for sections subjected to bending and 10×10^{-3} for sections subjected to tension

For design in ultimate limit state, the rectangular diagram in Figure 3.26 can also be used. This was however not used in this report.

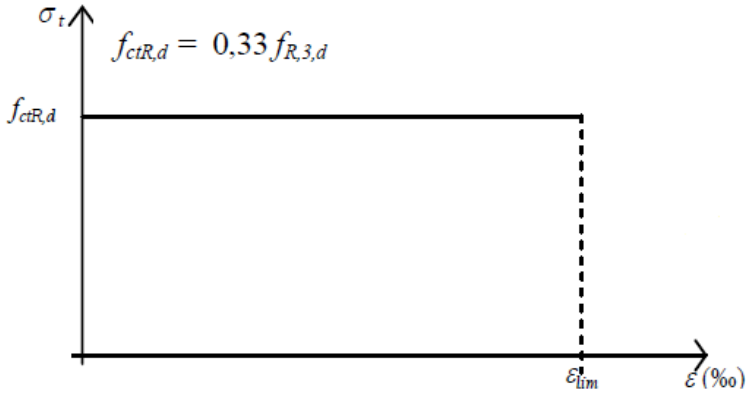

Figure 3.26 Rectangular stress strain diagram, from EHE-08

For the definition of variables, see equation (3.79).

3.4.2 Moment resistance

For the calculation of the moment resistance, EHE-08 gives a limitation formula, see equation (3.81), where fibres can be treated alone or in combination with ordinary reinforcement. It should however be noted that, no partial safety factors were used for the design in this report due to comparison with experimental results.

$$A_p f_{pd} \frac{d_p}{d_s} + A_s f_{yd} + \frac{z_f}{z} A_{ct} f_{ctR,d} \geq \frac{W_1}{z} f_{ctm} + \frac{P}{z}\left(\frac{W_1}{A} + e\right) \qquad (3.83)$$

where

$z_f A_{ct} f_{ctR,d}$ are the fibre contributions

z_f is the lever arm for the tensile zone

A_{ct} is area of the tensile zone

$f_{ctR,d}$ is the design residual tensile strength

f_{pd} is the design value of the tensile strength of bonded active reinforcement

A_p is the area of bonded active reinforcement

d_p is the depth of active reinforcement from the most compressed fibre in the section

f_{yd} is the design value of the tensile strength of passive reinforcement

A_s is the area of the passive reinforcement

z is the lever arm of the section

W_1 is the section modulus

e is the eccentricity of the prestressing relative to the center of gravity of the gross section

f_{ctm} is the mean flexural tensile strength

P is the prestressing force

A is the gross concrete section area

d_s is the depth passive reinforcement

Since no prestressing is considered in this report, equation (3.83) is reduced to equation (3.84).

$$A_s f_{yd} + \frac{z_f}{z} A_{ct} f_{ctR,d} \geq \frac{W_1}{z} f_{ctm} \qquad (3.84)$$

This limitation is to guarantee that no brittle failure occurs. This also means that ordinary reinforcement and fibres complement one another and in case there is no ordinary reinforcement, the fibre volume is to be increased.

The moment curvature diagrams for beams with 8 mm reinforcement bars are presented in Figure 3.27, where it is confirmed that the moment capacity increases with the addition of fibres.

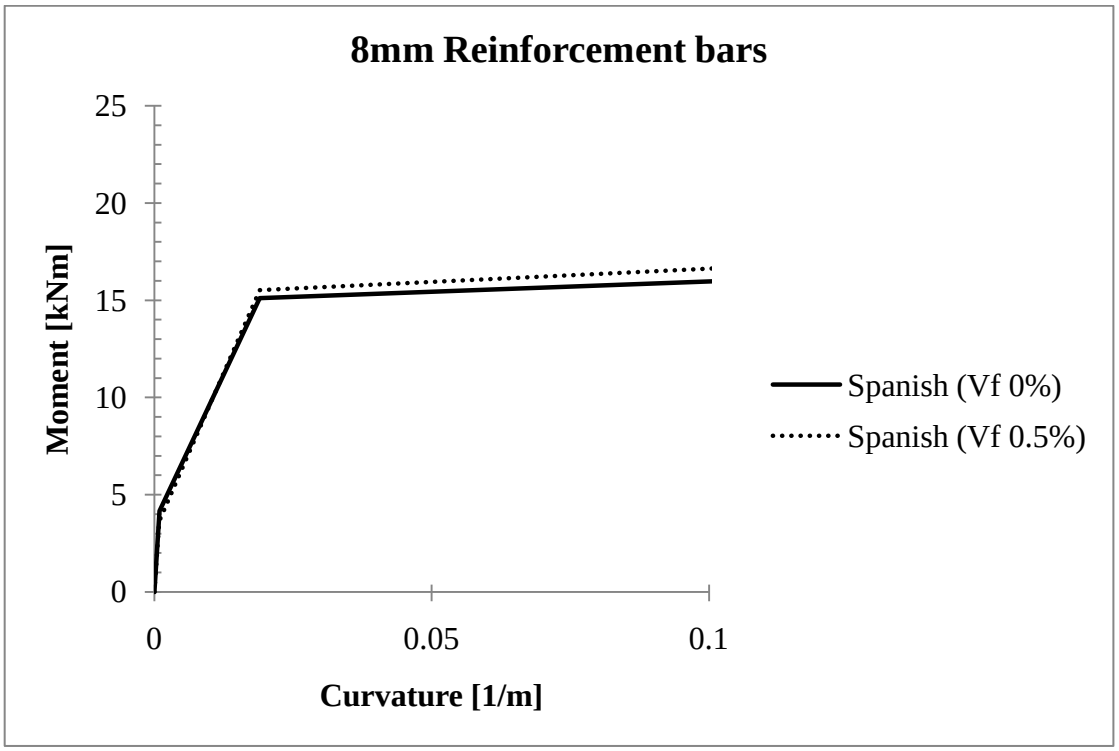

Figure 3.27 Moment curvature results from design according to EHE-08 for beams with 8 mm diameter reinforcement bars

The moment curvature diagrams in Figure 3.28 represent the beam series with 6 mm ordinary reinforcement bars. Here it is observed that the moment capacity increases slightly with increased fibre volume.

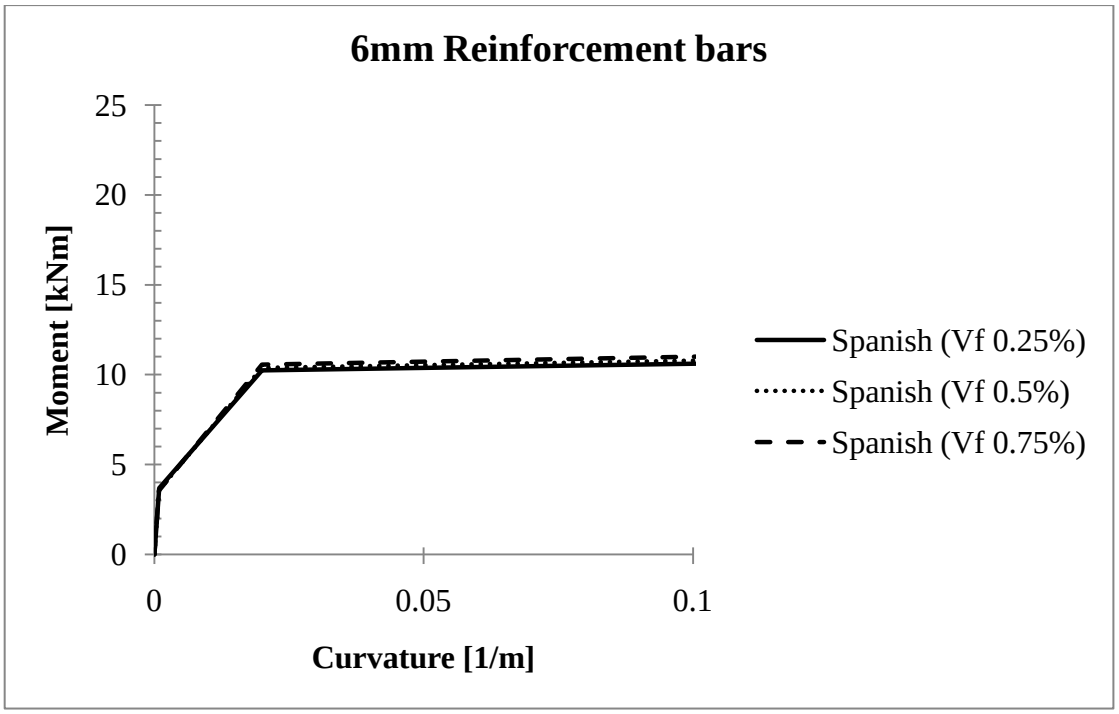

Figure 3.28 Moment curvature results from design according to EHE-08 for beams with 6 mm diameter reinforcement bars

The results in Table 3.29 show that addition of 0.5% volume fibre in ordinary reinforced concrete increases the moment resistance with approximately 1.8%.

Table 3.29 Ultimate moment capacities for beam series with 8 mm reinforcement bars, designed according to EHE-08

Series	V_f (%)	Reinforcement	Moment Capacity (kNm)	Increase of capacity due to addition of fibres (%)
1	0	3ø8	16.8	-
2	0.5	3ø8	17.1	1.8

From the results in Table 3.30, it can be noted that the moment capacity increases with increasing fibre volume

Table 3.30 Ultimate moment capacities for beam series with 6 mm reinforcement bars, designed according to EHE-08

Series	V_f (%)	Reinforcement	Moment Capacity (kNm)	Increase of capacity due to varying fibre volume (%)
4	0.25	3ø6	11.1	-
3	0.50	3ø6	11.3	1.8
5	0.75	3ø6	11.5	3.6

No information regarding ductility requirements can be found in the EHE-08, for fibre reinforced concrete design.

Design of fibre reinforced concrete, without ordinary reinforcement, leads to further reduction of equation (3.84), disregarding the contribution of ordinary reinforcement bars, see equation (3.85)

$$z_f A_{ct} f_{ctR,d} \geq W_1 f_{ctm} \quad (3.85)$$

For definition of variables see equation (3.83)

Design of ultimate moment capacity shows an increase with increasing fibre volume, see Table 3.31. The fibre fractions, used in this report, however give very low ultimate moment capacities. EHE-08 proposes, in equation (3.85), that the ultimate moment capacity should be greater than the cracking moment in order to avoid brittle failure. This requires the use of ordinary reinforcement or a strain hardening material.

Table 3.31 Ultimate moment capacities, designed using EHE-08, for beams without ordinary reinforcement bars

Series	Fibre Volume (%)	$M_{ultimate}$ (kNm)	Percentage increase (%)
4	0.25	0.411	-
3	0.5	0.614	49
5	0.75	0.867	111

The cracking moment, see Table 3.32, is greater than the ultimate moment resistance in all beam series without ordinary reinforcement. Thus making the results unacceptable, according to EHE-08, and resulting into brittle failure in all beams.

Table 3.32 Cracking moments, designed using EHE-08, for beams without ordinary reinforcement bars

Series	Fibre Volume (%)	M_{crack} (kNm)
4	0.25	3.69
3	0.5	3.59
5	0.75	3.54

3.4.3 Shear capacity

Shear resistance,V_{u2}, for steel fibre reinforced concrete with or without ordinary reinforcement can be calculated according to formula presented by EHE-08, given in equation (3.86)

$$V_{u2} = V_{cu} + V_{su} + V_{fu} \quad (3.86)$$

where

V_{cu}, is the shear resistance for members without shear reinforcement given in equation (3.87)

$$V_{cu} = \left[\frac{0.18}{\gamma_c}\xi[100\rho_1 f_{cv}]^{\frac{1}{3}} + 0.15\sigma_{cd}\right] bd \quad (3.87)$$

where

σ_{cd} is the contribution from axial compressive force or pre-stressing

f_{cv} is the compressive strength

ρ_1 is the steel reinforcement ratio

ξ is a size factor calculated as in equation (3.88)

$$\xi = 1 + \sqrt{\frac{200}{d}} \text{ with d given in (mm) and } \xi \leq 2 \quad (3.88)$$

d is the effective depth

b is the width of the specimen

γ_c is the partial safety factor, not considered in design in this report due to comparison with experiments

V_{su} is the contribution of transverse reinforcement to the shear strength, which is zero since there is no shear reinforcement in the evaluated beams.

V_{fu} is the contribution of fibres to shear resistance given in equation (3.89).

$$V_{fu} = 0.7\xi\tau_{fd}bd \quad (3.89)$$

where

τ_{fd} is the design value of fibre induced increase in shear strength. See equation (3.90).

$$\tau_{fd} = 0.5 f_{ctR,d} \quad (3.90)$$

with

$f_{ctR,d}$ being the design residual tensile strength

The shear resistance was also calculated according to EHE-08 and the results are presented in Table 3.33 and Table 3.34. Addition of fibres increased the shear resistance in all the beam series evaluated.

Table 3.33 Shear resistance results for beam series with 8 mm reinforcement bars, designed according to EHE-08.

Series	V_f (%)	Reinforcement	Shear Resistance (kN)	Change of capacity due to addition of fibres (%)
1	0	3ø8	26.0	-
2	0.5	3ø8	29.8	14.6

Table 3.34 Shear resistance results for beam series with 6 mm reinforcement bars, designed according to EHE-08.

Series	V_f (%)	Reinforcement	Shear Resistance (kN)	Change of capacity due to varying fibre volume (%)
4	0.25	3ø6	24.1	-
3	0.50	3ø6	24.8	2.9
5	0.75	3ø6	25.9	7.4

The bar diagram in Figure 3.29 illustrates the comparison of shear resistances calculated, according to EHE-08, with the experimental shear loads in all the beam series. The results show that the shear resistance is underestimated in the beam series1 and 2, with 8 mm ordinary reinforcement bars, which is not acceptable since shear was not the failure mode but flexure. The results from beam series 3, 4 and 5, with 6 mm ordinary reinforcement bars, overestimated the experimental shear loads which is logical.

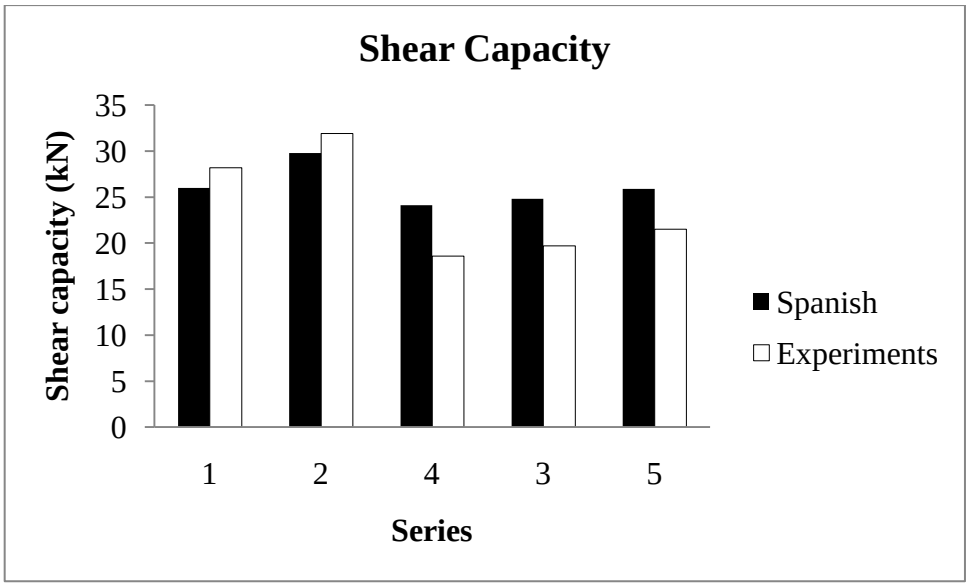

Figure 3.29 Shear resistance compared to experimental shear for all beam series

No design method regarding shear resistance for beams without ordinary reinforcement could be found. Equation (3.89), for the fibre contribution depends on presence of ordinary reinforcement.

3.4.4 Crack width

The Spanish EHE-08 does not consider the design in serviceability limit state with regard to fibre reinforced concrete and therefore, no crack width calculations for the design are available.

3.4.5 Comparison with experimental results

Figure 3.30 and Figure 3.31 illustrate the comparison between the calculated moment curvature diagrams and the experimental results. It is clear that there is an underestimation in all beam series with fibres, except series 4 where the capacity is overestimated.

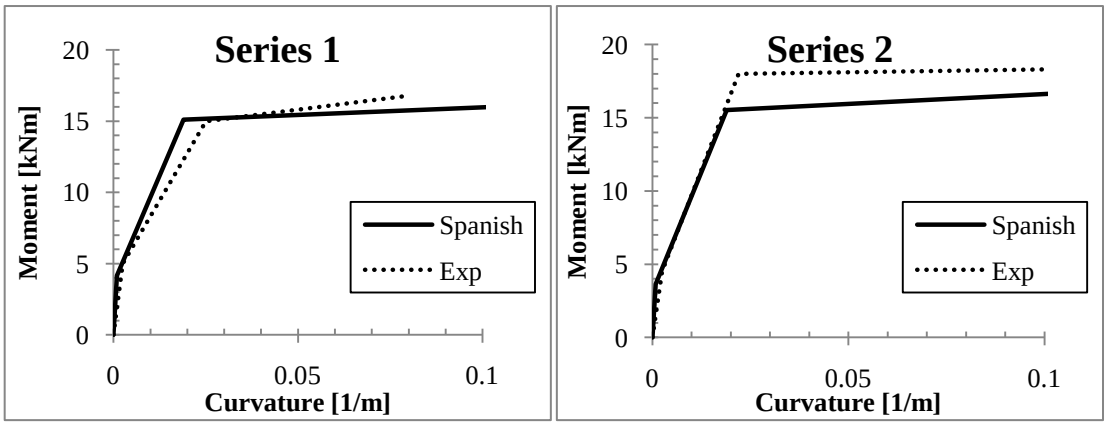

(a) *(b)*

Figure 3.30 Moment curvature results, for beam series with 8 mm rebars, from design according to EHE-08 and the experimental results for (a) beams with V_f = 0%, (b) beams with V_f = 0.5 %

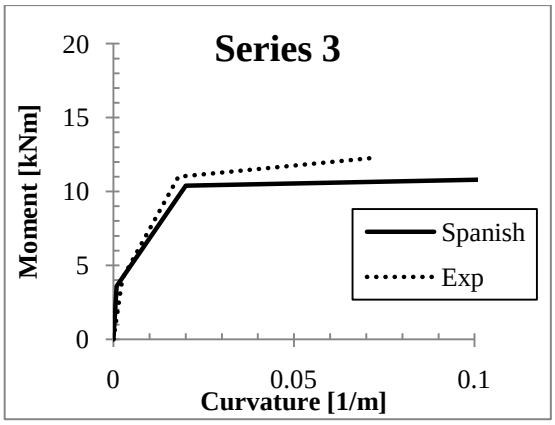

(a)

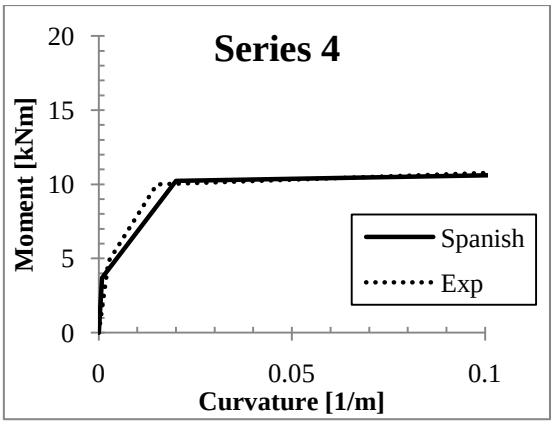

(b)

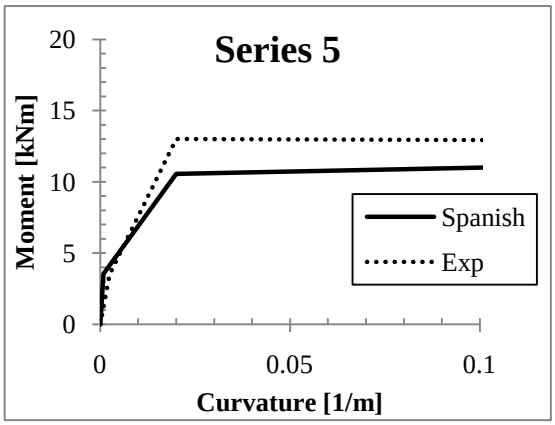

(c)

Figure 3.31 Moment curvature results, for beam series with 6 mm rebars, from design according to EHE-08 and the experimental results for (a) beams with V_f = 0.5%, (b) beams with V_f = 0.25 % , (c) beams with V_f = 0.75 %

Table 3.35 Ultimate moment capacities designed, according to EHE-08 and experiments for beams with 8 mm reinforcement bars

$M_{ultimate}$		
Series	1	2
V_f (%) and reinforcement	0 3Ø8mm	0.5 3Ø8mm
Spanish Guidelines	16.8	17.1
Experimental	16.8	18.9
Difference (%)	-	-9.5

The ultimate moment capacities are shown in Table 3.35 and Table 3.36. The tables also show the percentage underestimation with largest underestimation being 10.1% in series 5.

Table 3.36 Ultimate moment capacities, designed according to EHE-08 and experiments for beams with 6 mm reinforcement bars

$M_{ultimate}$			
Series	4	3	5
V_f (%) and reinforcement	0.25 3Ø6mm	0.5 3Ø6mm	0.75 3Ø6mm
Spanish Guidelines	11.1	11.3	11.5
Experimental	11.3	12.3	12.8
Difference (%)	-1.8	-8.1	-10.1

3.4.6 Conclusions

The moment resistance, designed according to the Spanish EHE-08, gave underestimations when compared to the experimental results. Maximum underestimation was 10.1%. The reason for this underestimation can be due to the variation in experimental results, as the values used are mean values from three beam tests in each series. The variation of the moment resistances in the experimental results was up to 1.5 kNm within the beams having the same material properties.

The shear resistance, designed according to EHE-08, increased with addition of fibres, see Tables 3.33. Varying the fibre volume, as seen in Table 3.34, also increased the shear resistance. This increase in shear resistance was however small. When the shear resistance was compared to the experimental shear load, slight underestimations were revealed in the beam series 1 and 2 with 8 mm diameter reinforcement bars. This is unacceptable since shear was not the failure mode but flexure. There were however large overestimations in the beam series 3, 4 and 5, with 6 mm diameter reinforcement bars, which is more accurate since shear failure was not reached.

The Spanish EHE-08 does not consider crack control for fibre reinforced concrete beams and therefore no calculations were possible.

3.5 Discussion

In general, all the codes and guidelines evaluated in this report use the same approach with regard to designing fibre reinforced concrete. Some minor exceptions concerning assumed post cracking stress strain distribution were found, giving differences in the equations used.

The design results did not differ considerably when compared with one another but when compared to the experimental results, underestimations were noticed in almost all cases, see Figure 3.32. The design approach suggested by the FIB model code gave the largest underestimations, with moment capacities differing up to 12.5% from the experimental results, see Table 3.37 and Table 3.38.

Table 3.37 Over- underestimations of the design codes and guidelines in comparison with experiments for beams with 8 mm reinforcement bars

	Series 1		Series 2	
	$M_{ultimate}$ (kNm)	Difference (%)	$M_{ultimate}$ (kNm)	Difference (%)
Experiments	16.8	-	18.9	-
FIB	16.9	0.6	17.0	-10.1
Rilem	17.2	2.4	17.2	-9.0
Spanish	16.8	-	17.1	-9.5

Table 3.38 Over- underestimations of the design codes and guidelines in comparison with experiments for beams with 6 mm reinforcement bars

	Series 4		Series 3		Series 5	
	$M_{ultimate}$ (kNm)	Difference (%)	$M_{ultimate}$ (kNm)	Difference (%)	$M_{ultimate}$ (kNm)	Difference (%)
Experiments	11.3	-	12.3	-	12.8	-
FIB	11.0	-2.7	11.1	-9.7	11.2	-12.5
Rilem	11.2	-0.8	11.3	-8.1	11.5	-10.2
Spanish	11.1	-1.8	11.3	-8.1	11.5	-10.2

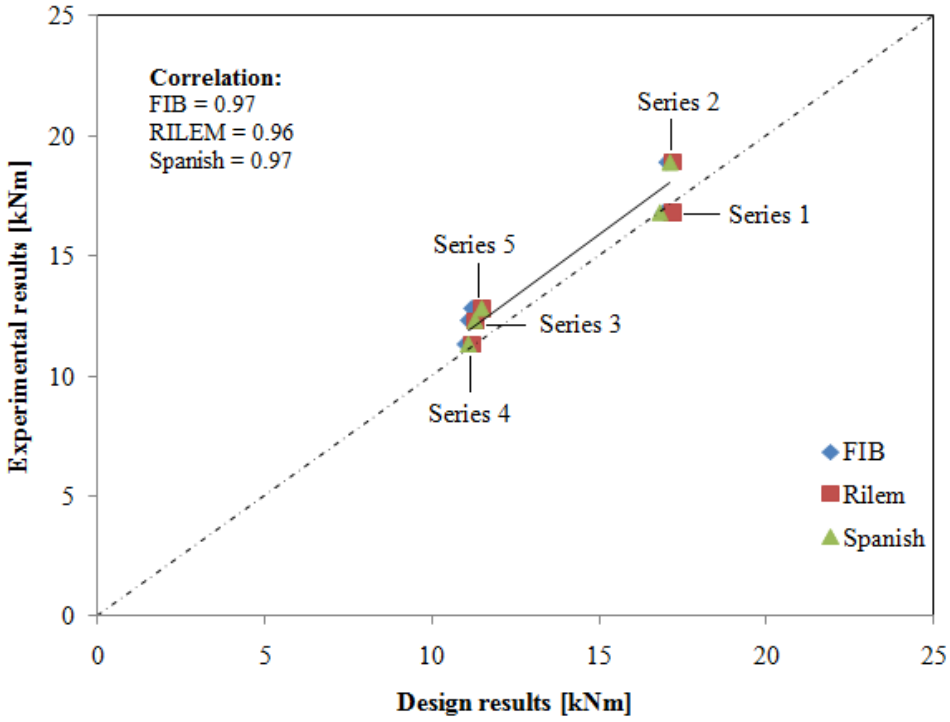

Figure 3.32 Comparison between design ultimate moment resistances and experimental results

The design approach suggested by the FIB model code and the Spanish EHE-08, proved to be most accurate when compared with the experimental results for the reason that both had the correlation ratio closest to 1, which was 0.97, see Figure 3.32.

Table 3.39 and Table 3.40 show the experimental results, obtained from the beam tests performed by Gustafsson and Karlsson (2006), used for comparison in this report. It is obvious that large variation occurs within beams having the same material properties. It can be noted that the largest variation in ultimate moment resistances is 9.5%, see Table 3.40. This makes it difficult to determine the accuracy of the design codes and guidelines, but using the mean values of the ultimate moment resistances, the Spanish EHE-08 proved to be the most accurate.

Table 3.39 Variation in ultimate moment capacities obtained from experiments on the three beams tested in each series, with 8 mm reinforcement bars

Experiments	Series 1		Series 2	
	$M_{ultimate}$ (kNm)	Difference (%)	$M_{ultimate}$ (kNm)	Difference (%)
Beam 1	17.3	5.5	19.2	2.7
Beam 2	16.9	3.1	18.7	-
Beam 3	16.4	-	19.8	5.9

Table 3.40 Variation in ultimate moment capacities obtained from experiments on the three beams tested in each series, with 6 mm reinforcement bars

Experiments	Series 4		Series 3		Series 5	
	$M_{ultimate}$ (kNm)	Difference (%)	$M_{ultimate}$ (kNm)	Difference (%)	$M_{ultimate}$ (kNm)	Difference (%)
Beam 1	11.6	2.7	12.7	9.5	12.3	-
Beam 2	11.3	-	12.1	4.3	12.7	3.3
Beam 3	11.3	-	11.6	-	13.2	7.3

The comparison of shear resistance with the experimental shear load, revealed underestimations for the beam series 1 and 2, reinforced with 8 mm reinforcement bars, which is not okay since the experimental shear load was not the cause of failure but bending. There were overestimations for the beam series 3, 4 and 5, reinforced with 6 mm reinforcement bars, for design according to both the Spanish EHE-08 and the FIB model code which is acceptable as shear failure is higher than the experimental shear load. Regarding RILEM TC-162-TDF (2003), all beam series with 8 mm reinforcement were highly underestimated, while the beam series reinforced with 6 mm ordinary reinforcement bars were slightly underestimated. Since there was no difference in applicability, regarding shear resistance design, it is believed that the shear resistance formula, see equation (3.61), proposed by RILEM TC-162-TDF (2003), has a hidden partial safety factor, as $\frac{0.18}{\gamma_c}$ is 0.12, which is the value used for design. The shear resistance design formulas for the FIB model code and the Spanish EHE-08 can be seen in equation (3.30) and equation (3.87).

Crack widths, calculated using the methods proposed by FIB model code and RILEM TC-162-TDF (2003), were evaluated. Spanish EHE-08 does not have any verification in serviceability limit state, regarding fibre reinforced concrete elements, and therefore, no crack width evaluation was possible. The results obtained from analysis, according to FIB model code, proved that addition of fibres has a positive effect on the crack width, as it decreased with increasing fibre volume. The results from analysis, according RILEM TC-162-TDF (2003), however showed that, fibres have a negative impact on the crack width as it increased with increasing fibre fractions. The reason for this unanticipated outcome is that, RILEM TC-162-TDF (2003) only considered the fibres slenderness ratios in the final crack spacing design formula, implying that the amount of fibres had no effect. And since the concrete tensile strength decreased with increasing fibre volume, such results were obtained.

The results from analysis of fibre reinforced concrete beams without ordinary reinforcement revealed that, very large amounts of fibres are needed in order to compensate the absence of ordinary reinforcement, as the largest fibre fraction of 0.75% was far from enough. Larger fibre fractions than the limit of 2% using the premix method, suggested by Bentur and Mindess (2006), are needed when using

fibre reinforced concrete with a softening behaviour. Considering other mixing methods and the use of fibre reinforced concrete elements with hardening material behaviour, is required in order for fibres to partly or entirely replace ordinary reinforcement.

4 Design of slab elements

In this chapter simply supported concrete slabs are designed, according to the FIB model code, in ultimate limit state. This is done for concrete slabs reinforced with ordinary reinforcement and for steel fibre reinforced concrete slabs.

4.1 FIB model code

For design of fibre reinforced concrete slab elements without ordinary reinforcement, subjected to bending actions, the FIB model code recommends the rigid plastic relationship, see Chapter 3 and in particular section 3.2.1. The rigid plastic model, proposed by the FIB model code, makes assumptions that the compressive force is concentrated in the top fibre of the section, see Figure 4.1. When using the rigid plastic model, f_{Ftu} is obtained from formula in equation (4.1), suggested by the FIB model code.

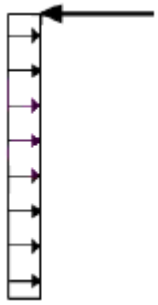

f_{Ftu}

Figure 4.1 Simplified model to determine the ultimate tensile strength, f_{Ftu}, from FIB model code

$$f_{Ftu} = \frac{f_{R3}}{3} \tag{4.1}$$

The moment resistance,m_{Rd}, for slab elements without ordinary reinforcement is calculated using the formula given in equation (4.2)

$$m_{Rd} = \frac{f_{Ftu}h^2}{2} \tag{4.2}$$

where

f_{Ftu} is the residual tensile strength of the fibres, calculated according to equation (4.1)

h is the height of the slab element

It should be noted that the moment resistance, m_{Rd}, in equation (4.2), is given in kNm/m.

4.2 Moment resistance

Simply supported slabs with distributed load, reinforced with 8 mm and 6 mm ordinary reinforcement bars with spacing 250 mm, were used as reference slabs when design of fibre reinforced concrete slabs without ordinary reinforcement was carried out, see Figure 4.2 and Figure 4.3. The moment resistance for the slabs with fibres was compared to the reference slabs in order to determine the effect of fibres. Due to difficulties in retrieving data on full scale fibre reinforced concrete slab experiments,

regarding fibre content and residual tensile strength, the results of the wedge splitting tests in chapter 3 were used.

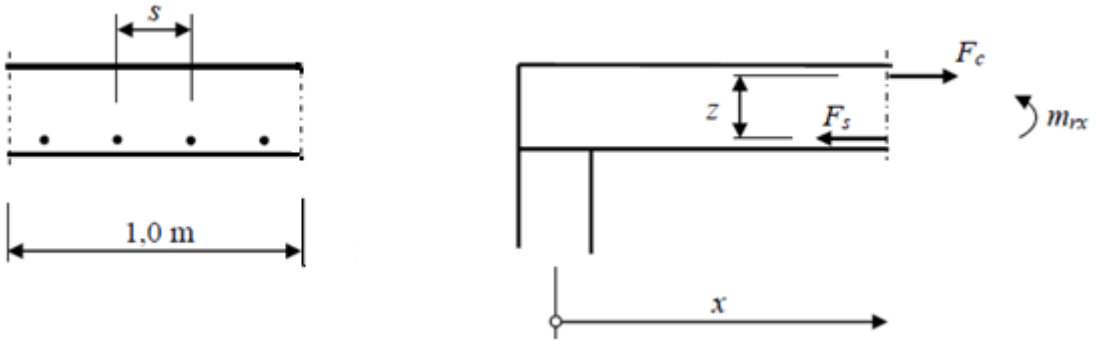

Figure 4.2 Slab cross-section in the x-direction, from Engström (2009)

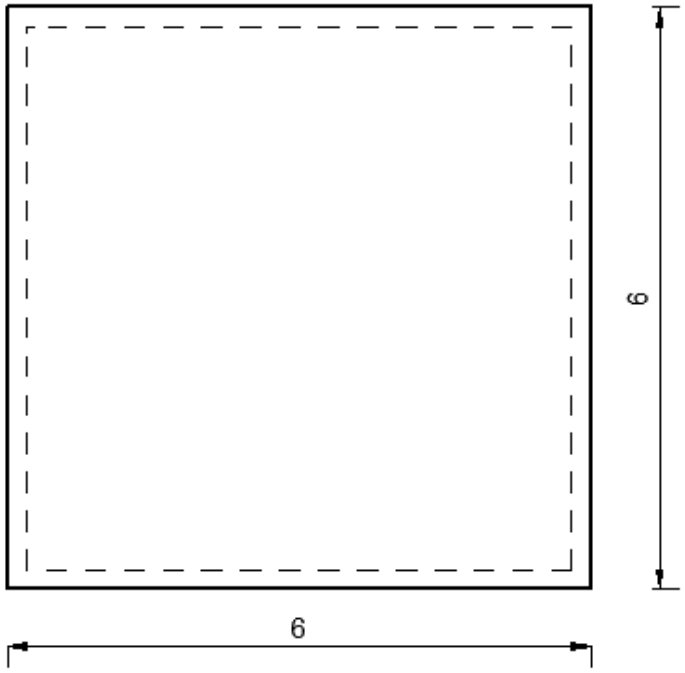

Figure 4.3 The designed simply supported slab, with dimensions in meters

The results obtained from the design, using the rigid plastic model proposed by the FIB model code, can be seen in Table 4.1. From Table 4.1 it is clear that the moment resistance increases with increasing fibre volume.

When compared with ordinary reinforced concrete slabs, it is clear that in order to substitute or replace ordinary reinforcement, large fibre fractions are needed. In Table 4.1, the moment resistances of the fibre reinforced concrete slabs are compared to the moment resistances of the reference slabs.

Table 4.1 Moment resistance results for slabs reinforced with fibres or ordinary reinforcement

V_f (%)	Reinforcement (mm)	Moment resistance (kNm/m)
0	ϕ8 s250	20.5
0	ϕ6 s250	12.9
0.25	-	3.0
0.50	-	4.5
0.75	-	6.4

No combination of fibres and ordinary reinforcement was done in this report, for the reason that, the FIB model code does not propose any methods for verification of moment resistance, for fibre reinforced concrete slabs with ordinary reinforcement. The FIB model code however states that it can be done using non-linear analysis.

Regarding shear resistance in slab members without ordinary reinforcement or prestressing, the FIB model code claims that the shear is not dominant unless there is a high load concentration close to the support.

4.3 Conclusion

Design of fibre reinforced concrete slab elements, revealed that fibres in low quantities have little influence on the moment resistance. It was more obvious in slab design than in beam design, that fibres are capable of replacing ordinary reinforcement entirely, if used in sufficient amounts as the increase of moment resistance with fibre volume was clearer. A benefit of using fibres in concrete slab elements is that only the direction with the maximum moment needs to be studied, since the moment resistance of fibre reinforced concrete is the same in all directions.

5 Discussion

The aim of the project was to detect possible difficulties, limitations and possibilities from the evaluated design codes.

Regarding difficulties, design in ultimate limit state has shown that a reduction of ordinary reinforcement and addition of fibres, for the fibre amounts used in this project, was far from enough. Design of elements without ordinary reinforcement proved that very large amounts of fibres are needed in order to compensate for the absence of ordinary reinforcement. According to Bentur and Mindess, the amount of fibres that can be applied using the premix method is limited to 2% which is in this evaluation not sufficient enough to partly or entirely replace ordinary reinforcement. Another difficulty is in the design of fibre reinforced concrete elements without ordinary reinforcement, where the design of shear resistance and crack width require further attention as no design suggestions are yet proposed.

Regarding serviceability limit state, for elements reinforced with ordinary reinforcement, the results obtained in this project revealed that fibres have a positive effect on crack control, as a reduction of the crack width was noticed with addition and increasing amounts of fibres.

With regard to limitations, concrete materials with strain hardening behaviour are required, according to the FIB model code, in order to carry out design on fibre reinforced concrete elements without ordinary reinforcement.

With sufficient fibre fractions, it is possible to adopt this method in more complex members, which are usually only designed to resist membrane forces not bending. Addition of sufficient amount fibres to a complex member would add a resistance to bending as well as controlling cracks.

In thin walled complex members where ordinary reinforcement is needed, there is a problem with regard to the positioning of the reinforcement, as the requirements for covering have to be met. This leads to a reduction of the effective depth of the reinforcement as the reinforcing bars have to be placed closer to the neutral axis of the cross section, thus the lever arm decreases and therefore, reducing the resisting moment. In this case addition of fibres in the mix could contribute to increased moment resistance as they are randomly scattered in the mix.

6 Conclusions

Fibre reinforced concrete requires large quantities of fibres in order to make a difference regarding resistance. According to Bentur and Mindess (2006), maximum about 2% fibre volume can be added using the premix method, due to difficulties in handling. This is the method that was applied for the experiments viewed in this report. The fibre fractions used for design in this report were up to 0.75%, which was not sufficient enough to partly or entirely replace ordinary reinforcement. From the results, it was obvious that fibre fractions much larger than 0.75% are needed in order to make a difference in capacity. It was however clear, that fibres had a considerable effect on crack width calculations in the serviceability limit state, where the crack width was decreased with more fibre fractions.

Experimental results on beam tests, performed by Gustafsson and Karlsson (2006), were used for comparison with design results obtained when designed according to, the FIB model code, RILEM TC-162-TDF (2003) and the Spanish EHE-08 in order to determine the accuracy of the design methods. The comparison showed that the different methods had little variation in the design results. When compared to the experimental results, underestimations, up to 12.5%, in ultimate moment resistances and both under- and overestimations in shear resistances, depending on the diameter of the ordinary reinforcement bars, were revealed. These over- underestimations might be caused by the use of the simplified linear post cracking behaviours, presented by the design codes and guidelines. It should also be mentioned that mean values of the experimental results were used due to the large variation in the material behaviour of the beam specimen. This variation in the ultimate moment resistance was up to 9.5% for beams with the same material properties and could also be a cause for the underestimations obtained.

Regarding accuracy, the FIB model code and the Spanish EHE-08 were most accurate with a correlation ratio of 0.97 compared to 0.96 for RILEM TC-162-TDF (2003).

Regarding applicability, the FIB model code was more complete compared to RILEM TC-162-TDF (2003) and the Spanish EHE-08, for the reason that, it was more detailed and clear. Unlike the other codes, the FIB model code also included ductility requirements and took the effect of fibres in crack width design more properly. For crack width design, RILEM TC-162-TDF (2003) only considered the slenderness ratio of the fibres, implying that fibre fractions had no effect on the final crack spacing, while the Spanish EHE-08 gave no suggestions for crack width calculations regarding fibre reinforced concrete. The FIB model code had also more limitations regarding design of fibre reinforced concrete elements without ordinary reinforcement, where the FIB model code required strain hardening materials for this design.

6.1 Further studies

In order to determine whether fibres can partly or entirely substitute ordinary reinforcement, more full scale tests with considerable amounts of fibres are needed. Experiments on strain hardening materials should also be considered, if fibres are to entirely replace ordinary reinforcement.

7 References

Bentur, A. and Mindess, S. (2006): *Fibre reinforced cementitious composites 2nd edition,* Taylor & Francis 2006.

Dupont, D, Vandewalle, CL. (2005): *Distribution of steel fibres in rectangular sections*. Cement and Concrete Composites 27, 2005, pp. 391-398.

EN 14651 (2005): T*est method for metallic fibered concrete – Measuring the flexural tensile strength (limit of proportionality (LOP), residual),* European Standard, pp. 18

Engström, B. (2009): *Design and analysis of slabs and flat slabs.* Department of Civil and Environmental Engineering, Division of Structural Engineering, Chalmers University of Technology, Göteborg, 2009.

fib (2010): *Model code 2010, first complete draft,* bulletin 55, vol. 1

fib (2010): *Model code 2010, first complete draft,* bulletin 56, vol. 2

fib (1999): *Structural concrete, Textbook on behaviour, Design and performance, updated knowledge of the CEB/FIP model code 1990,* bulletin 1, Vol. 1

fib (1999): *Structural concrete, Textbook on behaviour, Design and performance, updated knowledge of the CEB/FIP model code 1990,* bulletin 2, Vol. 2

fib (2009): *Structural concrete, Textbook on behaviour, Design and performance,* bulletin 51, Vol. 1

Gustafsson, M, Karlsson, S. (2006): *Fibre reinforced concrete structures – Analysis of crack spacing and crack width.* (In Swedish: Fiberarmerad betongkonstruktioner-analys av sprickavstånd och sprickbredd). Master's thesis, Department of Civil and Environmental Engineering, Division of Structural Engineering, Chalmers University of Technology, Göteborg, 2006.

Jansson, A. (2008): *Fibres in reinforced concrete structures- analysis, experiments and design.* Licentiate thesis, Department of Civil and Environmental Engineering, Division of Structural Engineering, Chalmers University of Technology, Göteborg, 2008.

Lutfi, A. (2004): *Steel fibrous cement based composites*. Ph.D. Thesis, Department of Civil and Architectural Engineering, Royal Institute of Technology, KTH, Stockholm, Sweden, 2004

Löfgren, I. (2005): *Fibre- reinforced concrete for industrial construction- a fracture mechanics approach to material testing and structural analysis.* Ph.D. Thesis. Department of Civil and Environmental Engineering, Division of Structural Engineering, Chalmers University of Technology, Göteborg, 2005.

Marcovic, I. (2006): *High-performance hybrid-fibre concrete*. Technical University of Delft, Delft, the Netherlands, 2006.

Naaman, A.E. (2003): *Engineered steel fibers with optimal properties for reinforcement of cement composites.* Journal of advanced concrete technology, Vol. 1, No. 3.

RILEM TC 162-TDF (2003): *Test and design methods for steel fibre reinforced concrete, σ-ε design method*. Materials and Structures, vol.36, pp. 560-567

Spanish EHE-08: *Code on structural concrete- articles and annexes.* Annex 14

Spanish EHE-08: *Code on structural concrete- articles and annexes.* Annex 17

Spanish EHE-08: *Code on structural concrete- articles and annexes.* Chapter 8

Spanish EHE-08: *Code on structural concrete- articles and annexes.* Chapter 10

Spanish EHE-08: *Code on structural concrete- articles and annexes.* Chapter 11

Özcan, DM et al. (2009*): Experimental and finite element analysis on the steel fiber-reinforced concrete (SFRC) beams ultimate behavior*. Construction and building materials 23, pp. 1064-1077

APPENDIX A: RESIDUAL TENSILE STRENGTH, ACCORDING TO RILEM TC-162 TDF (2003)

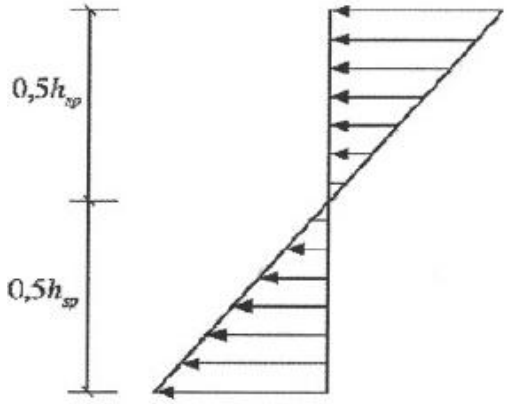

f_{R1}

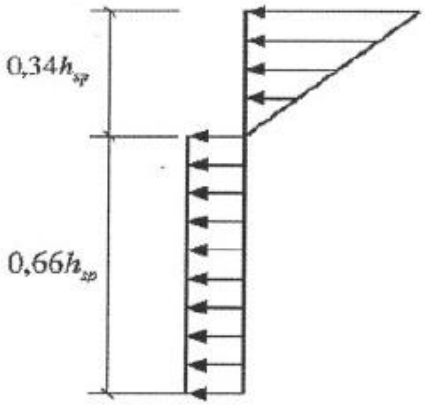

σ_1

f_{R1} and f_{R4} are calculated assuming linear elastic behaviour as shown in figure to the left. However, in reality the stress distribution is different. Rilem suggests assumptions as shown in the figure to the right meaning that the tensile stress in the cracked part of the steel fibre concrete section is constant.

The moment will be equal to:

$$M_1 = \frac{0.5 h_{sp} \cdot b}{2} \cdot \left(\frac{2}{3} \cdot 0.5 h_{sp} + \frac{2}{3} \cdot 0.5 h_{sp} \right) \cdot f_{R1}$$

$$M_2 = 0.66 h_{sp} \cdot b \cdot \left(\frac{0.66 h_{sp}}{2} + \frac{2}{3} \cdot 0.33 h_{sp} \right) \cdot \sigma_{f1}$$

$$M_1 = \frac{b \cdot h_{sp}^{\,2}}{6} \cdot f_{R1}$$

$$M_2 = 0.66 \cdot h_{sp} \cdot b \cdot 0.56 \cdot h_{sp} \cdot \sigma_{f1}$$

Requiring $M_1 = M_2$, σ_f can be expressed as:

$$\frac{b \cdot h_{sp}^{\,2}}{6} \cdot f_{R1} = 0.66 h_{sp} \cdot b \cdot 0.56 h_{sp} \cdot \sigma_{f1}$$

$$\sigma_{f1} = 0.45 \cdot f_{R1}$$

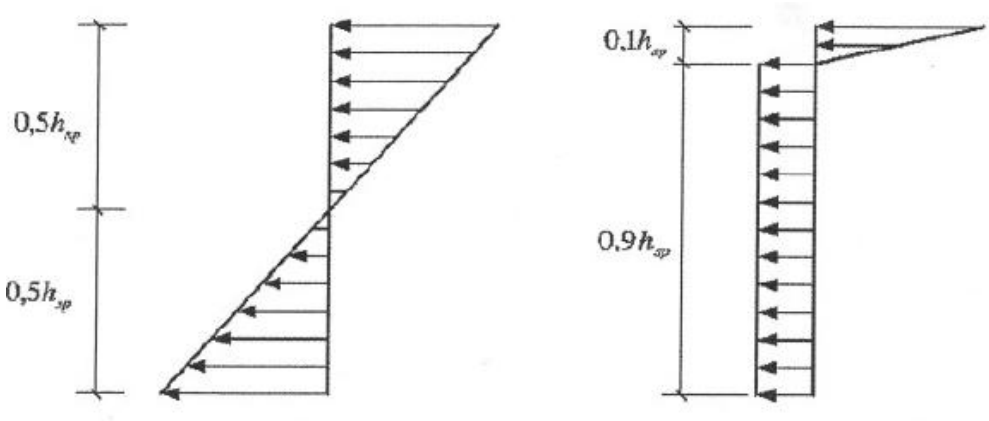

f_{R4} σ_4

The moment will be equal to:

$$M_1 = \frac{0.5h_{sp}\cdot b}{2}\cdot\left(\frac{2}{3}\cdot 0.5h_{sp} + \frac{2}{3}\cdot 0.5h_{sp}\right)\cdot f_{R4}$$

$$M_2 = 0.9h_{sp}\cdot b\cdot\left(\frac{0.9h_{sp}}{2} + \frac{2}{3}\cdot 0.1h_{sp}\right)\cdot\sigma_{f4}$$

$$M_1 = \frac{b\cdot h_{sp}^{\,2}}{6}\cdot f_{R4}$$

$$M_2 = 0.9\cdot h_{sp}\cdot b\cdot 0.51\cdot h_{sp}\cdot\sigma_{f4}$$

Requiring $M_1 = M_2$, σ_f can be expressed as:

$$\frac{b\cdot h_{sp}^{\,2}}{6}\cdot f_{R4} = 0.9h_{sp}\cdot b\cdot 0.51h_{sp}\cdot\sigma_{f4}$$

$$\sigma_{f4} = 0.37\cdot f_{R4}$$

APPENDIX B: RESIDUAL TENSILE STRENGTH, ACCORDING TO EHE-08

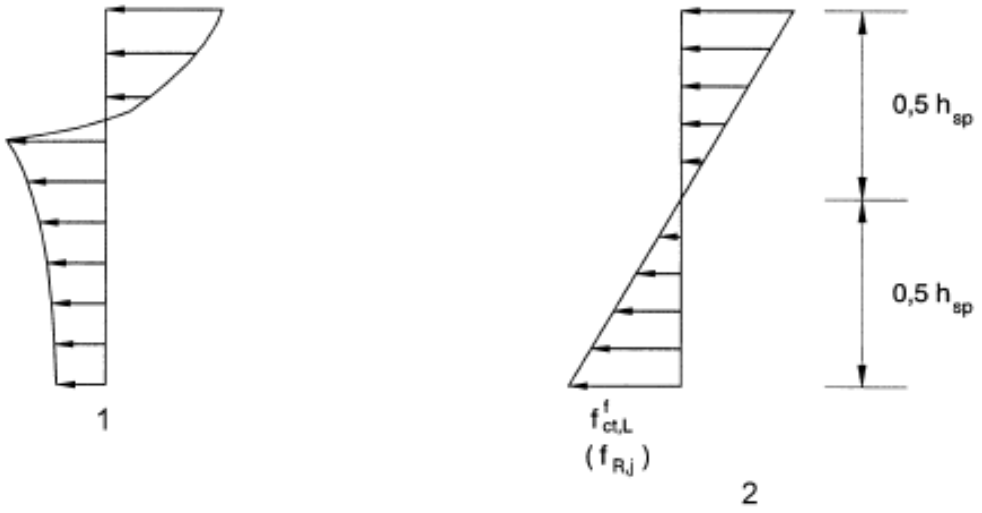

In order to get the residual flexural tensile strength f_{Rj}, the real stress distribution and behaviour in figure 1 is assumed to be linear as shown in figure 2.

The moment at midspan of a simply supported beam will be equal to:

$$M = \frac{F_j}{2} \cdot \frac{l}{2}$$

where,

F_j is the load corresponding to $CMOD_j$

l is the beam length

The residual flexural tensile stress will be:

$$f_{Rj} = \frac{M}{W}$$

where,

W is the section modulus

$$W = \frac{b \cdot h_{sp}^{2}}{6}$$

with b as the width of the beam and

h_{sp} is the height of the beam from the top of the notch

$$f_{Rj} = \frac{\frac{F_j}{2} \cdot \frac{l}{2}}{\frac{b \cdot h_{sp}^{2}}{6}}$$

$$f_{Rj} = \frac{3 \cdot F_j \cdot l}{2 \cdot b \cdot h_{sp}^{2}}$$

APPENDIX C: EXAMPLE OF VARIATION IN PROPERTIES OF THE SAME MATERIAL

An example of the variation in moment capacity of the experimental results, for the three beams of the same concrete fibre mix. In this particular case, it is series 2, 0.5% fibre volume and 8mm ordinary reinforcement bars.

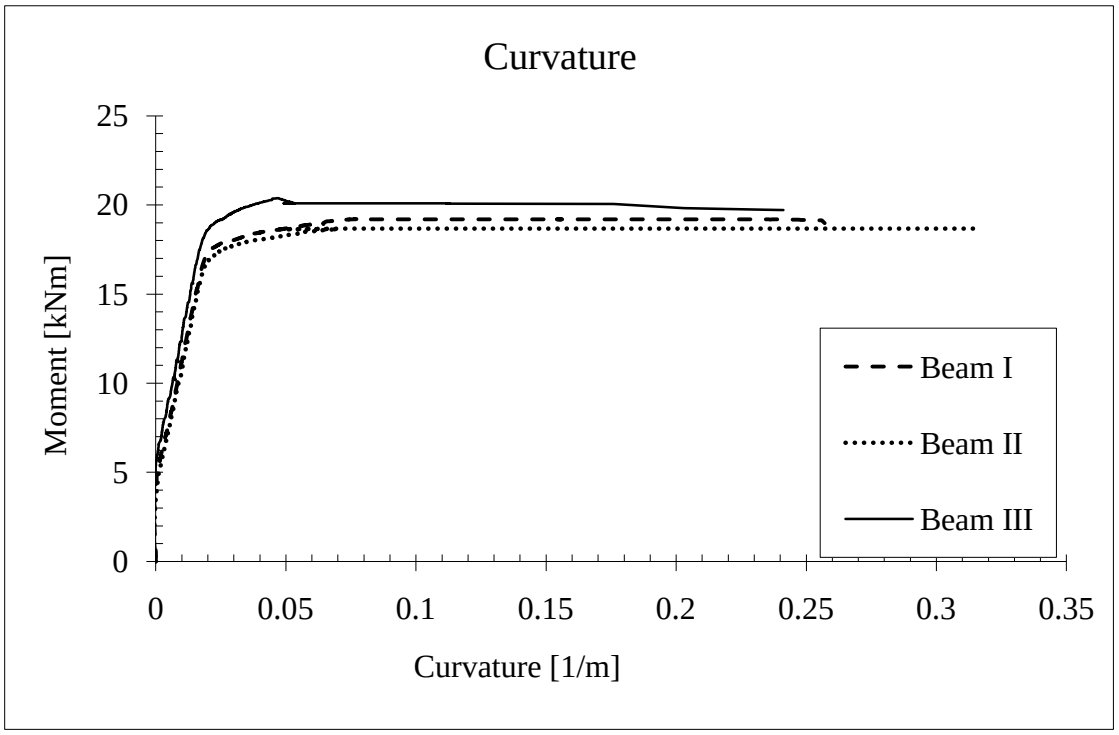

APPENDIX D: EXAMPLE FROM DESIGN OF BEAM ELEMENTS

FIB Model Code 2010:

BEAM SERIES 3: Vf 0.5%

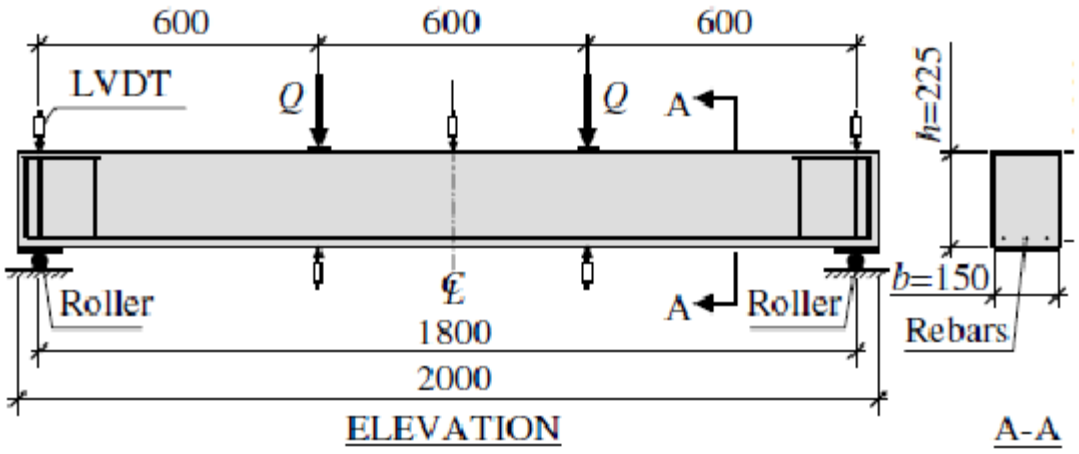

Beam Data used in experiments:

$b := 150mm$	width of the section
$h := 225mm$	height of the section
$d := 200mm$	distance to tension steel from top fibers
$l_s := 1800mm$	free span length
$l_t := 2040mm$	span length

Wedge Splitting tests:

$l_z := 100mm$	cube length
$h_z := 100mm$	cube height
$b_z := 100mm$	cube width

Materials:

Concrete:

$f_{ck3} := 37.7MPa$	strength from cube tests
$\gamma_c := 1.5$	parial safety factor for concrete

Conventional Reinforcing steel TEMPCORE:

$f_{sy} := 660MPa$ For 6mm dia bars

$f_{su} := 784MPa$

$\phi_s := 6mm$

$E_s := 200GPa$

$\varepsilon_y := \frac{f_{sy}}{E_s} = 3.3 \times 10^{-3}$

Steel Fibres Dramix RC-65/35-BN:

$V_f := 0.5$ percentage by volume of fibres in concrete matrix

$l_f := 35mm$ fibre length

$\phi := 0.55mm$ fibre diameter

$\eta_{b.exp} := 0.5$ fibre factor

Design:

$d = 200 \cdot mm$

$\phi_s := 6mm$

$A_{si} := \frac{\pi \cdot \phi_s^2}{4} = 28.274 \cdot mm^2$

$n := 3$

$A_s := n \cdot A_{si} = 84.823 \cdot mm^2$

Series 3:

$f_{ck3} := 37.7MPa$ Experimental result from cube tests

$f_{ck.cyl3} := 0.8 \cdot f_{ck3} = 30.16 \cdot MPa$ Equivalent cylinder strength

$f_{ctm3} := 0.3 \cdot \left(f_{ck.cyl3}\right)^{0.6}$

$f_{ctm3} := 2.8414887MPa$

$f_{cm3} := f_{ck.cyl3} + 8MPa = 38.16 \cdot MPa$

$E_{cm3} := 9500 \cdot \left(f_{cm3}\right)^{0.333}$

$E_{cm3} := 31.945\,GPa$

$\phi_s := 6mm$

$A_{si} := \frac{\pi \cdot \phi_s^2}{4} = 28.274 \cdot mm^2$

$n := 3$

$A_{s3} := n \cdot A_{si} = 84.823 \cdot mm^2$

$V_f := 0.5\%$ percentage by volume of fibres in concrete matrix

$F_1 := 3000N$ Load corresponding to CMOD=0.5

$F_4 := 2450N$ Load corresponding to CMOD=3.5

$F_3 := 2700N$ Load corresponding to CMOD=2.5

$F_L := 3.5kN$ Limit of proportionality

$a := 25mm$ height of notch

$h_{sp} := h_z - a = 0.075m$ h.sp is the distance of notch tip from top

$CMOD_1 := 0.5mm$

$CMOD_3 := 2.5mm$

Residual flexural tensile strength in SLS:

$f_{R1.exp} := 3 \cdot \frac{F_1 \cdot l_z}{2 \cdot b \cdot h_{sp}^2} = 0.533 \cdot MPa$

$\eta_{b.beam} := 0.5$ fibre effectivity factor

$f_{R1} := f_{R1.exp} \cdot \frac{\eta_{b.beam}}{\eta_{b.exp}} = 0.524 \cdot MPa$

Residual flexural tensile strength in ULS:

$f_{R3.exp} := 3 \cdot \frac{F_3 \cdot l_z}{2 \cdot b \cdot h_{sp}^2} = 0.48 \cdot MPa$

$$f_{R3} := f_{R3.exp} \cdot \frac{\eta_{b.beam}}{\eta_{b.exp}} = 0.471 \cdot MPa$$

$$f_{L.exp} := 3 \cdot \frac{F_L \cdot l_z}{2 \cdot b \cdot h_{sp}^2} = 0.622 \cdot MPa$$

$$f_L := f_{L.exp} \cdot \frac{\eta_{b.beam}}{\eta_{b.exp}} = 0.611 \cdot MPa$$

Fibre reinforced concrete can substitute the ordinary reinforcement in ultimate limit state if the relationships below are fulfilled.

$$\frac{f_{R1}}{f_L} > 0.4$$

$$\frac{f_{R3}}{f_{R1}} > 0.5$$

$\frac{f_{R1}}{f_L} = 0.857$ which is larger than 0.4 - OK

$\frac{f_{R3}}{f_{R1}} = 0.9$ which is larger than 0.5 - OK

Sectional Analysis:

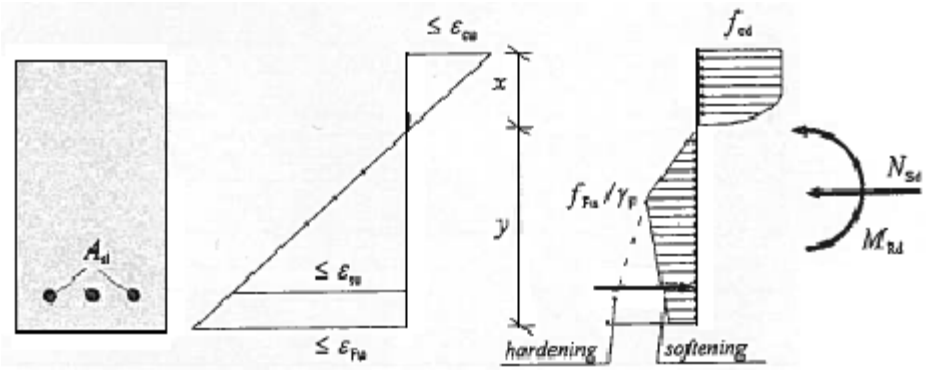

$f_{Fts3} := 0.45 \cdot f_{R1} = 0.236 \cdot MPa$ ultimate residual strength from Linear model

$\tau_{bm} := 1.8 \cdot f_{ctm3} = 5.115 \cdot MPa$ mean bond strength between reinforcement bars and concrete

$x_y := 32.567mm$ value calculated below in yield moment calculation

$$A_{c.ef} := \min\left[2.5 \cdot (h - d) \cdot b, \frac{(h - x_y)}{3} \cdot b\right]$$

$$A_{c.ef} = 9.375 \times 10^{-3}\,m^2$$

$$\rho_{s.ef} := \frac{A_{s3}}{A_{c.ef}} = 9.048 \times 10^{-3}$$

$$l_{s.max} := \frac{1}{4} \cdot \frac{(f_{ctm3} - f_{Fts3})}{\tau_{bm}} \cdot \frac{\phi_s}{\rho_{s.ef}} = 0.084\,m$$

$s_{rm} := \frac{2}{3} \cdot l_{s.max} = 0.056\,m$ average crack spacing for stabilized cracking

$y := h - x_y = 0.192\,m$

$l_{cs} := \min(s_{rm}, y)$ structural characteristic length

$l_{cs} = 0.056\,m$

$\varepsilon_{Fu} := 0.02$

$w_u := \varepsilon_{Fu} \cdot l_{cs} = 1.126 \cdot mm$ ultimate crack width

$f_{Ftu3} := f_{Fts3} - \frac{w_u}{CMOD_3} \cdot (f_{Fts3} - 0.5 \cdot f_{R3} + 0.2 \cdot f_{R1})$ ultimate residual strength from Linear model

$k := \frac{w_u}{CMOD_3}$

$f_{Ftu3} := 0.45 \cdot f_{R1} - k \cdot (0.45 \cdot f_{R1} - 0.5 \cdot f_{R3} + 0.2 \cdot f_{R1}) = 0.188\,MPa$

$\varepsilon_{SLS} := \frac{CMOD_1}{l_{cs}} = 8.879 \times 10^{-3}$ corresponds to f.Fts

$\varepsilon_{ULS} := \frac{w_u}{l_{cs}} = 0.02$ corresponds to f.Ftu

Details for the tensile stress block area and neutral axis:

$$p1 := \frac{\varepsilon_{SLS}}{\varepsilon_{ULS}} = 0.444$$

$$p2 := \frac{\varepsilon_{ULS} - \varepsilon_{SLS}}{\varepsilon_{ULS}} = 0.556$$

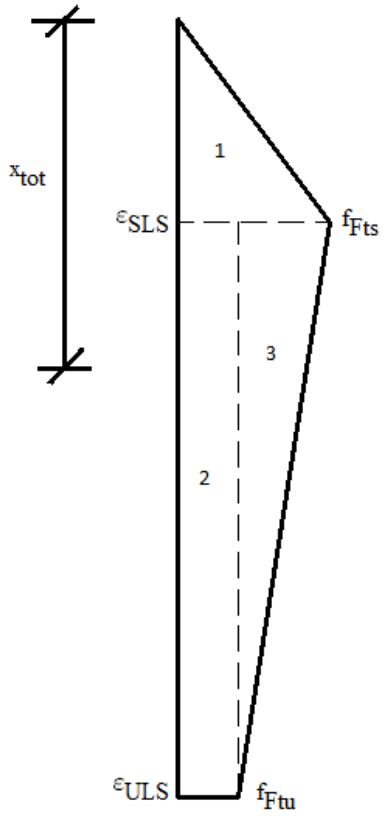

$$A_1 := \frac{1}{2} \cdot p1 \cdot f_{Fts3} = 0.052 \cdot \text{MPa}$$

$$A_2 := p2 \cdot f_{Ftu3} = 0.105 \cdot \text{MPa}$$

$$A_3 := \frac{1}{2} \cdot p2 \cdot \left(f_{Fts3} - f_{Ftu3}\right) = 0.013 \cdot \text{MPa}$$

$A_{tot} := A_1 + A_2 + A_3 = 0.17 \cdot \text{MPa}$ A.tot is the total stress of the tensile stress block

Neutral axis for individual areas:

$$x_1 := \frac{2}{3} \cdot p1 = 0.296$$

$$x_2 := \frac{1}{2} \cdot p2 = 0.278$$

$$x_3 := \frac{1}{3} \cdot p2 = 0.185$$

Neutral axis for the Tensile stress block:

$$x_{tot} \cdot A_{tot} = A_1 \cdot x_1 + A_2 \cdot x_2 + A_3 \cdot x_3$$

$$x_{tot} := \frac{A_1 \cdot x_1 + A_2 \cdot x_2 + A_3 \cdot x_3}{A_{tot}} = 0.276$$ it is 0.276 of the total tensile stress block height.

Cracking moment:

$$W_1 := \frac{b \cdot h^2}{6} = 1.266 \times 10^{-3}\, m \cdot m^2$$ section modulus

According to eq.3.3-65, FIB model code bulletin 51, the cracking moment is:

$$M_{cr} := W_1 \cdot f_{ctm3}$$

$$M_{cr} = 3.596 \cdot kN \cdot m$$

Yield Moment:

Horizontal Equilibrium:

Yielding starts when $\varepsilon_s = \varepsilon_{sy}$

$$f_{Ft} := A_{tot}$$

$$\sigma_{c3} := E_{cm3} \cdot \varepsilon_{c3}$$

$$\varepsilon_{sy} := \frac{f_{sy}}{E_s} = 3.3 \times 10^{-3}$$

$$\sigma_{c3} := E_{cm3} \cdot \left[\frac{\varepsilon_{sy}}{\left(\frac{d - x_y}{x_y} \right)} \right]$$

$$\frac{1}{2} \cdot b \cdot x_y \cdot \sigma_{c3} = f_{sy} \cdot A_{s3} + f_{Ft} \cdot b \cdot (h - x_y)$$

$$x_y := 0.1m$$

Given

$$\frac{1}{2} \cdot b \cdot x_y \cdot \left[E_{cm3} \cdot \left[\frac{\varepsilon_{sy}}{\left(\frac{d - x_y}{x_y} \right)} \right] \right] = f_{sy} \cdot A_{s3} + f_{Ft} \cdot b \cdot (h - x_y)$$

$x_y := \text{Find}(x_y)$

$x_y = 35.566 \cdot mm$

$$\varepsilon_{c3} := \frac{\varepsilon_{sy}}{\left(\frac{d - x_y}{x_y}\right)} = 7.138 \times 10^{-4}$$

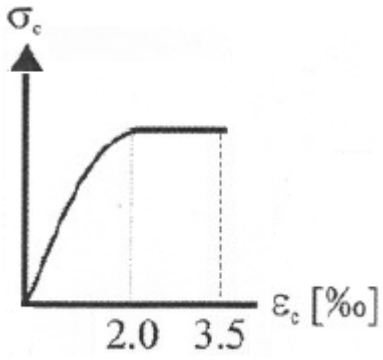

$\varepsilon_{c3} = 0.71 \cdot 10^{-3} < 2.0 \cdot 10^{-3}$ the compressive stress block is triangular

$$\frac{1}{2} \cdot b \cdot x_y \cdot \left[E_{cm3} \cdot \left[\frac{\varepsilon_{sy}}{\left(\frac{d - x_y}{x_y}\right)} \right] \right] = f_{sy} \cdot A_{s3} + f_{Ft} \cdot b \cdot (h - x_y)$$

$$M_{Rdy} := f_{sy} \cdot A_{s3} \cdot \left(d - \frac{2x_y}{3}\right) + f_{Ft} \cdot (h - x_y) \cdot b \cdot \left[\frac{2x_y}{3} + x_{tot} \cdot (h - x_y)\right]$$

$M_{Rdy} = 10.237 \cdot kN \cdot m$

Ultimate Moment:

Horizontal Equilibrium:

$$\frac{2}{3} \cdot b \cdot x_u \cdot f_{cm3} = f_{sy} \cdot A_{s3} + f_{Ft} \cdot b \cdot (h - x_u)$$

$x_u := 0.1mm$

Given

$$\frac{2}{3} \cdot b \cdot x_u \cdot f_{cm3} = f_{sy} \cdot A_{s3} + f_{Ft} \cdot b \cdot (h - x_u)$$

$x_u := \text{Find}(x_u)$

$x_u = 16.069 \cdot mm$

$\beta := 0.5$

$M_{Rdu} := f_{sy} \cdot A_{s3} \cdot \left(d - \beta x_u\right) + f_{Ft} \cdot \left(h - x_u\right) \cdot b \cdot \left[\beta \cdot x_u + x_{tot} \cdot \left(h - x_u\right)\right]$

$M_{Rdu} = 11.041 \cdot kN \cdot m$

Ductility:

Ductility requirements are satisfied when the need for minimum reinforcement is fulfilled.

$A_{s.min} = k_c \cdot k \cdot \left(f_{ctm3} - f_{Fts3}\right) \cdot \frac{A_{ct}}{\sigma_s}$

$k_c := 1$ for rectangular cross sections; k.c is the factor taking into account the stress distribution in the cross section just before cracking and the change of inner lever arm

$k := 1$ is the factor taking into account non-uniform self-equilibrating stresses leading to reduction of cracking force

$A_{ct} := b \cdot \left(h - x_u\right) = 0.031 m^2$ is the area of the tensile part of concrete cross section

$\sigma_s := f_{sy}$ is the maximum tensile reinforcement at cracking stage

$A_{s.min} := k_c \cdot k \cdot \left(f_{ctm3} - f_{Fts3}\right) \cdot \frac{A_{ct}}{\sigma_s}$

$A_{s.min} = 123.737 \cdot mm^2$

$A_{s3} = 84.823 \cdot mm^2$

$A_{s3} < A_{s.min}$ Ductility requirements not fulfilled

In all FRC structures without minimum conventional reinforcement, one of the following conditions has to be fulfilled.

$\delta_u \geq 20 \cdot \delta_{SLS}$

$\delta_{peak} \geq 5 \cdot \delta_{SLS}$

$\delta_{SLS} := 1mm$ displacement at service load when computed by performing a linear elastic analysis with assumption of uncracked conditions and initial elastic Young's modulus

$\delta_{peak} := 19mm$ displacement at maximum load

$\delta_u := 24mm$ ultimate displacement

$\frac{\delta_u}{\delta_{SLS}} = 24$ $24 > 20$ so ductility fulfilled

$\frac{\delta_{peak}}{\delta_{SLS}} = 19$ $19 > 5$ so ductility fulfilled

CURVATURES:

Curvature at Cracking:

$$\varepsilon_r := \frac{f_{ctm3}}{E_{cm3}} = 8.895\times 10^{-5}$$

$$k_{cr} := \frac{\varepsilon_r}{\frac{h}{2}} = 7.907\times 10^{-4}\,m^{-1}$$

Curvature at Yielding:

$$k_0 := \frac{\varepsilon_{c3}}{x_y} = 0.02\,m^{-1}$$

Ultimate Curvature:

$$\varepsilon_{cu} := 3.5\cdot 10^{-3}$$

$$k := \frac{\varepsilon_{cu}}{x_u} = 0.218\,m^{-1}$$

$$M := \begin{pmatrix} 0 \\ 3.596 \\ 10.665 \\ 11.098 \end{pmatrix} kN\cdot m \qquad k_t := \begin{pmatrix} 0 \\ 7.907\cdot 10^{-4} \\ 0.02 \\ 0.218 \end{pmatrix} \frac{1}{m}$$

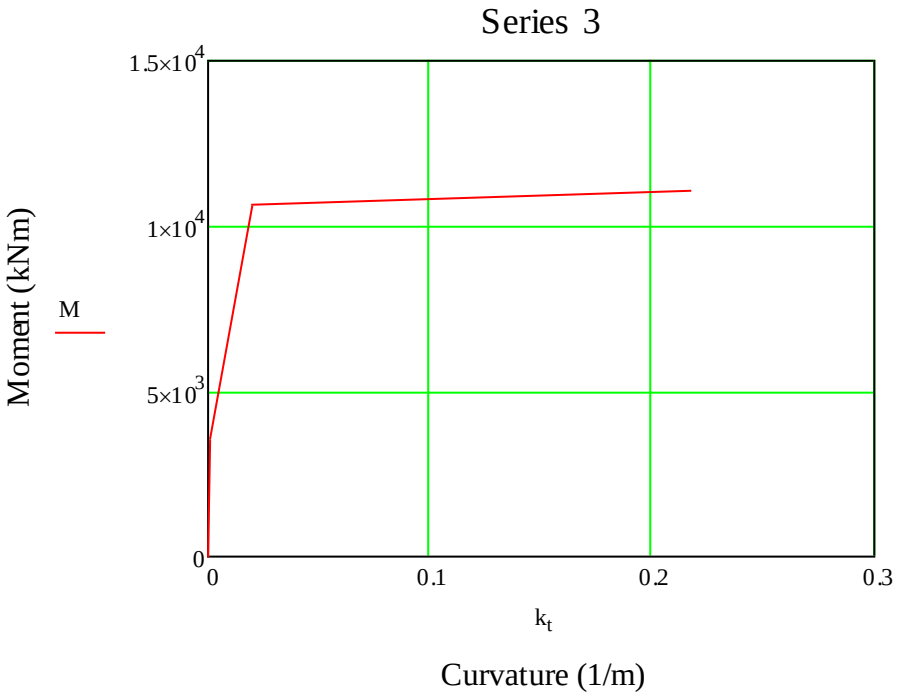

SHEAR CAPACITY:

Series 3

$\gamma_c := 1.5$ partial safety factor for the concrete without fibres

$d_1 := 200$ effective depth in mm

$b := 150 \cdot mm$

$k := 1 + \sqrt{\frac{200}{d_1}}$

$k = 2$

$\phi_s := 6mm$

$A_{si} := \frac{\pi \cdot \phi_s^2}{4} = 28.274 \cdot mm^2$

$n := 3$

$A_{s3} := n \cdot A_{si} = 84.823 \cdot mm^2$

$\rho_1 := \frac{A_{s3}}{b \cdot d}$

$\rho_1 = 2.827 \times 10^{-3}$

$w_u := 1.5mm$ for shear design according to FIB. Refer to section 7.7.3.2.2

$f_{Ftu3} := f_{Fts3} - \frac{w_u}{CMOD_3} \cdot \left(f_{Fts3} - 0.5 \cdot f_{R3} + 0.2 \cdot f_{R1}\right)$

$f_{Ftu3} = 0.173 \cdot MPa$

$\sigma_{cp} := 0$ no axial force or prestressing

$$V_{Rd} := \left[0.18 \cdot k \cdot \left[100 \cdot \rho_1 \cdot \left(1 + 7.5 \cdot \frac{f_{Ftu3}}{f_{ctm3}}\right) \cdot f_{ck.cyl3}\right]^{\frac{1}{3}} + 0.15 \cdot \sigma_{cp}\right] \cdot b \cdot d$$

$$V_{Rd} := \left[0.18 \cdot 2 \cdot \left[100 \cdot \rho_1 \cdot (1 + 7.5 \cdot 0.061) \cdot 30.16\right]^{\frac{1}{3}} + 0.15 \cdot \sigma_{cp}\right] \cdot 150 \cdot 200 = 2.502 \times 10^4$$

$V_{Rd} = 2.502 \times 10^{4}$ in Newton

$\nu_{min} := 0.035 \cdot k^{\frac{3}{2}} \cdot f_{ck.cyl3}^{\frac{1}{2}}$

$\nu_{min} := 0.035 \cdot k^{\frac{3}{2}} \cdot 30.16^{\frac{1}{2}} = 0.544$

$\nu_{min} = 0.544$ in Newton

$V_{Rd.Fmin} := (\nu_{min} + 0.15 \cdot \sigma_{cp}) \cdot b \cdot d$

$V_{Rd.Fmin} := (\nu_{min} + 0.15 \cdot \sigma_{cp}) \cdot 150 \cdot 200$

$V_{Rd.Fmin} = 1.631 \times 10^{4}$ in Newton

$V_{Rd.F3} := \max(V_{Rd}, V_{Rd.Fmin})$

$V_{Rd.F3} = 2.502 \times 10^{4}$ in Newton

CRACK WIDTH:

Series 3

$\alpha_{e3} := \frac{E_s}{E_{cm3}} = 6.261$

From Area balance in state-II:

$\frac{b \cdot x_{II.3}^{2}}{2} = \alpha_{e3} \cdot A_{s3} \cdot (d - x_{II.3})$

$x_{II.3} := 0.1mn$

Given

$\frac{b \cdot x_{II.3}^{2}}{2} = \alpha_{e3} \cdot A_{s3} \cdot (d - x_{II.3})$

$x_{II.3} := \text{Find}(x_{II.3})$

$x_{II.3} = 34.258 \cdot mm$

Moment of Inertia in state-II

$$I_{II.3} := \frac{b \cdot x_{II.3}^{3}}{3} + b \cdot x_{II.3} \cdot \left(x_{II.3} - \frac{x_{II.3}}{2}\right)^{2} + \alpha_{e3} \cdot A_{s3} \cdot \left(d - x_{II.3}\right)^{2} = 1.811 \times 10^{-5}\, m^{4}$$

$z_s := d - x_{II.3} = 0.166m$ for stress at steel level

Stabilized cracking is reached when the moment is between cracking and yield moment. To make a fair comparison between the design crack widths, a moment of 15kNm is used for series 1 and 2 and a moment of 10 kNm is used for series 3,4 and 5.

$M_{345} := 10kN \cdot m$

$$\sigma_{c3} := \frac{M_{345}}{I_{II.3}} \cdot z_s = 91.539 \cdot MPa$$ Concrete Stress

$\sigma_{s3} := \alpha_{e3} \cdot \sigma_{c3} = 573.102 \cdot MPa$ Steel Stress in a crack

From eq.7.7-12 of FIB Model code 2010, the general equation for design value of crack width is:

$$w_d := \frac{1}{2} \cdot \frac{\phi_s}{\rho_{s.ef}} \cdot \frac{\left(f_{ctm3} - f_{Fts3}\right)}{\tau_{bm}} \cdot \left(\sigma_{s3} - \beta \cdot \sigma_{sr} + \eta_r \cdot \varepsilon_r \cdot E_s\right)$$

For short term: $\eta_r := 0$

The equation is reduced to:

$$w_d := \frac{1}{2} \cdot \frac{\phi_s}{\rho_{s.ef}} \cdot \frac{\left(f_{ctm3} - f_{Fts3}\right)}{\tau_{bm}} \cdot \left(\sigma_{s3} - \beta \cdot \sigma_{sr}\right)$$

$$A_{c.ef} := \min\left[2.5 \cdot (h - d) \cdot b, \frac{\left(h - x_{II.3}\right)}{3} \cdot b\right]$$

$A_{c.ef} = 9.375 \times 10^{-3}\, m^{2}$

$$\rho_{s.ef} := \frac{A_{s3}}{A_{c.ef}} = 9.048 \times 10^{-3}$$

$$\rho_s := \frac{A_{s3}}{b \cdot d} = 2.827 \times 10^{-3}$$

$$\sigma_{sr} := \frac{f_{ctm3}}{\rho_{s.ef}} \cdot \left(1 + \alpha_{e3} \cdot \rho_s\right) = 319.613 \cdot MPa$$

$\beta := 0.6$ From table 7.6-2 FIB model code

$$\tau_{bm} := 1.8 \cdot f_{ctm3} = 5.115 \cdot MPa$$

$$w_d := \frac{1}{2} \cdot \frac{\phi_s}{\rho_{s.ef}} \cdot \frac{\left(f_{ctm3} - f_{Fts3}\right)}{\tau_{bm}} \cdot \left(\sigma_{s3} - \beta \cdot \sigma_{sr}\right) \cdot \frac{1}{E_s} = 0.322 \cdot mm$$

APPENDIX E: EXAMPLE FROM DESIGN OF BEAM ELEMENTS

RILEM TC-162 TDF (2003):

BEAM SERIES 4: Vf 0.25%

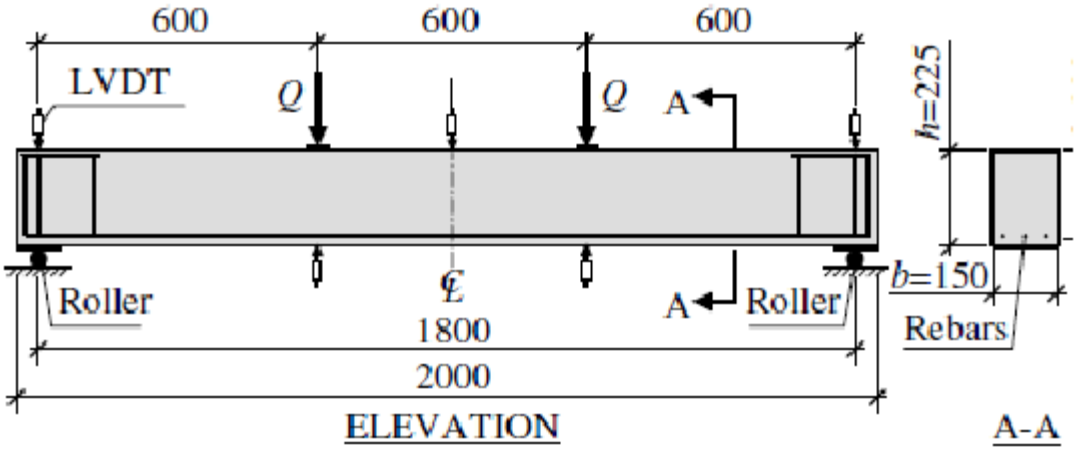

Beam Data used in experiments:

$b := 150mm$	width of the section
$h := 225mm$	height of the section
$d := 200mm$	distance to tension steel from top fibers
$l_s := 1800mm$	free span length
$l_t := 2040mm$	span length

Wedge Splitting tests:

$l_z := 100mm$	cube length
$h_z := 100mm$	cube height
$b_z := 100mm$	cube width

Materials:

Concrete:

$f_{ck.4} := 39.2MPa$	strength from cube tests
$\gamma_c := 1.5$	parial safety factor for concrete

Conventional Reinforcing steel TEMPCORE:

$f_{sy} := 660MPa$ For 8mm dia bars

$f_{su} := 784MPa$

$\phi_s := 6mm$

$E_s := 200GPa$

$\varepsilon_y := \frac{f_{sy}}{E_s} = 3.3 \times 10^{-3}$

Steel Fibres Dramix RC-65/35-BN:

$V_f := 0.25$ percentage by volume of fibres in concrete matrix

$L := 35mm$ fibre length

$\phi := 0.55mm$ fibre diameter

$\eta_{b.exp} := 0.49$ fibre factor

Design:

$d = 200mm$

$\phi_s := 6mm$

$A_{si} := \frac{\pi \cdot \phi_s^2}{4} = 28.274mm^2$

$n := 3$

$A_{s4} := n \cdot A_{si} = 84.823mm^2$

Series 4:

$f_{ck4} := 39.2MPa$ Experimental result from cube tests

$f_{ck.cyl4} := 0.8 \cdot f_{ck4} = 31.36MPa$ Equivalent cylinder strength

$f_{ctm4} := 0.3\left(f_{ck.cyl4}\right)^{\frac{2}{3}}$ from RILEM section 2.2

$f_{ctm4} := 2.98336MPa$

$f_{cm4} := f_{ck.cyl4} + 8MPa = 39.36\,MPa$

$E_{cm4} := 9500\left(f_{cm4}\right)^{\frac{1}{3}}$

$E_{cm4} := 32.32GPa$

$V_{f4} := 0.25\%$ percentage by volume of fibres in concrete matrix

$F_1 := 1900N$ Load corresponding to CMOD=0.5

$F_4 := 1400N$ Load corresponding to CMOD=3.5

$F_3 := 1600N$ Load corresponding to CMOD=2.5

$a := 25mm$ notch height

$h_{sp} := h_z - a = 0.075m$ h.sp is the distance of notch tip from top.

$CMOD_3 := 2.5mm$

$CMOD_4 := 3.5mm$

Residual flexural tensile strength in SLS:

$$f_{R1} := 3\cdot\frac{F_1\cdot l_z}{2\cdot b\cdot h_{sp}^{\,2}} = 0.338MPa$$

$\eta_{b.beam} := 0.54$ fibre effectivity factor

$$f_{R1.beam} := f_{R1}\cdot\frac{\eta_{b.beam}}{\eta_{b.exp}} = 0.372MPa$$

Residual flexural tensile strength in ULS:

$$f_{R4} := 3\cdot\frac{F_4\cdot l_z}{2\cdot b\cdot h_{sp}^{\,2}} = 0.249MPa$$

$$f_{R4.beam} := f_{R4}\cdot\frac{\eta_{b.beam}}{\eta_{b.exp}} = 0.274MPa$$

$$f_{R3} := 3 \cdot \frac{F_3 \cdot l_s}{2 \cdot b \cdot h_{sp}^{\,2}} = 5.12\,\text{MPa}$$

Tensile strength decreasing due to softening behaviour

Sectional Analysis:

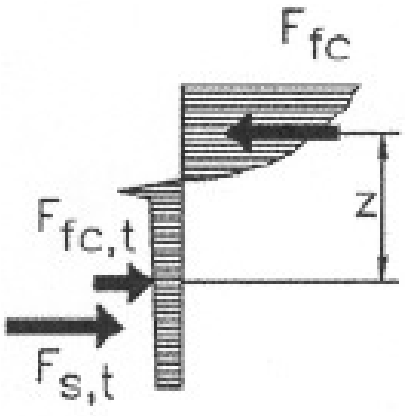

$h_1 := 22.5$ height in cm

$k_h := 1.0 - 0.6 \frac{h_1 - 12.5}{47.5} = 0.874$ size factor for $12.5 \le h_1 \le 60$ (cm)

$\sigma_2 := 0.45 \cdot f_{R1.beam} \cdot k_h = 0.146\,\text{MPa}$ serviceability residual strength from Linear model

$\sigma_3 := 0.37 \cdot f_{R4.beam} \cdot k_h = 0.089\,\text{MPa}$ ultimate residual strength from Linear model

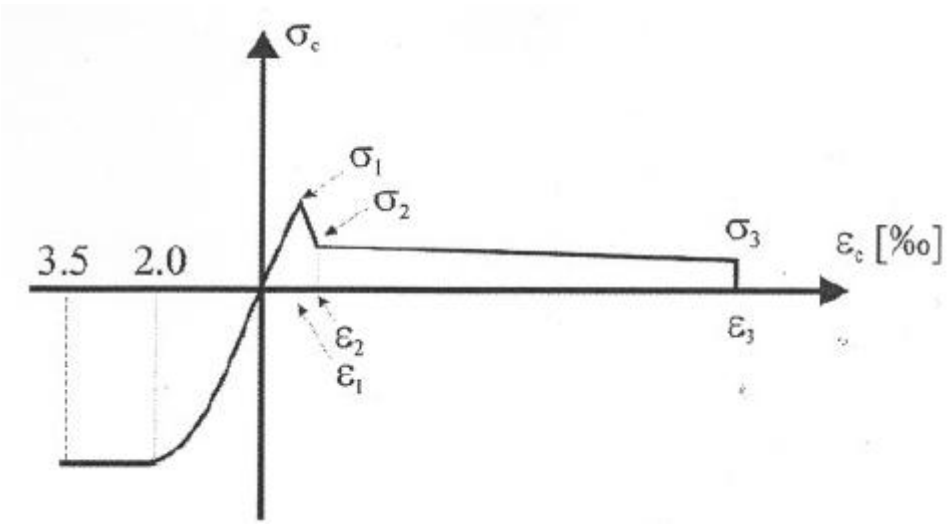

$d_1 := 0.2$ effective depth in m

$\sigma_1 := 0.7 \cdot f_{ctm4} \cdot (1.6 - d_1) = 2.924\,MPa$

$\varepsilon_1 := \frac{\sigma_1}{E_{cm4}} = 9.046 \times 10^{-5}$

$\varepsilon_2 := \varepsilon_1 + \frac{0.1}{1000} = 1.905 \times 10^{-4}$

$\varepsilon_3 := 0.025$

Details for the tensile stress block area and neutral axis:

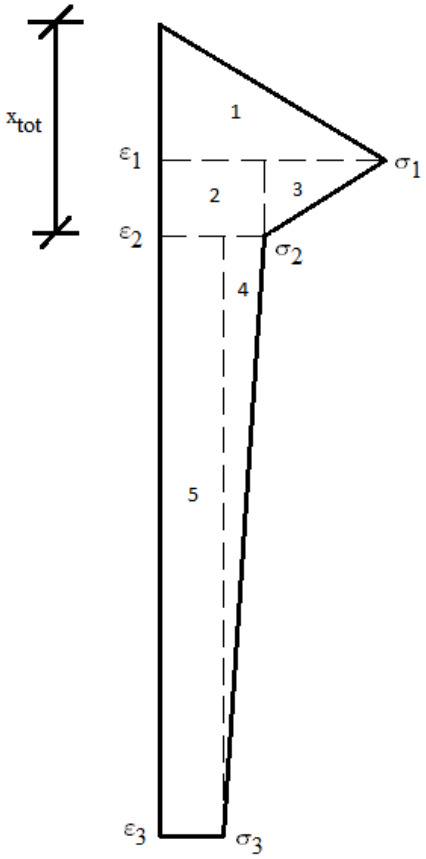

$p1 := \frac{\varepsilon_1}{\varepsilon_3} = 3.618 \times 10^{-3}$

$p2 := \frac{\varepsilon_2 - \varepsilon_1}{\varepsilon_3} = 4 \times 10^{-3}$

$$p3 := \frac{\varepsilon_3 - \varepsilon_2}{\varepsilon_3} = 0.992$$

$$A_1 := \frac{1}{2}\cdot p1\cdot\sigma_1 = 5.29\times 10^{-3}\cdot MPa$$

$$A_2 := p2\cdot\sigma_2 = 5.854\times 10^{-4}\cdot MPa$$

$$A_3 := \frac{1}{2}\cdot p2\cdot\left(\sigma_1 - \sigma_2\right) = 5.555\times 10^{-3}\cdot MPa$$

$$A_4 := \frac{1}{2}\cdot p3\cdot\left(\sigma_2 - \sigma_3\right) = 0.029 MPa$$

$$A_5 := p3\cdot\sigma_3 = 0.088 MPa$$

$$A_{tot} := A_1 + A_2 + A_3 + A_4 + A_5 = 0.128 MPa$$

A.tot is the total stress of the tensile stress block

Neutral axis for individual areas:

$$x_1 := \frac{2}{3}\cdot p1 = 2.412\times 10^{-3}$$

$$x_2 := \frac{1}{2}\cdot p2 = 2\times 10^{-3}$$

$$x_3 := \frac{1}{3}\cdot p2 = 1.333\times 10^{-3}$$

$$x_4 := \frac{1}{3}\cdot p3 = 0.331$$

$$x_5 := \frac{1}{2}\cdot p3 = 0.496$$

Neutral axis for the Tensile stress block:

$$x_{tot}\cdot A_{tot} = A_1\cdot x_1 + A_2\cdot x_2 + A_3\cdot x_3 + A_4\cdot x_4 + A_5\cdot x_5$$

$$x_{tot} := \frac{A_1\cdot x_1 + A_2\cdot x_2 + A_3\cdot x_3 + A_4\cdot x_4 + A_5\cdot x_5}{A_{tot}} = 0.415$$

It is 0.415 of the total tensile stress block height.

Cracking moment:

$W_b := \frac{b \cdot h^2}{6} = 1.266 \times 10^{-3}\, m \cdot m^2$ section modulus

$M_f := W_b \cdot \sigma_1$

$M_f = 3.7 \cdot kN \cdot m$

Yield Moment:

Horizontal Equilibrium:

Yielding starts when $\varepsilon_s = \varepsilon_{sy}$

$\varepsilon_{sy} := \frac{f_{sy}}{E_s} = 3.3 \times 10^{-3}$

The mean stress of the tensile stress block is equal to the area of the stress block:

$\sigma_m := A_{tot}$

$\sigma_m = 0.128\, MPa$

$\sigma_{c4} := E_{cm4} \cdot \varepsilon_{c4}$

$\sigma_{c4} := E_{cm4} \cdot \left[\frac{\varepsilon_{sy}}{\left(\frac{d - x_{y4}}{x_{y4}} \right)} \right]$

$\frac{1}{2} \cdot b \cdot x_{y4} \cdot \sigma_{c4} = f_{sy} \cdot A_{s4} + \sigma_m \cdot b \cdot (h - x_{y4})$

$x_{y4} := 0.1 mm$

Given

$\frac{1}{2} \cdot b \cdot x_{y4} \cdot \left[E_{cm4} \cdot \left[\frac{\varepsilon_{sy}}{\left(\frac{d - x_{y4}}{x_{y4}} \right)} \right] \right] = f_{sy} \cdot A_{s4} + \sigma_m \cdot b \cdot (h - x_{y4})$

$x_{y4} := \text{Find}(x_{y4})$

$x_{y4} = 35.065 mm$

$$\varepsilon_{c4} := \frac{\varepsilon_{sy}}{\left(\frac{d - x_{y4}}{x_{y4}}\right)} = 7.016 \times 10^{-4}$$

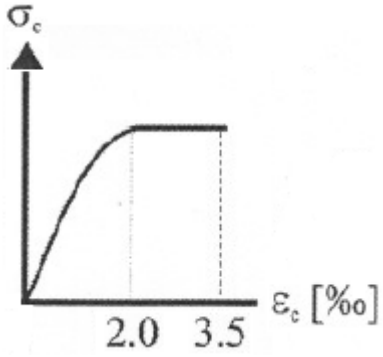

$\varepsilon_{c3} = 0.7 \cdot 10^{-3} < 2.0 \cdot 10^{-3}$ the compressive stress block is triangular

$$M_{Rdy4} := f_{sy} \cdot A_{s4} \cdot \left(d - \frac{2x_{y4}}{3}\right) + \sigma_m \cdot (h - x_{y4}) \cdot b \cdot \left[\frac{2x_{y4}}{3} + x_{tot} \cdot (h - x_{y4})\right]$$

$M_{Rdy4} = 10.261 \cdot kN \cdot m$

Ultimate Moment:

$\frac{2}{3} \cdot b \cdot x_{u4} \cdot f_{cm4} = f_{sy} \cdot A_{s4} + \sigma_m \cdot b \cdot (h - x_{u4})$ area of parabolic stress block is approximately 2/3 the area of rectangular stress block

$x_{u4} := 0.1mm$

Given

$$\frac{2}{3} \cdot b \cdot x_{u4} \cdot f_{cm4} = f_{sy} \cdot A_{s4} + \sigma_m \cdot b \cdot (h - x_{u4})$$

$x_{u4} := \text{Find}(x_{u4})$

$x_{u4} = 15.247mm$

$\beta := 0.5$

$$M_{Rdu4} := f_{sy} \cdot A_{s4} \cdot (d - \beta \cdot x_{u4}) + \sigma_m \cdot (h - x_{u4}) \cdot b \cdot [\beta \cdot x_{u4} + x_{tot} \cdot (h - x_{u4})]$$

$M_{Rdu4} = 11.096 kN \cdot m$

Curvatures:

$$A_c := b \cdot h = 0.034 m^2$$

$$\alpha := \frac{E_s}{E_{cm4}} = 6.188$$

Curvature at Cracking:

$$\varepsilon_r := \frac{\sigma_1}{E_{cm4}} = 9.046 \times 10^{-5}$$

$$k_{cr} := \frac{\varepsilon_r}{\frac{h}{2}} = 8.041 \times 10^{-4} \frac{1}{m}$$

Curvature at Yielding:

$$k_0 := \frac{\varepsilon_{c4}}{x_{y4}} = 0.02 \frac{1}{m}$$

Ultimate Curvature:

$$\varepsilon_{cu} := 3.5 10^{-3}$$

$$k := \frac{\varepsilon_{cu}}{x_{u4}} = 0.23 \frac{1}{m}$$

$$M := \begin{pmatrix} 0 \\ 3.7 \\ 10.848 \\ 11.151 \end{pmatrix} kN \cdot m \qquad k_t := \begin{pmatrix} 0 \\ 8.041 10^{-4} \\ 0.019 \\ 0.23 \end{pmatrix} \frac{1}{m}$$

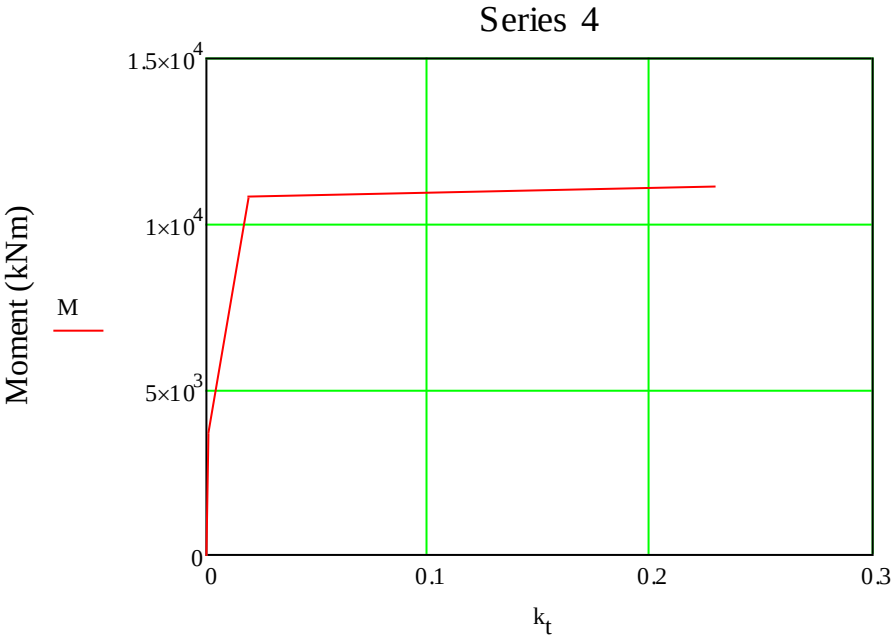

SHEAR RESISTANCE:

Series 4:

$V_{Rd.3} := V_{cd} + V_{fd} + V_{wd}$

$V_{wd} := 0$ is the contribution of transverse reinforcement

$d_1 := 200$ effective depth in mm

$k_1 := 1 + \sqrt{\frac{200}{d_1}}$ factor that takes size effect into account

$k_1 = 2$

The design value of the increase in shear strength due to steel fibres.

$\tau_{fd} := 0.12 \cdot f_{R4} = 0.03 \cdot MPa$

$k_f := 1 + n \cdot \left(\frac{h_f}{b}\right) \cdot \left(\frac{h_f}{d}\right)$

h_f is the height of the flange which is 0 in this case giving k.f equal to 1

$k_f := 1$

$V_{fd} := 0.7 \cdot k_f \cdot k_1 \cdot \tau_{fd} \cdot b \cdot d$ is the contribution of steel fibres

$V_{fd} = 1.254\,kN$

$\gamma_c := 1.5$ partial safety factor for the concrete without fibres

$\rho_1 := \frac{A_{s4}}{b \cdot d}$ longitudinal reinforcement ratio

$\rho_1 = 2.827 \times 10^{-3}$

$\sigma_{cp} := 0$ no axial force or prestressing

$f_{fck} := f_{ck.cyl4}$

$V_{cd} := \left[(0.12) \cdot k \cdot \left(100 \cdot \rho_1 \cdot f_{fck} \right)^{\frac{1}{3}} + 0.15\,\sigma_{cp} \right] \cdot b \cdot d$

$V_{cd} := \left[(0.12) \cdot 2 \cdot \left(100 \cdot \rho_1 \cdot 31.36 \right)^{\frac{1}{3}} + 0.15\,\sigma_{cp} \right] \cdot 150 \cdot 200 = 1.49 \times 10^{4}$

$V_{cd} = 1.49 \times 10^{4}$ in Newton

$V_{cd} := 14.9\,kN$

$V_{Rd.3} := V_{cd} + V_{fd} = 16.154\,kN$

CRACK WIDTH CALCULATION:

Series 4

$\alpha := \frac{E_S}{E_{cm4}} = 6.188$

From Area balance in state-II:

$\frac{b \cdot x_{II}^{2}}{2} = \alpha \cdot A_{s4} \cdot \left(d - x_{II} \right)$

$x_{II} := 0.1\,mm$

Given

$$\frac{b \cdot x_{II}^2}{2} = \alpha \cdot A_{s4} \cdot (d - x_{II})$$

$x_{II} := \text{Find}(x_{II})$

$x_{II} = 34.077\,mm$

Moment of Inertia in state-II

$$I_{II} := \frac{b \cdot x_{II}^3}{12} + b \cdot x_{II} \cdot \left(x_{II} - \frac{x_{II}}{2}\right)^2 + (1 + \alpha) \cdot A_{s4} \cdot (d - x_{II})^2 = 1.876 \times 10^{-5}\,m^4$$

$z_s := d - x_{II} = 0.166\,m$ for stress at steel level

Stabilized cracking is reached when the moment is between cracking and yield moment. To make a fair comparison between the design crack widths, a moment of 15kNm is used for series 1 and 2 and a moment of 10 kNm is used for series 3,4 and 5.

$M_{345} := 10\,kN \cdot m$

$$\sigma_c := \frac{M_{345}}{I_{II}} \cdot z_s = 88.425\,MPa$$ Concrete Stress

$\sigma_s := (\alpha \cdot \sigma_c) - 0.45 \cdot f_{R1.beam} = 547.014\,MPa$ Steel Stress in a crack

The steel stress σ .s and σ .sr have to be calculated taking into account, that the tensile stress in steel fibre reinforced concrete after cracking is not equal to zero but equal to 0.45*f.R1, which is constant all over the cracked part of the cross section.

$$\sigma_{cr} := \left(\frac{M_f}{I_{II}} \cdot z_s\right)$$

$\sigma_{sr} := \alpha \cdot \sigma_{cr} - (0.45 \cdot f_{R1.beam}) = 202.306\,MPa$

$\beta := 1.7$ for load induced cracking. section 4.4 RILEM TC-162-TDF-Test and design methods for steel fibre reinforced concrete

$\beta_1 := 1.0$ for high bond bars

$\beta_2 := 1.0$ for single short term loading

$$\varepsilon_{sm} := \frac{\sigma_s}{E_s}\cdot\left[1 - \beta_1\cdot\beta_2\cdot\left(\frac{\sigma_{sr}}{\sigma_s}\right)^2\right] = 2.361\times 10^{-3}$$

$k_1 := 0.8$ coefficient taking into account bond properties/0.8 for high bond bars

$k_2 := 0.5$ coefficient taking into account the form of the strain distribution/0.5 for bending

$\phi_b := 6$ bar size in mm

$A_{c.eff} := 2.5(h - d)\cdot b = 9.375\times 10^{-3}\,m^2$

$\rho_r := \frac{A_{s4}}{A_{c.eff}} = 9.048\times 10^{-3}$ effective reinforcement ratio

$s_{rm} := \left(50 + 0.25 k_1\cdot k_2\cdot\frac{\phi_b}{\rho_r}\right)\cdot\left(\frac{50}{\frac{L}{\phi}}\right) = 91.39$ average final crack spacing for members subjected to flexure (in mm)

$w_k := \beta\cdot s_{rm}\cdot\varepsilon_{sm} = 0.367$ in mm

APPENDIX F: EXAMPLE FROM DESIGN OF BEAM ELEMENTS

Spanish EHE-08:

BEAM SERIES 5: Vf 0.75%

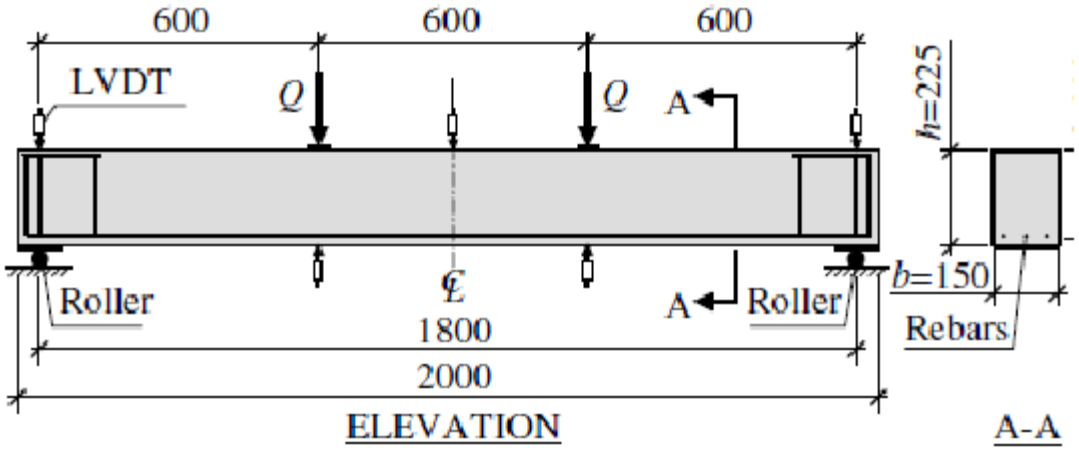

Beam Data used in experiments:

$b := 150mm$	width of the section
$h := 225mm$	height of the section
$d := 200mm$	distance to tension steel from top fibers
$l_s := 1800mm$	free span length
$l_t := 2040mm$	span length

Wedge Splitting tests:

$l_z := 100mm$	cube length
$h_z := 100mm$	cube height
$b_z := 100mm$	cube width

Materials:

Concrete:

$f_{ck.5} := 36.8MPa$	strength from cube tests
$\gamma_c := 1.5$	parial safety factor for concrete

Conventional Reinforcing steel TEMPCORE:

$f_{sy} := 660MPa$ For 6mm dia bars

$f_{su} := 784MPa$

$\phi_s := 6mm$

$E_s := 200GPa$

$\varepsilon_y := \frac{f_{sy}}{E_s} = 3.3 \times 10^{-3}$

Steel Fibres Dramix RC-65/35-BN:

$V_f := 0.75$ percentage by volume of fibres in concrete matrix

$l_f := 35mm$ fibre length

$\phi := 0.55mm$ fibre diameter

$\eta_{b.exp} := 0.56$ fibre factor

Design:

$d = 200mm$

$\phi_s := 6mm$

$A_{si} := \frac{\pi \cdot \phi_s^2}{4} = 28.274mm^2$

$n := 3$

$A_{s5} := n \cdot A_{si} = 84.823mm^2$

Series 5:

$f_{ck5} := 36.8MPa$ Experimental result from cube tests

$f_{ck.cyl5} := 0.8 \cdot f_{ck5} = 29.44MPa$ Equivalent cylinder strength

$f_{ctm5} := 0.3\left(f_{ck.cyl5}\right)^{0.66}$

$f_{ctm5} := 2.797MPa$

$f_{cm5} := f_{ck.cyl5} + 8MPa = 37.44MPa$

$E_{cm5} := 8500\sqrt[3]{f_{cm5}}$

$E_{cm5} := 28.436GPa$

$V_{f5} := 0.75\%$ percentage by volume of fibres in concrete matrix

$F_1 := 4075N$ Load corresponding to CMOD=0.5

$F_4 := 3500N$ Load corresponding to CMOD=3.5

$F_3 := 3900N$ Load corresponding to CMOD=2.5

$a := 25mm$ notch height

$h_{sp} := h_z - a = 0.075m$ h.sp is the distance of notch tip from top.

$CMOD_3 := 2.5mm$

$CMOD_4 := 3.5mm$

Residual flexural tensile strength in SLS:

$$f_{R1.exp} := 3 \cdot \frac{F_1 \cdot l_z}{2 \cdot b \cdot h_{sp}^2} = 0.724MPa$$

$\eta_{b.beam} := 0.54$ fibre effectivity factor

$$f_{R1} := f_{R1.exp} \cdot \frac{\eta_{b.beam}}{\eta_{b.exp}} = 0.699MPa$$

Residual flexural tensile strength in ULS:

$$f_{R4} := 3 \cdot \frac{F_4 \cdot l_z}{2 \cdot b \cdot h_{sp}^2} = 0.622MPa$$

$$f_{R3.exp} := 3 \cdot \frac{F_3 \cdot l_z}{2 \cdot b \cdot h_{sp}^2} = 0.693MPa$$ tensile strength decreasing due to softening behaviour

$$f_{R3} := f_{R3.exp} \cdot \frac{\eta_{b.beam}}{\eta_{b.exp}} = 0.669MPa$$

Sectional Analysis:

$f_{ctR1.d5} := 0.45 \cdot f_{R1} = 0.314\,MPa$ serviceability residual strength from Linear model

$k_1 := 1$ for sections subjected to bending

$f_{ctR3.d5} := k_1 \cdot (0.5 \cdot f_{R3} - 0.2 \cdot f_{R1})$ ultimate residual strength from Linear model

$f_{ctR3.d5} = 0.195\,MPa$

$f_{ct.d} := f_{ctm5}$

$\varepsilon_r := \frac{f_{ct.d}}{E_{cm5}} = 9.836 \times 10^{-5}$

$\varepsilon_1 := \varepsilon_r + \frac{0.1}{1000} = 1.984 \times 10^{-4}$

$\varepsilon_2 := 20 \cdot 10^{-3}$

$\varepsilon_2 = 0.02$

$p1 := \frac{\varepsilon_r}{\varepsilon_2} = 4.918 \times 10^{-3}$

$p2 := \frac{\varepsilon_1 - \varepsilon_r}{\varepsilon_2} = 5 \times 10^{-3}$

$p3 := \frac{\varepsilon_2 - \varepsilon_1}{\varepsilon_2} = 0.99$

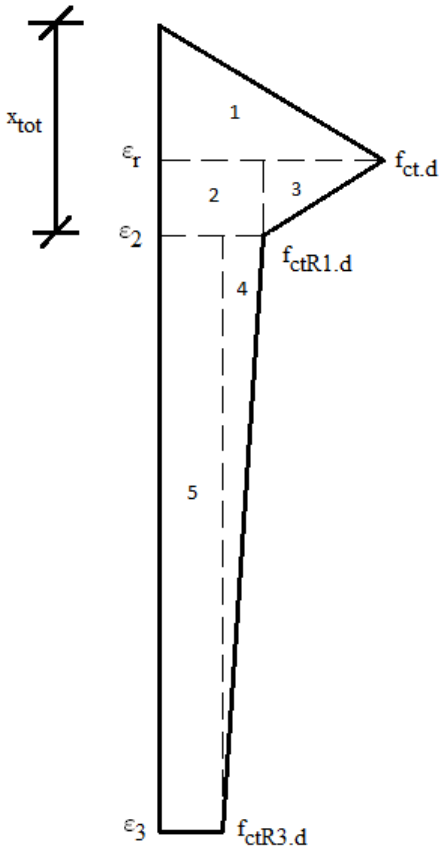

$$A_1 := \frac{1}{2}\cdot p1\cdot f_{ct.d} = 6.878\times 10^{-3}\cdot MPa$$

$$A_2 := p2\cdot f_{ctR1.d5} = 1.572\times 10^{-3}\cdot MPa$$

$$A_3 := \frac{1}{2}\cdot p2\cdot\left(f_{ct.d} - f_{ctR1.d5}\right) = 6.207\times 10^{-3}\cdot MPa$$

$$A_4 := \frac{1}{2}\cdot p3\cdot\left(f_{ctR1.d5} - f_{ctR3.d5}\right) = 0.059 MPa$$

$$A_5 := p3\cdot f_{ctR3.d5} = 0.193 MPa$$

$$A_{tot} := A_1 + A_2 + A_3 + A_4 + A_5 = 0.267 MPa$$

A.tot is the total stress of the tensile stress block

Neutral axis for individual areas:

$$x_1 := \frac{2}{3}\cdot p1 = 3.279\times 10^{-3}$$

$$x_2 := \frac{1}{2}\cdot p2 = 2.5\times 10^{-3}$$

$$x_3 := \frac{1}{3}\cdot p2 = 1.667\times 10^{-3}$$

$$x_4 := \frac{1}{3}\cdot p3 = 0.33$$

$$x_5 := \frac{1}{2}\cdot p3 = 0.495$$

Neutral axis for the Tensile stress block:

$$x_{tot}\cdot A_{tot} = A_1\cdot x_1 + A_2\cdot x_2 + A_3\cdot x_3 + A_4\cdot x_4 + A_5\cdot x_5$$

$$x_{tot} := \frac{A_1\cdot x_1 + A_2\cdot x_2 + A_3\cdot x_3 + A_4\cdot x_4 + A_5\cdot x_5}{A_{tot}} = 0.431$$

It is 0.431 of the total tensile stress block height.

Cracking moment:

$$W_1 := \frac{b\cdot h^2}{6} = 1.266\times 10^{-3}\,m\cdot m^2$$ section modulus

According to Article.50.2.2.2, Chapter 11, Spanish recommendations EHE-08, the cracking moment is:

$$M_{cr} := W_1\cdot f_{ctm5}$$

$$M_{cr} = 3.54\cdot kN\cdot m$$

Yield Moment:

Yielding starts when $\varepsilon_s = \varepsilon_{sy}$

$$\varepsilon_{sy} := \frac{f_{sy}}{E_s} = 3.3\times 10^{-3}$$

$$f_{ctRt} := A_{tot}$$

$$f_{ctRt} = 0.267\cdot MPa$$

$$\sigma_{c5} := E_{cm5}\cdot \varepsilon_{c5}$$

$$\sigma_{c5} := E_{cm5} \cdot \left[\frac{\varepsilon_{sy}}{\left(\frac{d - x_{y5}}{x_{y5}} \right)} \right]$$

$$\frac{1}{2} \cdot b \cdot x_{y5} \cdot \sigma_{c5} = f_{sy} \cdot A_{s5} + f_{ctRt} \cdot b \cdot \left(h - x_{y5} \right)$$

$x_{y5} := 0.1mm$

Given

$$\frac{1}{2} \cdot b \cdot x_{y5} \cdot \left[E_{cm5} \cdot \left[\frac{\varepsilon_{sy}}{\left(\frac{d - x_{y5}}{x_{y5}} \right)} \right] \right] = f_{sy} \cdot A_{s5} + f_{ctRt} \cdot b \cdot \left(h - x_{y5} \right)$$

$x_{y5} := \text{Find}\left(x_{y5} \right)$

$x_{y5} = 38.195mm$

$$\varepsilon_{c5} := \frac{\varepsilon_{sy}}{\left(\frac{d - x_{y5}}{x_{y5}} \right)} = 7.79 \times 10^{-4}$$

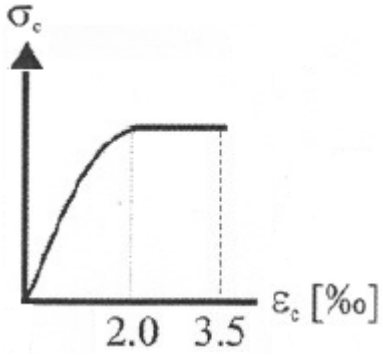

$\varepsilon_{c3} = 0.77 \cdot 10^{-3} < 2.0 \cdot 10^{-3}$ the compressive stress block is triangular

$\beta := \frac{2}{3}$

$$M_{Rdy5} := f_{sy} \cdot A_{s5} \cdot \left(d - \beta \cdot x_{y5} \right) + f_{ctRt} \cdot \left(h - x_{y5} \right) \cdot b \cdot \left[x_{tot} \cdot \left(h - x_{y5} \right) + \beta \cdot x_{y5} \right]$$

$M_{Rdy5} = 10.563kN \cdot m$

Ultimate Moment:

$$\frac{2}{3}\cdot b\cdot x_{u5}\cdot f_{cm5} = f_{sy}\cdot A_{s5} + f_{ctRt}\cdot b\cdot\left(h - x_{u5}\right)$$

$x_{u5} := 0.1\,mm$

Given

$$\frac{2}{3}\cdot b\cdot x_{u5}\cdot f_{cm5} = f_{sy}\cdot A_{s5} + f_{ctRt}\cdot b\cdot\left(h - x_{u5}\right)$$

$x_{u5} := \mathrm{Find}\left(x_{u5}\right)$

$x_{u5} = 17.173\,mm$

$\beta := 0.5$

$M_{Rdu5} := f_{sy}\cdot A_{s5}\cdot\left(d - \beta\cdot x_{u5}\right) + f_{ctRt}\cdot\left(h - x_{u5}\right)\cdot b\cdot\left[x_{tot}\cdot\left(h - x_{u5}\right) + \beta\cdot x_{u5}\right]$

$M_{Rdu5} = 11.475\,kN\cdot m$

Curvatures:

$A_c := b\cdot h = 0.034\,m^2$

$\alpha := \frac{E_s}{E_{cm5}} = 7.033$

Curvature at Cracking:

$\varepsilon_r := \frac{f_{ctm5}}{E_{cm5}} = 9.836\times 10^{-5}$

$k_{cr} := \frac{\varepsilon_r}{\frac{h}{2}} = 8.743\times 10^{-4}\,\frac{1}{m}$

Curvature at Yielding:

$k_0 := \frac{\varepsilon_{c5}}{x_{y5}} = 0.02\,\frac{1}{m}$

Ultimate Curvature:

$\varepsilon_{cu} := 3.5\,10^{-3}$

$k := \frac{\varepsilon_{cu}}{x_{u5}} = 0.204\,\frac{1}{m}$

$M := \begin{pmatrix} 0 \\ 3.54 \\ 10.564 \\ 11.574 \end{pmatrix} kN{\cdot}m \qquad k_t := \begin{pmatrix} 0 \\ 8.74310^{-4} \\ 0.02 \\ 0.204 \end{pmatrix} \frac{1}{m}$

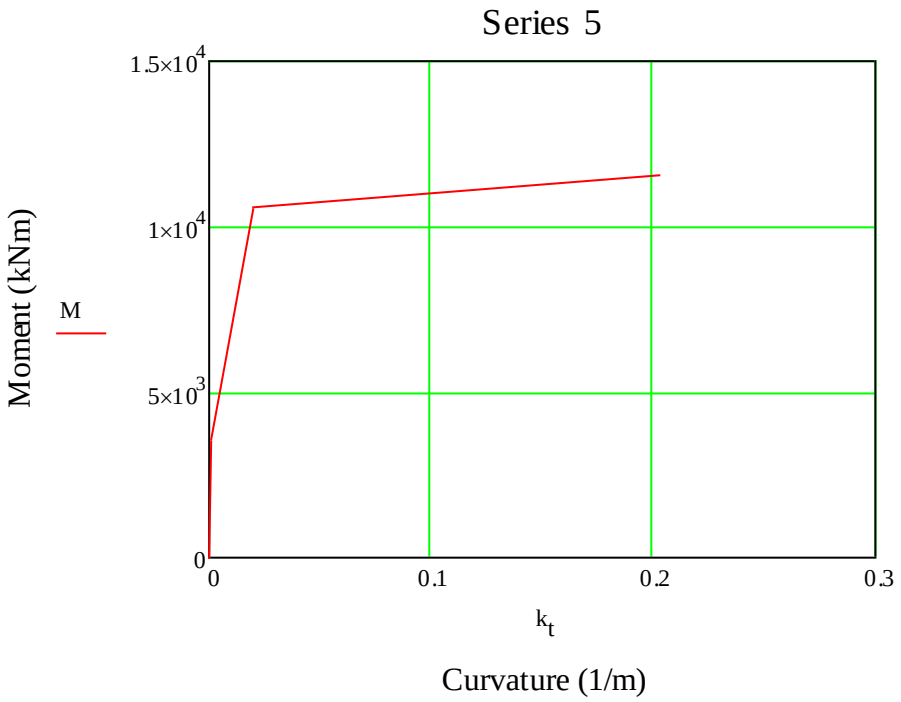

SHEAR RESISTANCE:

Series 5

$V_{Rd} := V_{u2}$

$V_{u2} := V_{cu} + V_{su} + V_{fu}$

$V_{su} := 0$ is the contribution of transverse reinforcement

$d_1 := 200$ effective depth in mm

$\xi := 1 + \sqrt{\frac{200}{d_1}}$ factor that takes size effect into account

$\xi = 2$

$\tau_{fd} := 0.5 \cdot f_{ctR3.d5} = 0.097 \cdot MPa$ design value of the increment in shear strength due to the fibres taken from article 44.2.3.2.3, Spanish recommendations EHE-08, Annex-14

$V_{fu} := 0.7 \cdot \xi \cdot \tau_{fd} \cdot b \cdot d$ is the contribution of steel fibres

$V_{fu} = 4.086\,kN$

$\gamma_c := 1.5$ partial safety factor for the concrete without fibres

$\rho_1 := \frac{A_{s5}}{b \cdot d}$ longitudinal reinforcement ratio

$\rho_1 = 2.827 \times 10^{-3}$

$\sigma_{cd} := 0$ no axial force or prestressing

$f_{cv} := f_{ck.cyl5}$

$$V_{cu} := \left[0.18 \xi \cdot \left(100 \cdot \rho_1 \cdot f_{ck.cyl5}\right)^{\frac{1}{3}} + 0.15 \sigma_{cd}\right] \cdot b \cdot d$$

$$V_{cu} := \left[0.18 \cdot 2 \cdot \left(100 \cdot \rho_1 \cdot 29.44\right)^{\frac{1}{3}} + 0.15 \sigma_{cd}\right] \cdot 150 \cdot 200 = 2.189 \times 10^{4}$$

$V_{cu} = 2.189 \times 10^{4}$ in Newton

$V_{cu} := 21.89\,kN$

$V_{u2} := V_{cu} + V_{fu} = 25.976\,kN$

APPENDIX G: EXAMPLES FROM DESIGN OF SLAB ELEMENTS

DESIGN OF SLABS - FIB MODEL CODE

Slab Data:

$b := 6m$ width of the section

$h := 0.2m$ height of the section

$l := 6m$ free span length

$A_c := h \cdot b = 1.2m^2$

Wedge Splitting tests:

$l_z := 100mm$ cube length

$h_z := 100mm$ cube height

$b_z := 100mm$ cube width

Materials:

Concrete:

$f_{ck} := 36.8MPa$ strength from cube tests

$f_{ck.cyl} := 0.8 \cdot f_{ck} = 29.44MPa$ Equivalent cylinder strength

$f_{ctm} := 0.3\left(f_{ck.cyl}\right)^{0.66}$ for concrete classes below 50 MPa

$f_{ctm} := 2.79653MPa$

$f_{cm} := f_{ck.cyl} + 8MPa = 37.44MPa$

$f_{ctk.0.05} := 0.7 \cdot f_{ctm} = 1.958MPa$

$f_{ctk.0.95} := 1.3 \cdot f_{ctm} = 3.635MPa$

$E_{cm} := 9500\left(f_{cm}\right)^{0.33}$

$E_{cm} := 31.743GPa$

Steel Fibres Dramix RC-65/35-BN:

$V_f := 0.75$ percentage by volume of fibres in concrete matrix

$l_f := 35mm$ fibre length

$\phi := 0.55mm$ fibre diameter

$\eta_{b.exp} := 0.56$ fibre factor

Same concrete mix as used in beam experiments is assumed for the slab design due to lack of experimental results for slabs. The values are taken from the file FIB-Beam series 5

$F_1 := 4075N$ Load corresponding to CMOD=0.5

$F_4 := 3500N$ Load corresponding to CMOD=3.5

$F_3 := 3900N$ Load corresponding to CMOD=2.5

$F_L := 2.7kN$ Limit of proportionality

$a := 25mm$ height of notch

$h_{sp} := h_z - a = 0.075m$ distance of notch tip from top

$CMOD_1 := 0.5mm$

$CMOD_3 := 2.5mm$

$CMOD_4 := 3.5mm$

Residual flexural tensile strength in SLS:

$$f_{R1.exp} := 3 \cdot \frac{F_1 \cdot l_z}{2 \cdot b_z \cdot h_{sp}^2} = 1.087MPa$$

$\eta_{b.slab} := 0.52$ fibre effectivity factor

$$f_{R1} := f_{R1.exp} \cdot \frac{\eta_{b.slab}}{\eta_{b.exp}} = 1.009MPa$$

Residual flexural tensile strength in ULS:

$$f_{R3.exp} := 3 \cdot \frac{F_3 \cdot l_z}{2 \cdot b_z \cdot h_{sp}^2} = 1.04MPa$$

$$f_{R3} := f_{R3.exp} \cdot \frac{\eta_{b.slab}}{\eta_{b.exp}} = 0.966\,MPa$$

$$f_{L.exp} := 3 \cdot \frac{F_L \cdot l_z}{2 \cdot b_z \cdot h_{sp}^{\,2}} = 0.72\,MPa$$

$$f_L := f_{L.exp} \cdot \frac{\eta_{b.slab}}{\eta_{b.exp}} = 0.669\,MPa$$

$f_{Fts} := 0.45 \cdot f_{R1} = 0.454\,MPa$ serviceability residual strength from Linear model

$f_{Ftu} := \frac{f_{R3}}{3} = 0.322\,MPa$ ultimate residual strength from Rigid-plastic model

$f_{Ftu} = 0.322\,MPa$

Ultimate Moment:

For slab members without conventional reinforcement, the resistance moment M.Rd is evaluated by considering a rigid-plastic model.

$$m_{Rd} := \frac{f_{Ftu} \cdot h^2}{2} = 6.438\,kN \cdot \frac{m}{m}$$